AD NUMBER
AD475509
NEW LIMITATION CHANGE

TO

Approved for public release, distribution unlimited

FROM

Distribution: No Foreign

AUTHORITY

USAFML ltr., 29 May 1972

DETERMINATION OF NATIVE DEFECTS AND ENDOTAXIAL GROWTH OF METAL-METALLOID CRYSTAL SYSTEMS EXPERIMENTAL RESULTS IN TiO$_2$ (RUTILE)

N. E. FARB

NAVIGATION SYSTEMS DIVISION
AUTONETICS
A DIVISION OF NORTH AMERICAN AVIATION, INC.

SEPTEMBER 1965

NOTICES

When Government drawings, specifications, or other data are used for any
purpose other than in connection with a definitely related Government procure-
ment operation, the United States Government thereby incurs no responsibility
nor any obligation whatsoever; and the fact that the Government may have
formulated, furnished, or in any way supplied the said drawings, specifications,
or other data, is not to be regarded by implication or otherwise as in any
manner licensing the holder or any other person or corporation, or conveying
any rights or permission to manufacture, use, or sell any patented invention
that may in any way be related thereto.

Qualified users may obtain copies of this report from the Defense Documen-
tation Center.

The distribution of this report is limited because it contains technology identi-
fiable with items on the Mutual Defense Assistance Control List excluded from
export under U. S. Export Control Act of 1949, as implemented by AFR 400-10.

Copies of this report should not be returned to the Research and Technology
Division unless return is required by security considerations, contractual obli-
gations, or notice on a specific document.

400 - November 1965 - 18-322-773

AFML-TR-65-232

DETERMINATION OF NATIVE DEFECTS AND ENDOTAXIAL GROWTH OF METAL–METALLOID CRYSTAL SYSTEMS EXPERIMENTAL RESULTS IN TiO$_2$ (RUTILE)

N. E. FARB

NAVIGATION SYSTEMS DIVISION
AUTONETICS
A DIVISION OF NORTH AMERICAN AVIATION, INC.

FOREWORD

This report was prepared by the Navigation Systems Division, Autonetics, Anaheim, California, under USAF Contract No. AF33-(615)1552. This contract was initiated under Project No. 7350, titled "Refractory, Inorganic Non-metalic Materials", Task No. 735001, "Non-Graphitic". The work was administered under the direction of the Air Force Materials Laboratory, Metals and Ceramics Division, with L. L. Fehrenbacher acting as project scientist.

This report covers work conducted from May 1964 to June 1965.

This technical document has been reviewed and approved.

W. G. Ramke
Chief, Ceramics and Graphite Branch
Metal and Ceramics Division
Air Force Materials Laboratory

ii

ABSTRACT

This work was undertaken so that an understanding of the anomalous nonstoichiometric and high temperature behavior of TiO_2 (rutile) could be ascertained. The experiment was of such a nature that the question (which has been a subject of controversy for years) concerning the type of defect--that is, whether the nonstoichiometric defect was cation interstitials or oxygen vacancies, could be answered immediately. The defect that had been considered in most of the early work (oxygen vacancies) was not the predominant effect found in this experiment. The result of the experiment was a crystalline regrowth on the high partial pressure O_2 surface. The course of the work followed an initial experimental program to determine which of the two assumptions was correct, then a combination of theoretical and experimental correlation, and, finally, a theoretical study to outline a general tool for the determination of the native imperfections in metal-metalloid crystal systems in a single experiment. Experimental results also yielded experimental proof of a new purification technique for TiO_2, and the results are applied by theoretical discussion to other metal-metalloid systems. The regrowth of single crystal TiO_2 in this experiment also leads, by a simple extension, to an entirely new and, as yet, unexplored method of growing single crystals. This is also discussed theoretically. The growth of polycrystalline samples also points to the possibility of new techniques in producing ~ 100 percent theoretical density polycrystalline material. This experiment has also yielded a new method of revealing dislocations in metal-metalloid crystals. The method is discussed theoretically.

The results obtained yield a physical proof of the existence of titanium interstitials in nonstoichiometric TiO_2 and an understanding of previous experimental inconsistencies.

CONTENTS

ILLUSTRATIONS

TABLES

1. INTRODUCTION

The theoretical determination of the type and degree of non-stoichiometry cannot at this time be determined from first principles. In fact, a satisfactory theory of the cohesive properties of solids does not exist. A completely satisfactory theory of the cohesive properties of solids would necessarily include the theoretical determination of the type and degree of nonstoichiometry a crystal would have in equilibrium with its environment.

The determination of the type and degree of nonstoichiometry by experimental techniques has led to different conclusions in all the thoroughly studied systems. Several reviews, articles, and chapters of textbooks have been written on this subject. (References 1-5) For example, one class of experiments dealing with the electrical properties will differ from the logical conclusions drawn from diffusion experiments.

The usual experimental techniques used to determine non-stoichiometry in metal-metalloid crystal systems can be listed where in all cases the magnitude and sign of the variation in the property is measured versus partial pressure. *

Variation of

1. Conduction

    a. Electronic

    b. Ionic

2. Hall effect as $f(T)$

    a. Electronic

    b. Ionic (has been attempted)

3. Thermoelectric power as $f(T)$

4. Tarnishing reactions

---

*Except No. 3 in certain cases

1

5. Loss of weight

    a. Thermogravimetry

6. Change in density

    a. Pycnometry

    b. X-ray techniques

7. Optical properties

    a. Absorption

    b. Fluorescence

    c. Polarization

    d. Thermoluminescence

8. Self-diffusion

9. Internal friction

10. Dielectric constant and loss

The key reason that confrontation of results exists is the word variation. Many simplifying assumptions necessarily have to be made in theoretical derivations to ascertain which of the four native imperfections--metal atom or ion vacancies or interstitials, metalloid atom or ion vacancies or interstitials (antistructure disorder will only be considered briefly)--yields the magnitude and sign of the variation in the measured property versus the partial pressure. These assumptions, for example, assume that:

1. Imperfections are ionized at a particular level so that they all affect the electrical properties, or that the ratio of ionized to unionized defects is large

2. The defect-defect interaction is small and can be neglected (Henry's Law and Raoult's Law)

3. One or the other type of defect leads to donors and acceptors

4. The rate of growth of a tarnished layer on a metal corresponds to interstitial or vacancy diffusion because of the value of D or D_O

5. The self-diffusion occurs by one or the other diffusion mechanisms

6. The optical properties correspond to one or the other ionized or unionized states.

However, from the entire spectrum of experimental data, some basic facts are clearly established:

1. Native imperfections do exist

2. Diffusion does occur because of imperfections

3. Diffusion of an imperfection species will occur under a concentration gradient of that species (Ficks' Law) if the imperfection specie diffusion is the rate limiting process.

4. The sign of the variation of the imperfection concentration with partial pressure can be determined (the magnitude of the slope being unimportant). Stated in other words, the law of mass action will determine that the concentration of imperfections is either directly or inversely proportional to some power of the partial pressure of the gas in equilibrium with the solid. The conclusions arrived at by the experimental technique described in this report are independent of the absolute value of the fractional value of the partial pressure exponent.

5. Different imperfection concentration gradients can be determined by conventional techniques, i. e. , some physical property other than diffusion is either directly or indirectly proportional to the concentration of the imperfections. Again, the absolute value of the physical property dependency upon partial pressure is not needed.

Using these facts, an experimental technique has been developed to yield a physical proof of the type or types of imperfections present in a crystal system. It must be emphasized that this determination is not dependent upon (1) the magnitude of the slope, (2) the relative degree of ionization, or (3) inferences from quantitative diffusion measurements as to whether the diffusion is by interstitial or vacancy mechanisms. In certain crystals there may be a large

3

difference in the activation energy for motion. In this instance, the greatest rate of crystal growth may be due to a specie which does not have the greatest concentration. However, this specie would be the most important defect as far as mass transport is concerned.

Regrcwth of the crystal will occur when the imperfections associated with the metal or metalloid are present. This type of regrowth on a single crystal has never been experienced except indirectly in tarnishing reactions. Purification of the crystal is also experienced. For background information regarding crystal growth and diffusion, see References 4 and 6 for crystal growth, and References 7 and 8 for diffusion. For background information concerning the direct observations of dislocations see Reference 9. In addition, this technique offers the possibility of sweeping out line and surface imperfections by a technique discussed in the theoretical section. Excellent background for this can be ascertained from Reference 6.

The TiO_2 body centered tetragonal (rutile) crystal system was used in the experimental portion of this work (4/28/64 to 4/28/65). This crystal system has been investigated considerably. The results of these investigations have led to different conclusions. Weight loss measurements by Buessem and Butler, Reference 10 and by Kofstad, Reference 11, led to the conclusion that oxygen vacancies were the predominant defect. Conductivity and thermoelectric measurements by Yahia, Reference 12, led to the conclusion that titanium interstitials were present below an O_2 partial pressure of 10 mm Hg and oxygen vacancies were present above this value. Hall and Just (Reference 13) measured the self-diffusion of oxygen by O_{18} mass spectrographic techniques to be

$$D = 1.1 \exp (-3.13 \text{ ev}/KT).$$

This value did not correlate directly with the experimental time required to reach a new value of nonstoichiometry, as reported by various investigators (References 10 and 11), even considering the difference between mass and self-diffusion. The fast diffusion indicated by these equilibrium times implies that a membrane experiment using steady state mass diffusion is possible, and that if there was a titanium imperfection, crystal regrowth would occur. The latter was found to be true.

II. THEORETICAL DISCUSSION

A perfect crystal is considered to be constructed by the infinite regular repetition in space of identical structural units. The smallest structural unit possible is the primary unit cell, which contains the ratio of atoms associated with the crystal. (This discussion will only consider metal-metalloid crystal systems of the form M_aX_b.)

However, an alternative consideration from an imperfection study standpoint is the view that a perfect M_aX_b crystal has atoms and vacant spaces associated with an infinite point set of interposed sublattices. The point sets can be associated with the center of the volumes normally occupied by atoms, and the point set associated with the center of the normally vacant interstitial volumes. The interstitial volumes can sometimes be associated with the normally occupied sublattice positions. Each sublattice is composed of an infinite set of points with a corresponding volume. Thus, in the M_aX_b crystal system it is assumed:

(1) M_M Normally occupied,

(2) X_X Normally occupied,

(3) V_i Normally unoccupied interstitial position.

Imperfections can be classified according to relative dimensions as:

(1) Point defects - of atomic size in three directions,

(2) Line defects - of atomic size in two directions,

(3) Surface defects - of atomic size in one direction.

Point defects can be subdived into:

(1) Atomic defects,

(2) Electronic defects

(3) Associated atomic-electronic defects.

Atomic defects can be subdivided into:

(1) Native and Foreign Atomic Imperfections

    a. V_M^x - vacancy at a normally occupied M lattice position*,

    b. V_X^x - vacancy at a normally occupied X lattice position,

    c. M_i^x - M atom at a normally unoccupied interstitial (V_i) position,

    d. X_i^x - X atom at a normally unoccupied interstitial position,

    e. F_M^x, F_X^x, F_i^x - Foreign atom at an M, X, or (V_i) position.

(2) Electronic Imperfection

    a. e' - quasi free electron in conduction band,

    b. h* - quasi free hole in valence band,

    c The symbols ', ', ^{x} indicate a negative, positive or neutral charge.

(3) Associated Defects

    a. V_M', V_M^2, $V_X^\cdot$, V_X^2, etc.

    b. $(V_M M_i)^x$, $(V_X X_i)^x$, $(V_M V_X)^x$, etc.

The definition of deviation from stoichiometry will be defined by the equation

$$\Delta = \frac{a}{b}\left\{ \frac{[X_i] - [V_X]}{[X]_{total}} - \frac{[M_i] - [V_M]}{[M]_{total}} \right\} \tag{1}$$

If $\Delta = 0$, the crystal is stoichiometric.

---

*The symbol ^{x} indicates a neutral charge.

A. DETERMINATION OF IMPERFECTIONS IN A METAL-METALLOID SYSTEM.

Consider the experimental arrangement as shown in Figure 1. A polished crystalline sample men.brane is placed inside a precision ground non-interacting ceramic ring and between two non-interacting metal washers. These components act as a gas seal between the impervious ceramic tubes and the disc sample. A partial pressure of X_2 is maintained on surface 1 greater than on surface 2, $(p_{X_2})_1 > (p_{X_2})_2$. The entire assembly is placed inside a furnace. For ionic conduction, the two surfaces would be electrically connected externally.

1. Surface Equilibrium Conditions

Let us now only consider vacancies and interstitials 'n the sublattices. For the moment, let us only consider those systems that exhibit only one predominant type of non-stoichiometric atomic defect in the partial pressure range of interest, and that the defect is nonionized. In this case the various solid state-gas reactions and their equilibrium are as follows:

2. Case 1. Metal Interstitials:

$$M_a X_b + \delta M(g) \rightleftharpoons M_a (\delta M_i) X_b \tag{2}$$

or

$$M(g) \rightleftharpoons M_i \tag{3}$$

thus

$$\frac{[M_i]_j}{(p_M)_j} = (K_{Mi})_j \tag{4}$$

but

$$M_a X_b \rightleftharpoons aM(g) + \frac{b}{2} X_2(g) \tag{5}$$
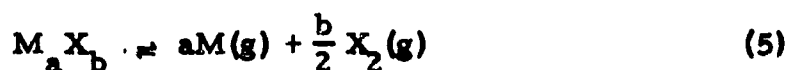
therefore

$$(p_M^a)_j \ (p_{X_2}^{\frac{b}{2}})_j = (K_{MX})_j \tag{6}$$
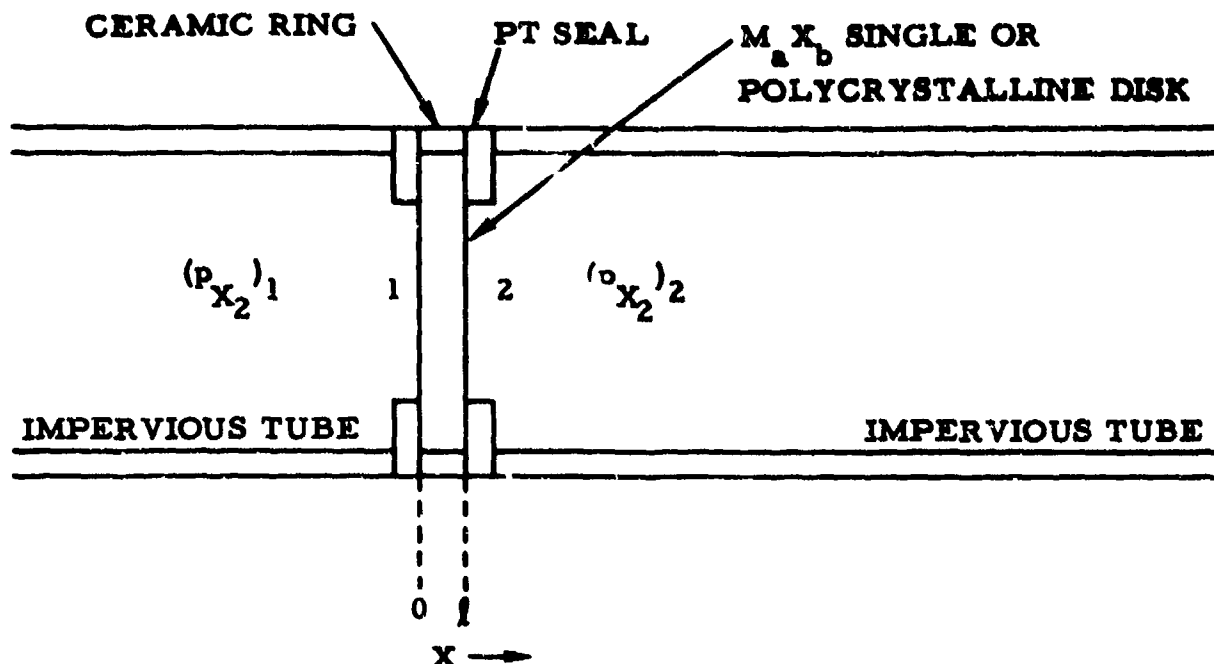
Figure 1. Membrane Experiment

since

$$[M_a X_b]_j \approx 1 \tag{7}$$

where the structural notation of Kroger and Vink (Reference 4) has been followed, and j indicates the surface (j = 1, 2). Henry's law will be assumed to be true for the moment. If $(p_{X_2}{}^{1/2})_1 > (p_{X_2}{}^{1/2})_2$, (8) the concentration of $\left[M_i \right]_2 > \left[M_i \right]_1$ (9) by the relation using Equations 3 and 5

$$[M_i]_2 = \frac{(K_{M_i}{}^{1/a})_2 \, (K_{MX}{}^{1/a})_2 \, (p_{X_2}{}^{b/2a})_1}{(K_{M_i}{}^{1/a})_1 \, (K_{MX}{}^{1/a})_1 \, (p_{X_2}{}^{b/2a})_2} [M_i]_1 \tag{10}$$

The equilibrium constants do not cancel unless the temperature and free energies are the same. It will be shown later that, indeed, the surface reactions are different resulting in exothermic and endothermic reactions which modify the equilibrium surface temperatures.

8

3. **Case 2: Metal Vacancies:**

$$\frac{b}{2} X_2(g) \rightleftharpoons bX_X + a\ V_M \tag{11}$$

The equilibrium constant can be written as

$$\frac{[V_M^a]_j}{(p_{X_2}^{\frac{b}{2}})_j} = (K_{VM})_j \tag{12}$$

The relation between the equilibrium values on the two surfaces is now

$$[V_M]_1 = \frac{(K_{VM})_1^{\frac{1}{a}}}{(K_{VM})_2^{\frac{1}{a}}} \ \frac{(p_{X_2}^{b/2a})_1}{(p_{X_2}^{b/2a})_2} [V_M]_2 \tag{13}$$

Thus, if

$$(p_{X_2}^{b/2})_1 > (p_{X_2}^{b/2})_2 \tag{14}$$

.then

$$[V_M]_1 > [V_M]_2 \tag{15}$$

which is opposite to the relation for metal interstitials.

4. **Case 3. Metalloid Interstitials:**

$$M_a X_b + \frac{\delta}{2} (X_2)_g \rightleftharpoons M_a X_b (\delta X_i) \tag{16}$$

or

$$\frac{1}{2} (X_2)_g \rightleftharpoons X_i \tag{17}$$

9

or

$$[X_i]_j = (K_{X_i})_j \, (p_{X_2}^{\frac{1}{2}})_j \tag{18}$$
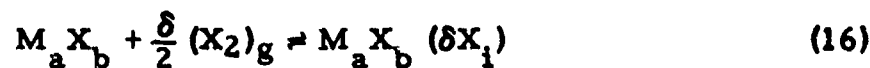
Thus,

$$[X_i]_1 = \frac{(K_{X_i})_1 \, (p_{X_2}^{\frac{1}{2}})_1}{(K_{X_i})_2 \, (p_{X_2}^{\frac{1}{2}})_2} [X_i]_2 \tag{19}$$

and if

$$(p_{X_2}^{\frac{1}{2}})_1 > (p_{X_2}^{\frac{1}{2}})_2 \tag{20}$$

then

$$[X_i]_1 > [X_i]_2 \tag{21}$$

5. Case 4. Metalloid Vacancies:

$$X_X = \frac{1}{2} X_2 \, (g) + V_X \tag{22}$$

Thus,

$$(p_{X_2}^{\frac{1}{2}})_j \, [V_X]_j = (K_{V_X})_j \tag{23}$$

or

$$[V_X]_j = (K_{V_X})_j \, (p_{X_2}^{-\frac{1}{2}})_j \tag{24}$$

therefore

$$[V_X]_1 = \frac{(K_{V_X})_1 \, (p_{X_2}^{-\frac{1}{2}})_1}{(K_{V_X})_2 \, (p_{X_2}^{-\frac{1}{2}})_2} [V_X]_2 \tag{25}$$

and if

$$(p_{X_2}^{\frac{1}{2}})_1 > (p_{X_2}^{\frac{1}{2}})_2 \tag{26}$$

10

then

$$[v_X]_2 > [v_X]_1 \qquad (27)$$

In summary then if $\quad (p_{X_2})_1 > (p_{X_2})_2$, $\qquad (28)$

(assuming equal temperatures here) then,

$$[M_i]_2 > [M_i]_1 \qquad (29)$$

$$[V_M]_1 > [V_M]_2 \qquad (30)$$

$$[X_i]_1 > [X_i]_2 \qquad (31)$$

$$[v_X]_2 > [v_X]_1 \qquad (32)$$

6. Diffusion

The above differences in concentration of imperfections results in a concentration gradient across the membrane which will result in a diffusion of that species. This diffusion can be depicted in the four cases as shown in Figure 2.

Let us now consider case 1 and 2, (i. e.) the metal defects. If one uses Fick's Law where the diffusion is independent of concentration and the crystal is at a uniform temperature,

$$j = -D \frac{dc}{dx} \qquad (33)$$

Fick's Law for case No. 1 is

$$j_{Mi} = -D_{Mi} \frac{d[M_i]}{dx} \qquad (34)$$

For case No. 2 it is

$$j_{V_M} = -D_{V_M} \frac{d[V_M]}{dx} \qquad (35)$$

11

METAL INTERSTITIALS:

$(p_{X_2})_1 > (p_{X_2})_2$

$\dfrac{d\,|M_i|}{dx} > 0$

$\dfrac{dT}{dx} < 0$

METAL VACANCIES:

$(p_{X_2})_1 > (p_{X_2})_2$

$\dfrac{d\,|V_M|}{dx} < 0$

$\dfrac{dT}{dx} > 0$

METALLOID INTERSTITIALS:

$(p_{X_2})_1 > (p_{X_2})_2$

$\dfrac{d\,|X_i|}{dx} < 0$

$\dfrac{dT}{dx} > 0$

METALLOID VACANCIES:

$(p_{X_2})_1 > (p_{X_2})_2$

$\dfrac{d\,|V_X|}{dx} > 0$

$\dfrac{dT}{dx} < 0$

a   b   c
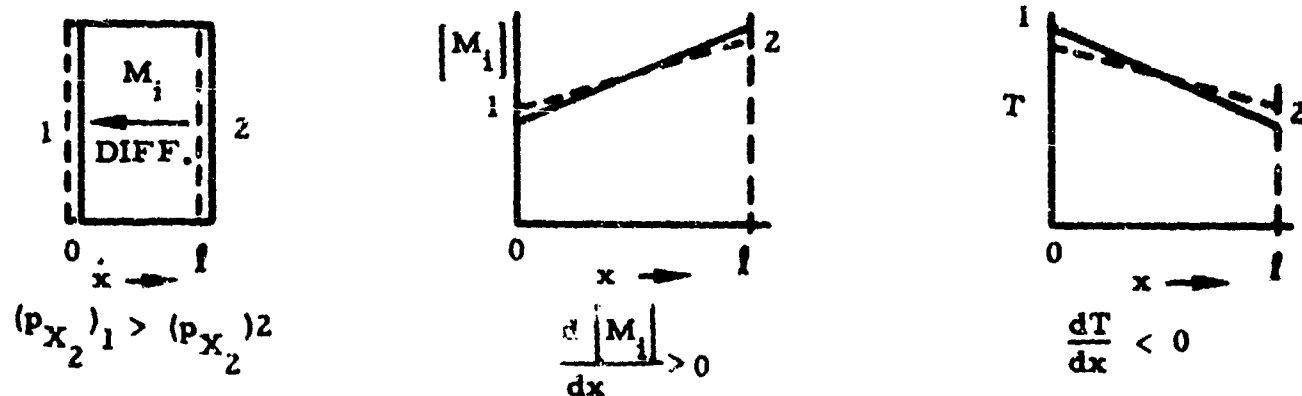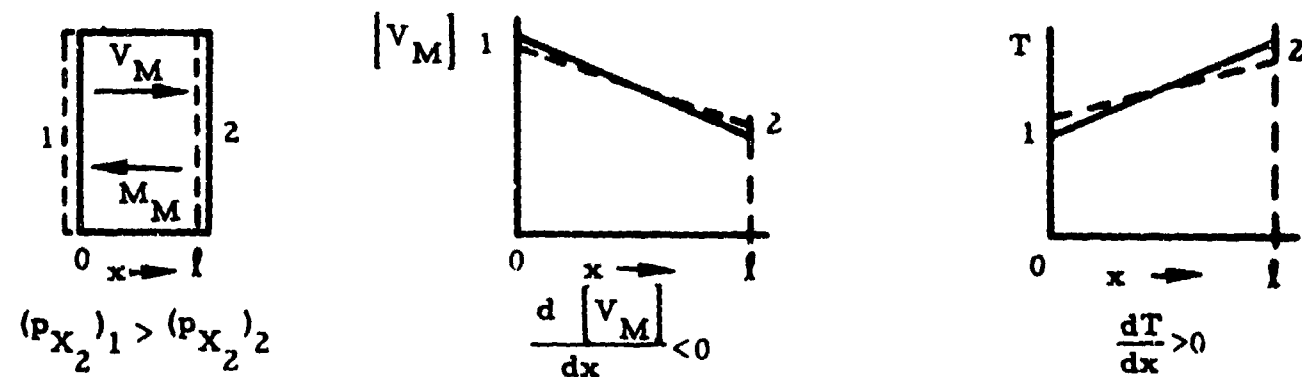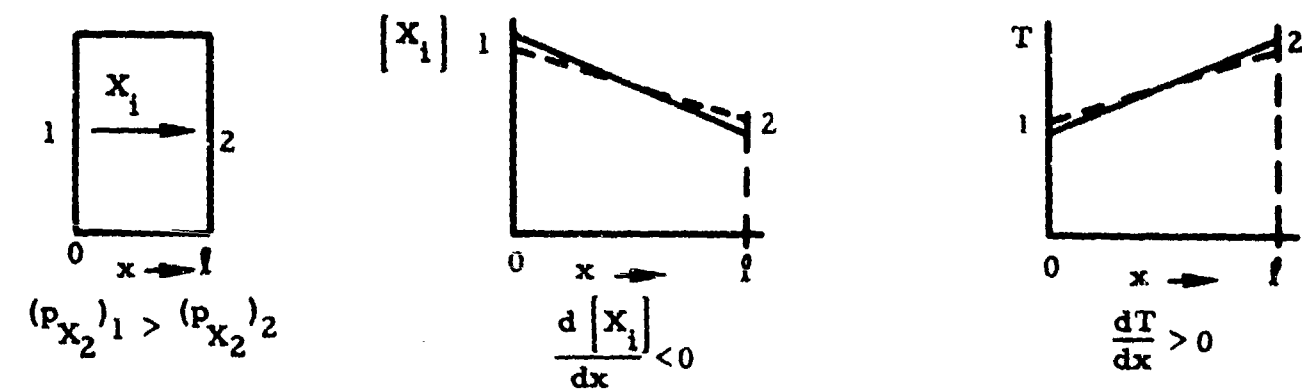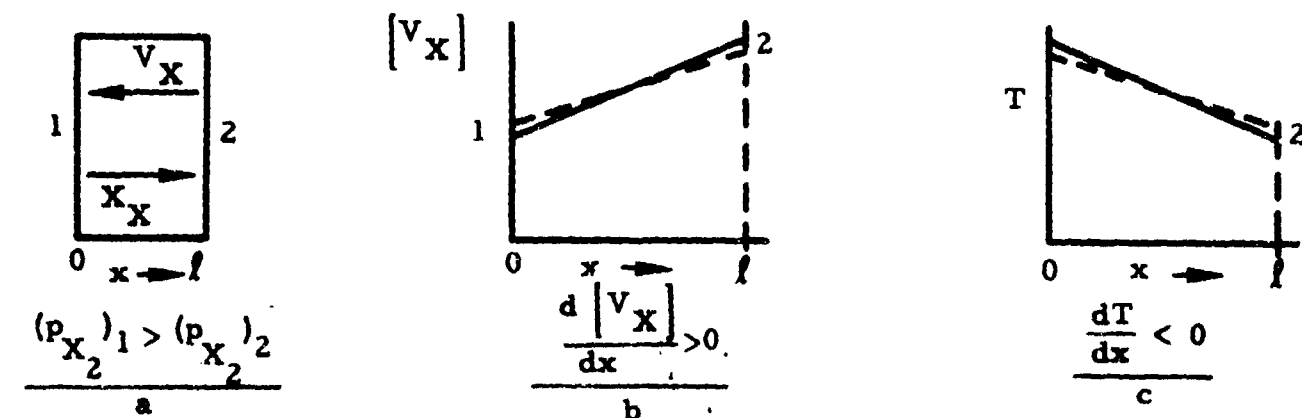
Figure 2. Diffusion Schematic Representation – Dashed
Slopes Represent Equilibrium Conditions

Now $\dfrac{d\left[M_i\right]}{dx} > 0$ and $\dfrac{d\left[V_M\right]}{dx} < 0$ so that for either case $j > 0$ resulting

in a diffusion of metal atoms towards surface 1. Diffusion of vacancies in one direction is equivalent to diffusion of atoms in the opposite direction i. e. $j_{V_M} = -j_{M_M}$.

For case 3 and 4 Fick's Law can be written

$$j_X = -D_{x_i} \frac{d\left[X_i\right]}{dx} \tag{36}$$

and

$$j_{V_X} = -D_{V_X} \frac{d\left[V_X\right]}{dx} \tag{37}$$

but again

$$\frac{d\left[X_i\right]}{dx} < 0 \text{ and } \frac{d\left[V_X\right]}{dx} > 0 \text{ so that in either case metalloid}$$

ator s move toward surface 2. Again $j_{V_X} = -j_X$.

7. Growth from Metal Atom Interstitials

Now, reconsider case No. 1 and No. 2 where metal atom imperfections are moving resulting in a mass diffusion of metal atoms towards surface 1. Case 1 has metal atom interstitials moving from surface 2 which is in equilibrium with a low partial pressure of $(P_{X_2})_2$ to the surface where the partial pressure $(P_{X_2})_1$ is higher. The resulting concentration of M_i (due to diffusion) is, therefore, higher than the equilibrium concentration at surface 1, and the excess interstitials react with the X_2 gas atoms driving the following equation from right to left

$$(1 - \delta_D) M_{a + \delta_1} X_b \rightleftharpoons M_{a + \delta_1} X_b + \delta_D (a M_i + \frac{b}{2} X_2 (g)) \quad (28)$$
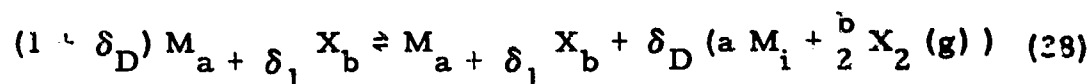
where δ_D is the excess concentration of M_i above δ_1 at surface 1 due to diffusion. Thus, the crystal grows on the high partial pressure X_2 surface. The low partial pressure surface continues to supply metal-atom interstitials in an attempt to maintain equilibrium on this surface. This is equivalent to the above equation being driven from left to right with

$$\delta_D \longrightarrow -\delta_D \text{ and } \delta_1 \longrightarrow \delta_2$$

or

$$(1 - \delta_D) M_{a + \delta_2} X_b \rightleftharpoons M_{a + \delta_2} X_b - \delta_D (a M_i + \frac{b}{2} X_2 (g))$$

$$(39)$$
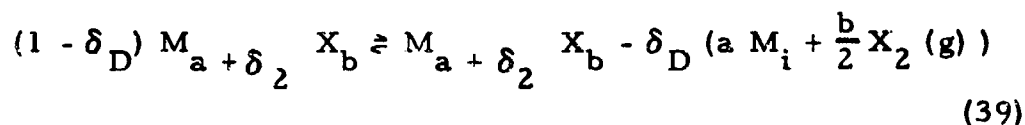
8. Growth from Metal Atom Vacancies

The atomic details of this process proceed as follows. A metal atom near the surface is promoted to the surface by thermal stimulation. The crystal in the presence of X_2 gas has a certain fraction of its surface sites occupied by X atoms (chemisorption, adsorption), and thus can react and form a $M_a X_b$ unit cell. The process also can occur by a collision with an X_2 molecule with the M surface atom. The following equation proceeds from left to right.

14

$$(1 - \frac{\delta}{a}) \, M_a X_b + \frac{\delta b}{2a} \, X_2 \rightleftharpoons M_{a - \delta} \, X_b + \delta \, V_M \qquad (40)$$

The high concentration of $[V_M]_1$ on surface 1 diffuses towards surface 2 where the equilibrium concentration of $[V_M]_2$ is now imbalanced, and the above Equation proceeds from right to left resulting in an annihilation of metalatom vacancies and an evolution of $\frac{\delta b}{2a} X_2$ gas molecules. Thus, crystal growth is obtained on the high pressure side, there is mass diffusion of cations in the cation sublattice through the membrane, X_2 gas molecules are deposited on the high pressure side, and X_2 gas molecules are released on the low pressure side that were originally crystal anions.

9. Metalloid Interstitials Diffusion

This does not directly result in crystal growth if a low partial pressure of X_2 is used. The equilibrium concentration of metalloid interstitials is higher on the high pressure surface (1), and metalloid interstitials diffuse through the crystal resulting in a higher than equilibrium concentration at surface two. Thus, at surface 1 Equation 15 is driven from left to right, and at surface 2 Equation 15 is driven from right to left. This results in an evolution of X_2 gas molecules at surface two.

10. Metalloid Vacancies Diffusion

This also does not directly result in crystal growth if a low partial pressure of X_2 is used. The concentration of metalloid vacancies is higher on the low partial pressure surface, and the diffusion of metalloid vacancies proceeds towards the high pressure surface. Here again, the equilibrium concentration of vacancies is lower so that metalloid vacancies are annihilated at this surface and are replaced by X atoms on the surface (chemisorbed or adsorbed) or from collision with an X_2 gas molecule.

The results are tabulated in the first three columns of Table 1.

15

Table 1. Diffusion Results

	Crystal Growth	Imperfection Gradient	Diffusion Mechanism	Surface 1 Reaction	Surface 2 Reaction	$\dfrac{dT}{dX}$
Metalatom Interstitials	Yes	$\dfrac{d[M_i]}{dx} > 0$	Interstitial Interstitialcy	Highly Exothermic	Endothermic	$\dfrac{dT}{dX} < 0$
Metalatom Vacancies	Yes	$\dfrac{d[V_M]}{dx} < 0$	Vacancy	Endothermic	Exothermic	$\dfrac{dT}{dX} > 0$
Metalloid Interstitials	No	$\dfrac{d[X_i]}{dx} < 0$	Interstitial Interstitialcy	Endothermic	Exothermic	$\dfrac{dT}{dX} > 0$
Metalloid Vacancies	No	$\dfrac{d[V_X]}{dx} > 0$	Vacancy	Exothermic	Endothermic	$\dfrac{dT}{dX} < 0$

From the above results one can readily determine the type of imperfection prevalant in a crystal. If crystal growth occurs, the imperfection is either metal atom vacancies or metal atom interstitials. If crystal growth does not occur and loss of X_2 gas on the high pressure side occurs, the imperfection is either metalloid vacancies or metalloid interstitials. To separate the two possibilities, i. e., metal atom interstitials from metal atom vacancies, when crystal growth occurs, the concentration gradient across the membrane must be determined. A rapid quenching from high temperatures will freeze in the concentration gradient. The membrane can then be cut so as to reveal a cross section, or thinner membranes can be cut from the original membrane. Then, some physical parameter such as optical absorption, conductivity, etc. that varies with the concentration of the imperfection can be measured to determine the concentration gradient. The concentration gradient being greater than zero indicates metal atom interstitial imperfections. A concentration gradient less than zero indicates a metal atom vacancy imperfection.

In a similar manner if crystal growth does not occur, the separation of metalloid vacancies from metalloid interstitials can be determined from the concentration gradient, being >0 (metalloid vacancies) or <0 (metalloid interstitials). In the determination of the concentration gradient by some physical property due to the imperfections, the only fact required is that the physical property be directly or indirectly proportional to the concentration of imperfections. The magnitude of the proportionality is not important. Thus, the five elementary assumptions have been employed to determine the type of defect.

Consider now the individual surface reactions at each face in regard to type of chemical reaction--that is, exothermic or endothermic reactions. In each of the four cases the imperfections are created at one surface and annihilated at the other surface. Metal atom interstitials and metalloid vacancies are formed at the low partial pressure surface; metal atom vacancies and metalloid interstitials are formed on the high partial pressure surface and annihilated at the low partial pressure surface. The creation of the imperfections requires energy in each case and the annihilation releases energy in each case. Here, a detailed analysis of an appropriate Born-Haber cycle for an ionic or covalent crystal would have to be analyzed, but, in general, the creation of imperfections requires energy.

17

If the creation of imperfections requires energy, then the reaction of case 1 on surface 2 (forming metal interstitials) will be endothermic, and surface 1 will be exothermic. The reaction of case 2 on surface 1 (forming metal vacancies) will be endothermic, and surface 2 will be exothermic. The reaction of case 3 on surface 1 will be endothermic (forming metalloid interstitials), and surface two will be exothermic. The reaction of case 4 on surface 2 will be endo-thermic (forming metalloid vacancies), and on surface 1 will be exo-thermic.

These reactions and their associated changes in local temp-erature, from the ambient, will change the equilibrium constants so that the resulting concentration gradients are always reduced in ab-solute magnitude. Therefore, the mass diffusion is reduced by this consideration. However, the temperature gradient is always of a nature to aid the mass diffusion. Thus, these competing effects will result in a new temperature and concentration gradient in the steady state. The resulting equilibrium concentration and temperature grad-ients are indicated in Figure 2 by dash lines. The results are summarized in the last three columns of Table 1.

In some crystal systems deviations from stoichiometry may occur at some partial pressure $(p_{X_2})_s$ that is spanned by $(p_{X_2})_1$ and $(p_{X_2})_2$ or

$$(p_{X_2})_1 > (p_{X_2})_s > (p_{X_2})_2 \tag{41}$$

In this situation, the prevalent type of imperfection may differ on each side of the crystal. This can lead to some interesting situations. Since we are considering four different types of imperfections on two surfaces, the number of situations we have not considered so far is $4^2 - 4$ or 12 different situations. However, of these 12, only four are possible. This can be seen from the matrix of Table 2.

Cases 1 through 4 have already been considered, and case (Z) is equivalent to the inverse of case (Z +6). Some of these situations, however, are not likely. These are indicated by an N in the matrix element. Cases 13, 15, and 16 are not likely, because this would indicate that

$$[V_X] \, \alpha \, (p_{X2})_1^{\frac{1}{2}} \tag{42}$$

18

Table 2. Imperfection Matrix

Surface 1 $(P_{X_2})_1$ \ Surface 2 $(P_{X_2})_2$	Metalatom Interstitials	Metalatom Vacancies	Metalloid Interstitials	Metalloid Vacancies
Metal Atom Interstitials	Case 1 Y	Case 5 ** N*	Case 6 ** N*	Case 7 ** N*
Metal Atom Vacancies	Case 11 ** Y	Case 2 Y	Case 8 ** N*	Case 9 ** Y
Metalloid Atom Interstitials	Case 12 ** Y	Case 14 ** N	Case 3 Y	Case 10 ** Y
Metalloid Atom Vacancies	Case 13 ** N*	Case 15 ** N*	Case 16 ** N*	Case 4 Y

N* $\approx$ not likely

**Nondiagonal elements assumed $(P_{X_2})_1 > (P_{X_2})_s > (P_{X_2})_2$

rather than

$$[V_X] \ \alpha \ (P_{X_2})_1^{-\frac{1}{2}}, \quad \text{(in contradiction to the law of mass action)} \quad (43)$$

when

$$(P_{X_2})_1^{\frac{1}{2}} > (P_{X_2})_s^{\frac{1}{2}} \quad (44)$$

Cases 5 and 14 are not likely, because this would indicate that

$$[V_M] \ \alpha \ (P_{X_2})_2^{-\frac{1}{2}} \quad (45)$$

rather than

$$[V_M] \ \alpha \ (P_{X_2})_2^{\frac{1}{2}} \quad \text{(in contradiction to the law of mass action)} \quad (46)$$

19

when

$$\left(P_{X_2}^{\frac{1}{2}}\right)_s \;>\; \left(P_{X_2}^{\frac{1}{2}}\right)_2. \tag{47}$$

Cases 6 and 8 are not likely, because this would indicate that

$$\left[X_i\right] \;\alpha\; \left(P_{X_2}^{-\frac{1}{2}}\right)_2 \tag{48}$$

rather than

$$\left[X_i\right] \;\alpha\; \left(P_{X_2}^{\frac{1}{2}}\right)_2 \qquad \text{(in contradiction to the} \atop \text{law of mass action)} \tag{49}$$

when

$$\left(P_{X_2}^{\frac{1}{2}}\right)_2 \;<\; \left(P_{X_2}^{\frac{1}{2}}\right)_s \tag{50}$$

Case 7 is not likely, because this would indicate that

$$\left[M_i\right] \;\alpha\; \left(P_{X_2}^{\frac{1}{2}}\right)_1 \tag{51}$$

rather than

$$\left[M_i\right] \;\alpha\; \left(P_{X_2}^{-\frac{1}{2}}\right)_1 \qquad \text{(in contradiction to the} \atop \text{law of mass action)} \tag{52}$$

when

$$\left(P_{X_2}^{\frac{1}{2}}\right)_1 \;>\; \left(P_{X_2}^{\frac{1}{2}}\right)_s \tag{53}$$

Thus, only four other diffusion problems need to be considered--Cases 9, 10, 11, and 12.

11. Consideration of Case 9

Anion vacancies are created at surface 2 and diffuse toward surface 1. Cation vacancies are created at surface 1 and diffuse toward surface 2. This would result in void formation internally in the crystal (because of association of V_M and V_X) with growth on the oxidizing side and loss of X_2 gas in the high partial pressure chamber due to growth. Schottky equilibrium is not involved here because the

20

formulation of the Schottky equation assumes the equilibrium transfer of atoms M and X from normal lattice sites to new sites at the surface of the crystal by the equation. [4]

$$O \rightarrow V_M^x + V_X^x \qquad (54)$$

with

$$\left[V_M^x \right]\left[V_X^x \right] = K_S \qquad (55)$$

The steady-state diffusion of V_M from one surface and V_X from the other surface will result in internal equilibrium by the reaction:

$$nV_M^x + m V_X^x \rightleftharpoons (nV_M m V_X)^x \qquad (56)$$

with

$$\frac{\left[(nV_M\, mV_X)^x \right]}{\left[V_M^x \right]^n \left[V_X^x \right]^m} = K_7 \qquad (57)$$

At the plane of association of V_M and V_X defined by the following equation which is derived later (see Equation 82).

$$x = \cfrac{\ell}{1 + \cfrac{a\ D_{V_X}\ [V_X]_2}{b\ D_{V_M}\ [V_M]_1}} \qquad (58)$$

the following sequence of steps will occur (see Figure 3).

1. A disc void will be created (the shape depends upon the surface free energies).

2. The continued diffusion of metal vacancies from surface one will be annihilated at the void with resulting release in the void of X_2 by the reaction

$$V_M + X_X \longrightarrow 1/2\ X_2 \qquad (59'$$
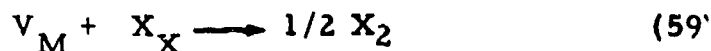
3. Thus the partial pressure of X_2 due to the surface 1 side of the void will be higher than the partial pressure of X_2 due to the surface 2 side of the void where V_X imperfections are arriving from surface 2.

4. Thus there will be gaseous transport of X_2 across the void tending to equilibrate the surface 2 side of the void.

5. Since the condition for the stoichiometric plane of association was $jv_M = jv_X$, the X_2 gas molecules will be just sufficient for the continued transport of X_X through the entire crystal (assuming surface reaction rates unimportant).

6. Thus, the surface 2 side of the void remains stationary but the surface 1 side of the void continues to move toward the original $x = 0$ position. This is depicted in Figure 3.

22.
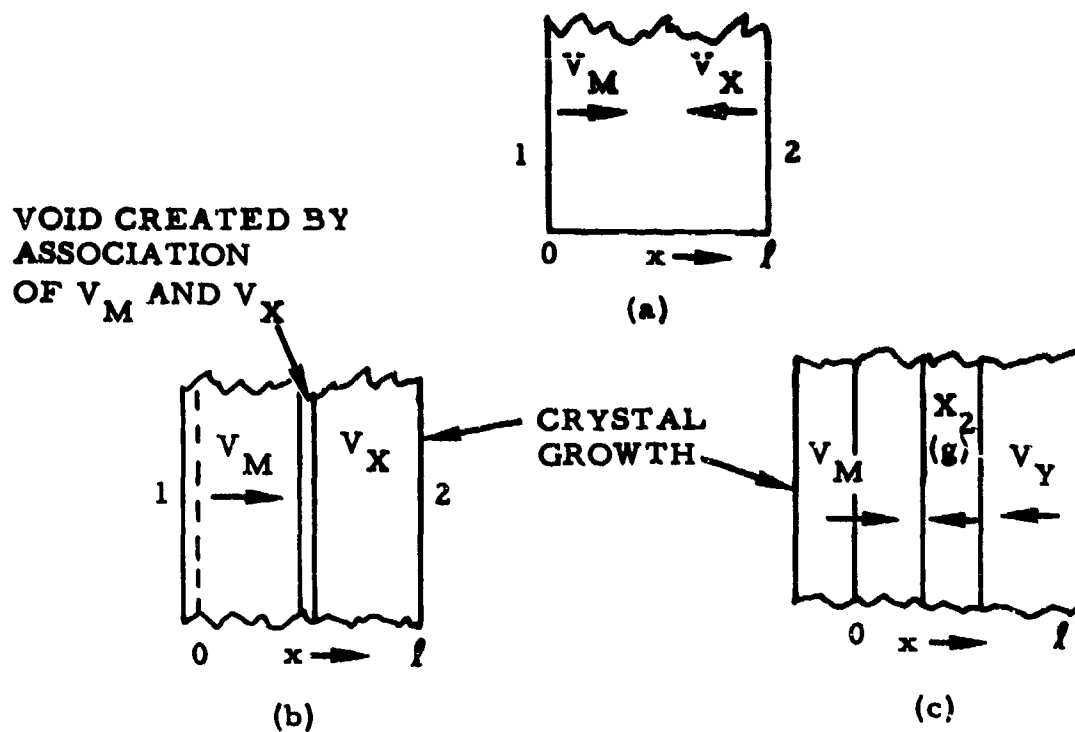
Figure 3. Case 9--Diffusion Result

12. Consideration of Case 10

Metalloid vacancies are created at surface 2 and diffuse towards surface 1. Metalloid interstitials are created at surface 1 and diffuse toward surface 2. Annihilation of metalloid vacancies and interstitials can occur internally by association. No crystal growth would normally occur.

$$V_X + X_i \; \rightleftarrows \; O. \tag{60}$$

13. Consideration of Case 11

Metal atom interstitials are formed at surface 2 and diffuse towards surface 1. Metal atom vacancies are formed at surface 1 and diffuse toward surface 2. Crystal growth occurs on surface 1 , and annihilation of metal atom vacancies and interstitials will occur internally.

$$V_M + M_i \; \rightleftarrows \; O. \tag{61}$$

23

14. Consideration of Case 12

Metalloid interstitials ar~ f..rmed at surface 1 and diffuse toward surface 2. Metal atom interstitials are formed at surface 2 and diffuse toward surface 1.' Crystal growth could occur, and the loss of $(X_2)_1$ gas is the result of crystal growth on surface 1 and the diffusion of anion interstitials to surface 2 where they are liberated. This case would be a particularly interesting diffusion problem to determine if there is a different "interstitial sublattice" for cations and anions and a p-n junction is likely to be formed if there is not a different sublattice. Also, association of M_i and X_i is likely to occur that will reduce the diffusion rate. The results are summarized in Table 3.

Table 3. Diffusion Results if There Exists a Stoichiometric Partial Pressure Spanned by $(P_{X_2})_1$ and $(P_{X_2})_2$

	Crystal Growth	Metalloid Atom Diffusion	Metalloid Atom Diffusion Results	Metal Atom Diffusion	Metal Atom Dif. Results
Case 9	Yes Surface 1	Vacancy	Annih. at Surface 1	Vacancy	Annih. at Surface 2
Case 10	No Surface 1	Vacancy & Interstitial	Annih. Internally in crystal	None	——
Case 11	Yes	None	——	Vacancy & Interst.	Annih. internally
Case 12	Yes Surface 1 None	Interst.	Removed at Surface 2	Interst.	Annih. at Surface 1

15. Reconsideration of all Cases Under a Real Metal Partial Pressure on Surface 2.

In all cases, the assumption is that the same defect will occur when the low X_2 partial pressure $(P_{X_2})_2$ is replaced by the

24

equivalent $(P_M)_2$ partial pressure by the following equations:

$$M_aX_b \rightleftarrows a M_{(g)} + \frac{b}{2}(X_2) \tag{62}$$

therefore

$$P_M = K_{M_aX_b} \, P_{X_2}^{-b/2a} \tag{63}$$

Case 1. In this case the cation interstitials are formed on surface 2 but now instead of the destruction of unit cells on surface 2 they remain intact. The metals atoms from the vapor become the interstitial atoms instead of metal atoms from the crystal unit cells. In this case etching of the surface does not occur.

The original crystal becomes larger by growing on the high X_2 pressure surface.

Case 2. In this case the metal vacancies formed on the high X_2 pressure surface are just annihilated at the metal partial pressure surface by a metal atom from the gas replacing the metal atom on a surface unit cell. The crystal growth occurs on the high metalloid partial pressure surface.

Case 3. In this case the metalloid interstitials are formed on the high partial pressure surface, diffuse through the crystal and by combining with the gaseous or adsorbed metal atoms form unit cells on the metal partial pressure surface. Thus the crystal grows on the metal partial pressure surface. This is an independent check for metalloid interstitials.

Case 4. In this case the metal partial pressure forms metalloid vacancies by forming unit cells on the surface and the crystal grows on this surface. This diffusion of oxygen vacancies to the high X_2 partial pressure surface will result in annihilation of oxygen vacancies by adsorbed X atoms on the high X_2 partial pressure surface.

25

Thus Case 3 and 4 will result in crystal growth on the metal partial pressure surface and Case 1 and 2 will not result in crystal growth on the metalloid partial pressure surface. In the prior considerations whereby a low partial pressure of X_2 was used, crystal growth occurred for Case 1 and Case 2 but not for Case 3 and Case 4.

Case 9. In this case the crystal grows on both surfaces, the surface 2 side of the vacancy disk remains at a constant X_0, and the surface 1 side of the vacancy disk recedes towards $x = O$.

Case 10. In this case the crystal only grows on the metal partial pressure surface and X_i imperfections annihilate V_x imperfections within the crystal by association.

Case 11. In this case the crystal grows only on the metalloid partial pressure surface and M_i imperfections annihilate V_M imperfections within the crystal by association.

Case 12 In this case the crystal does not grow unless the X_i imperfections can diffuse thru the portion of the crystal having an excess of M_i imperfections. If the respective imperfection are uncharged they are likely to do this. In this stance both surfaces will grow. Since the defects may be ionized then defect-defect interactions will occur and halt diffusion. A comparison of using different vapors is summarized in Table 4.

16. Discussion of the Determination of Defects

The determination of the type of defect is independent of the form of the crystal. That is, the membrane disk may be either polycrystalline or single crystal. There is little reason to believe that polycrystalline material would show a different type of defect than single crystal material under the same environmental conditions. The time required for diffusion results may be different because of the generally faster diffusion along grain boundaries.

The temperatures used would generally be above one half the melting temperature so that diffusion can proceed and surface reaction rates would be sufficiently fast. Temperatures very close to the melting point would be particular interesting because the large

26

Table 4. Comparison of Real Metal Vapor and Apparent Metal Vapor in Equilibrium With Surface 2 Membrane Experiments

		Growth on Surface 1	Growth on Surface 2	Diffusing Specie from Surface 1	Diffusion Specie from Surface 2	Internal Results of Diffusion
Case 1	$(PX_2)_2$	Yes	No (etches)	—	M_i	—
	$(P_M)_2$	Yes	No (non-etching)	—	M_i	—
Case 2	$(PX_2)_2$	Yes	No (etches)	V_M	—	—
	$(P_M)_2$	Yes	No (non-etching)	V_M	—	—
Case 3	$(PX_2)_2$	No	No	X_i	—	—
	$(P_M)_2$	No	Yes	X_i	—	—
Case 4	$(PX_2)_2$	No	No	—	V_X	—
	$(P_M)_2$	No	Yes	—	V_X	—
Case 9	$(PX_2)_2$	Yes	No	V_M	V_X	Association $(V_M V_X)$
	$(P_M)_2$	Yes	Yes	V_M	V_X	Association $(V_M V_X)$
Case 10	$(PX_2)_2$	No	No	X_i	V_X	Annihilation $X_i + V_X \rightleftharpoons 0$
	$(P_M)_2$	No	Yes	X_i	V_X	Annihilation $X_i + V_X \rightleftharpoons 0$
Case 11	$(PX_2)_2$	Yes	No (etches)	V_M	M_i	Annihilation $M_i + V_M \rightleftharpoons 0$
	$(P_M)_2$	Yes	No (non-etching)	V_M	M_i	Annihilation $M_i + V_M \rightleftharpoons 0$
Case 12	$(PX_2)_2$	"Yes"	No	X_i	M_i	Association $(X_i M_i)$
	$(P_M)_2$	"Yes"	"Yes"	X_i	M_i	Association $(X_i M_i)$

variation from stoichiometry that occurs at these temperatures.
This experiment, unlike many others, will yield results at these
temperatures. Various partial pressures can be used on either side
of the membrane and the ability to vary these partial pressures form
a very useful experimental tool. Either P_{X_2} or P_M may be used on
surface 2. The partial pressure span may be large and include the
stoichiometric partial pressure, or, be smaller and on either side of
the stoichiometric pressure. The control of temperatures is another
useful variable. Increasing the temperature is equivalent to chang-
ing the pressure through the law of mass action. Thus, a variation in
results will occur in particular systems with a change in temperature.

The five assumptions (Page 3) on which this determination
depends are valid in all ordered crystals including the intermetallics and
the ordered metal alloys. When conduction is by ionic diffusion only
($t_e=0$), the surfaces have to be electrically connected so that electronic
conduction occurs externally between the metal partial pressure surface
and the metalloid partial pressure surface.

The experimental apparatus would depend upon the temperatures
needed, the type of metalloid gases needed, e.g., oxygen, sulfur,
tellerium, antimony, selenium on the high and low X_2 pressure surfaces,
and, if needed, the type of M gases.

The ratio of the thickness to the diameter of the membrane
should be sufficiently small so that one-dimensional diffusion will occur
and the results will be simpler to interpret. One is not limited to this,
however, for a three pressure gas system may be used as shown in
Figure 4. The added possibilities with either metal or metalloid partial
pressure are involved but the results can be determined by analysis
similar to the prior discussion.

The determination of the type of defect is quite simple, (1)
surface conditions are analyzed in regard to growth, and etching or
nonetching conditions, (2) concentration gradients are determined,
and (3) internal crystal conditions are examined. The use of the two
different types of atmospheres on surface 2 provides an additional
consistency check, as will the determination of the temperature grad-
ient during the experiment. The monitoring of the quantities of gases
used or reacted on either surface also will serve as a correlation to
either the crystal growth or the permeability of the membrane to X_2.

The presence of impurities in the crystal will not effect
this determination of the native imperfections. The presence of im-
purities extrinsically controls the concentration of defects over some
partial pressure range. Thus, if the limit of partial pressure range
can be exceeded in either direction the determination of defects will
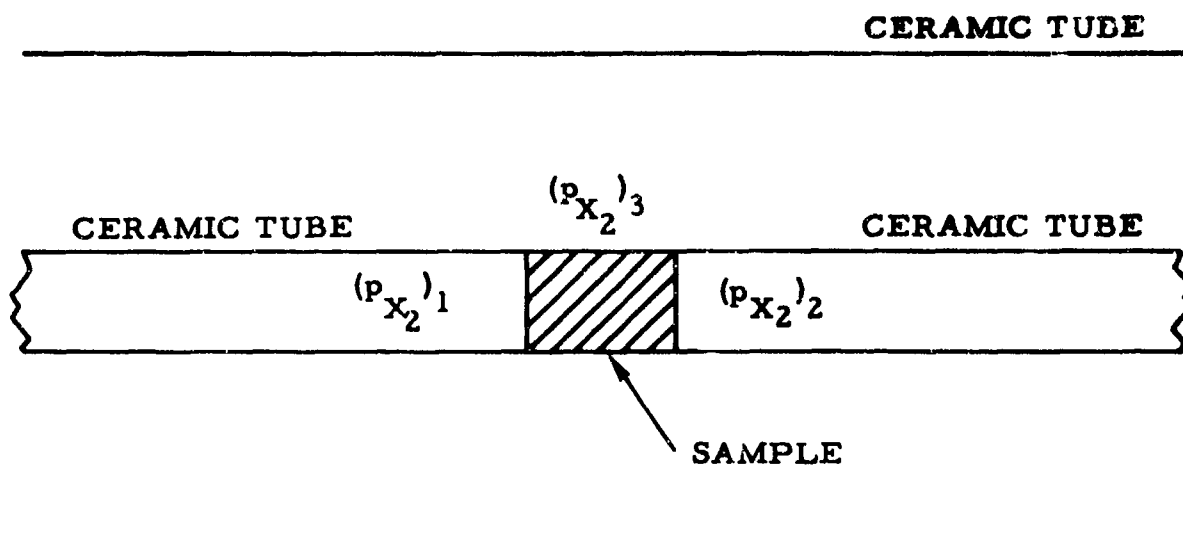occur. The diffusion will take place since the concentration of defects

28

Figure 4. Three Pressure Gas Experiment

is intrinsically controlled by the atmosphere on one side, and extrinsically controlled on the other side by the impurities, thus yielding a concentration gradient. Determining which surface grows and the concentration gradient is the same as before.

It should be noted that the experiment results are because of the diffusion of all the ionized states of the imperfection, and all the self associated states of the imperfection, such as $(V_X V_X)$. The diffusion may be different from one another but a concentration gradient would exist for any of the associated defects. Thus, the determination is independent of the associations, this is a reflection of the elementary assumptions.

There may be crystal systems where two defects are present simultaneously on one surface such as M_i and V_X with $[V_X]^x > [M_i]^x$ but that $D_{M_i} > D_{V_X}$ so that $|j_{M_i}| > |j_{V_X}|$. This analysis shows that the surface with the greatest growth rate does not necessarily have to be associated with the defect having the highest concentration but in fact always represents that defect having the greatest $j = D \dfrac{dc}{dx}$ Thus it

is always the most important defect in so far as mass transport is concerned. By using D_M in this case the crystal would grow on both surfaces because of some diffusion of the $[V_X]$.

29

CERAMIC TUBE $(P_{X_2})_3$ CERAMIC TUBE

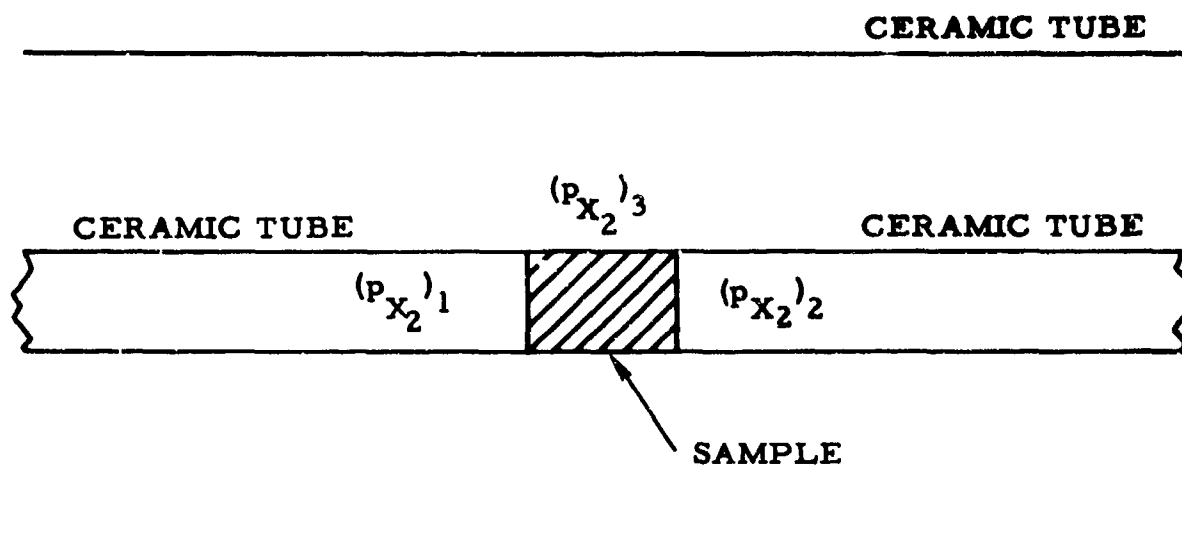$(P_{X_2})_1$ $(P_{X_2})_2$

SAMPLE

Figure 4. Three Pressure Gas Experiment

is intrinsically controlled by the atmosphere on one side, and extrinsically controlled on the other side by the impurities, thus yielding a concentration gradient. Determining which surface grows and the concentration gradient is the same as before.

It should be noted that the experiment results are because of the diffusion of all the ionized states of the imperfection, and all the self associated states of the imperfection, such as $(V_X V_X)$. The diffusion may be different from one another but a concentration gradient would exist for any of the associated defects. Thus, the determination is independent of the associations, this is a reflection of the elementary assumptions.

There may be crystal systems where two defects are present simultaneously on one surface such as M_i and V_X with $[V_X]^x > [M_i]^x$ but that $D_{M_i} > D_{V_X}$ so that $|j_{M_i}| > |j_{V_X}|$. This analysis shows that the surface with the greatest growth rate does not necessarily have to be associated with the defect having the highest concentration but in fact always represents that defect having the greatest $j = D \frac{dc}{dx}$ Thus it

is always the most important defect in so far as mass transport is concerned. By using D_M in this case the crystal would grow on both surfaces because of some diffusion of the $[V_X]$.

29

17. Antistructure Disorder Determination.

Antistructure disorder is believed to occur in those ordered ystems where the size and electonegativity of the species is not appreciably different.

Antistructure disorder occurs when one species is in the normal lattice position of the other species as represented by
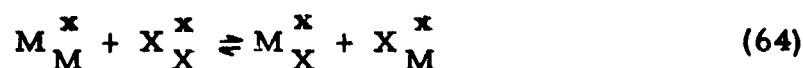
$$M_M^x + X_X^x \rightleftharpoons M_X^x + X_M^x \tag{64}$$

with its associated equilibrium constant

$$\frac{\left[M_X^x\right]\left[X_M^x\right]}{\left[M_M^x\right]\left[X_X^x\right]} = K_A \tag{65}$$

which is independent of the atmospheres.

Now, assume that (e.g.) a low partial pressure X_2 (g) produces V_X, and a membrane cell is used with the other surface a stoichiometric surface in regard to V_X, X, V_M, M, then growth of the membrane will occur because the V_X diffusion would bring M_X imperfections to the low partial pressure surface where they would form unit cells. Thus, the crystal could grow under a condition of metalloid vacancy diffusion that would not occur without antistructure disorder. Quantitative information as to the degree of antistructure disorder could be obtained if the other parameters are known by measuring the crystal growth.

30

The diffusion of V_X species would result in a diffusion of M atoms by the following relation

$$j_M = \frac{\left| M_X \right|}{\left| X_X \right|} j_{V_X} \qquad (66)$$

but since

$$j_X = -j_{V_X}$$

$$j_M = - \frac{\left| M_X \right|}{\left| X_X \right|} j_X \qquad (67)$$

Now the internal antistructure disordered will be maintained by

$$\left[M_X^x \right] \left[X_M^x \right] = K_A \qquad (68)$$

and it is not evident at this time what atomic details will take place internally. There are several possibilities, such as the production of V_M sites by the association of X_M, and V_X sites, etc. Further consideration of other nonstoichiometry and antistructure disorder can be determined by the reader.

18. Nonstoichiometric Diffusion Etching by Low Partial Pressures of X_2.

The preparation of the surface plays an important role in the diffusion of titanium interstitials in titania. It was found that an optically polished surface greatly reduced the reaction rate of the formation and/or the diffusion of titanium interstitials and the regrowth on the high O_2 partial pressure side Because of the similarity of the diffusion of titanium interstials and lithium interstitials in TiO_2, the author favors the limitation of the diffusion into the crystal as the controlling factor. Johnson (Reference 14) reported that lithium

31

interstitials will not diffuse thru a polished surface. A polished surface is a work hardened surface in that many dislocation loops are formed. The dislocations loops penetrate the volume of the crystal only a few microns.

The reactivity at a dislocation penetrating the surface may be high but the diffusion of the titanium interstials may be limited by the large number of intersecting dislocations. The size of the interstitial sites would be smaller in the compression region of the dislocations, the jump distance larger in the tension region, and the jump direction changed with the result that the diffusion may be greatly reduced and retarded.

If the work hardened surface is removed by chemical etching (fuming H_2SO_4) the intersecting dislocation region is removed so that only those dislocations that penetrate into the volume of the crystal for some distance are present. The rate of gaseous etching on the compression side of the dislocation would be larger because of the increased lattice energy. Interstitial diffusion along the dislocation into or in other directions away from the dislocation is now possible. However, there could very well be crystallographic surfaces where the surface reaction rates and diffusion of interstitials from this surface are sufficiently fast that etching may occur predominantly on these surfaces. Both of these possibilities are apparent in the experimental results.

Nonstoichiometric diffusion etching using low-vapor pressure of the X_2 gas has been shown experimentally to produce unusual tunneling. An explanation of this is in order. Consider Figure 5, which represents a single crystal membrane. Consider that for some reason a local area initially reduces faster by the production of metal interstitials. The metal interstitials diffuse in all directions from this local region leaving a small depression. At some distance, ℓ away, another similar area produces a small depression. The increase in the concentration of metal interstitials in the area between these two depressions will occur by diffusion from the depression regions. As this process continues the iso-nonstoichiometric diffusion concentrations (INDC) will have equal concentrative surfaces depicted by the dashed lines in Figure 5.

The regions of highest concentration gradients and therefore, greatest diffusion will be immediately below the depression areas. The surface between the two depressions will tend to arrive at a nonstoichiometric equilibrium, not because of its own surface
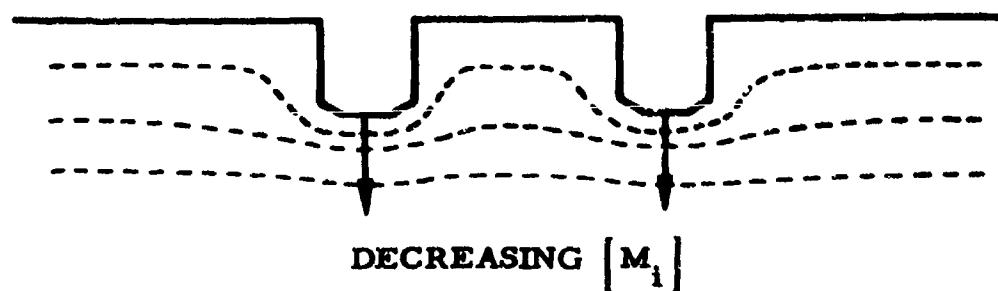
32

DECREASING $\left[M_i \right]$

Figure 5. Production of Channels or Tunnels by
Nonstoichiometric Diffusion.

reduction, but from defect diffusion produced at the depression. Thus,
the continuation of the process leads to nonstoichiometric diffusion
channels or tunnels.

18. Interacting and Noninteracting Gases

In order to develop the low partial pressures of metalloid associated with the crystal without resorting to ultra-vacuum techniques, it is necessary to use gases with very low equilibrium partial pressure of the metalloid. Gases involving H_2/H_2O and CO/CO_2 are normally used for the oxides. If the gas is a noninteracting gas, the equilibrium between the solid and the gas need only consider the solid surface-gas relationship. However, the influence of an interacting is may result in a foreign atom impurity doping reaction.
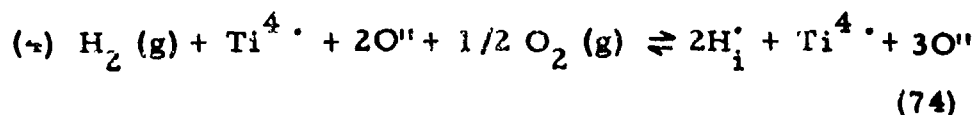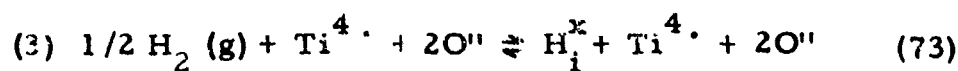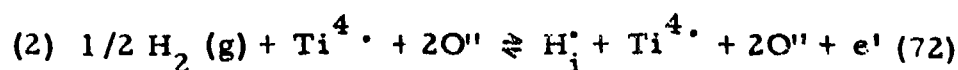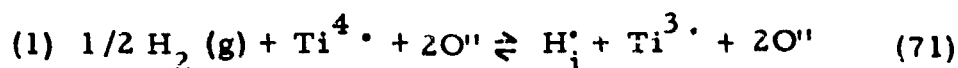
The H_2/H_2O system should be considered with great care because of the small size of the ion (i.e., a proton) and its fast interstial diffusion in many systems. The partial pressure of the oxygen can be determined by the reaction
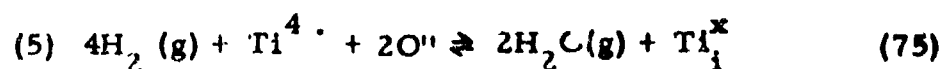
$$H_2O \text{ (g)} \rightleftharpoons H_2 \text{ (gas)} + 1/2 \, O_2 \text{ (g)} \tag{69}$$
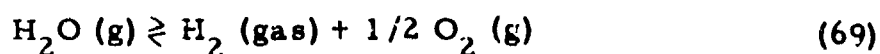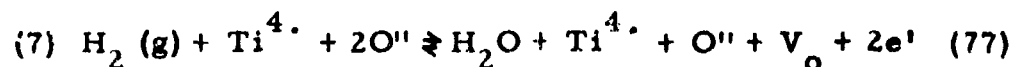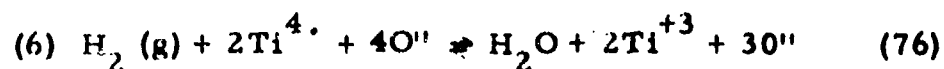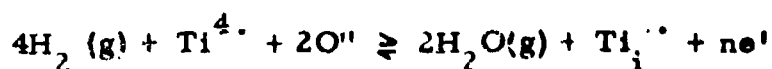
with its associated equilibrium Equation

$$\frac{P_{H_2} P_{O_2}^{1/2}}{P_{H_2O}} = K_{H_2O} \tag{70}$$

This will determine at any temperature the partial pressure of $O_2(g)$, if P_{H_2}/P_{H_2O} is known. However, this may not be the important reaction. The $H_2(g)$ may interact with the crystal as follows (using TiO_2 as an example)

$$\text{(1)} \quad 1/2 \, H_2 \text{ (g)} + Ti^{4\cdot} + 2O'' \rightleftharpoons H_i^\cdot + Ti^{3\cdot} + 2O'' \tag{71}$$

$$\text{(2)} \quad 1/2 \, H_2 \text{ (g)} + Ti^{4\cdot} + 2O'' \rightleftharpoons H_i^\cdot + Ti^{4\cdot} + 2O'' + e' \tag{72}$$

$$\text{(3)} \quad 1/2 \, H_2 \text{ (g)} + Ti^{4\cdot} + 2O'' \rightleftharpoons H_i^x + Ti^{4\cdot} + 2O'' \tag{73}$$

$$\text{(4)} \quad H_2 \text{ (g)} + Ti^{4\cdot} + 2O'' + 1/2 \, O_2 \text{ (g)} \rightleftharpoons 2H_i^\cdot + Ti^{4\cdot} + 3O'' \tag{74}$$

34

$$(5) \quad 4H_2\,(g) + Ti^{4\cdot} + 2O'' \rightleftharpoons 2H_2O(g) + Ti_i^x \qquad (75)$$

or

$$4H_2\,(g) + Ti^{4\cdot} + 2O'' \rightleftharpoons 2H_2O(g) + Ti_i^{\cdot\cdot} + ne' $$

$$(6) \quad H_2\,(g) + 2Ti^{4\cdot} + 4O'' \rightleftharpoons H_2O + 2Ti^{+3} + 3O'' \qquad (76)$$

$$(7) \quad H_2\,(g) + Ti^{4\cdot} + 2O'' \rightleftharpoons H_2O + Ti^{4\cdot} + O'' + V_o + 2e' \qquad (77)$$
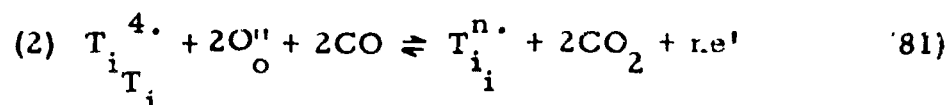
H_2/H_2O gas mixture enriched with deterium have resulted in optical absorptions bands that can be associated with H_i and D_i foreign impurity imperfections (Reference 15). Hydrogen reduced TiO_2 is also known to be an n-type conductor (Reference 16) and loses weight. Using these experimental facts, reactions, 71, 72, 73, or 74 are possibly occurring with the conclusion that hydrogen may be an interacting gas.
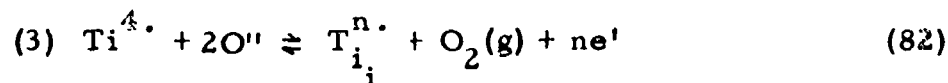
For CO/CO_2 the following reactions occur

$$(1) \quad CO_2 \rightleftharpoons CO + 1/2\,O_2 \qquad (78)$$

$$(2) \quad CO \rightleftharpoons C + 1/2\,O_2 \qquad (79)$$

with an associated equilibrium constant for reaction 79 extremely low. The likelihood of the CO molecule becoming an imperfection in TiO_2 is unlikely from an energy standpoint. Thus, the CO/CO_2 gas equilibrium with TiO_2 can be considered by the following reactions

$$(1) \quad CO_2 \rightleftharpoons CO + 1/2\,O_2 \qquad (80)$$

$$(2) \quad Ti_i^{4\cdot} + 2O_o'' + 2CO \rightleftharpoons Ti_i^{n\cdot} + 2CO_2 + ne' \qquad (81)$$

or

$$(3) \quad Ti^{4\cdot} + 2O'' \rightleftharpoons Ti_i^{n\cdot} + O_2(g) + ne' \qquad (82)$$

where the oxygen partial pressure is controlled by reaction 80. Thus, CO/CO_2 gas can be considered a noninteracting gas.

35

B. ENDOTAXY - CRYSTAL GROWTH

The growth of reasonable size crystals of ultra-high purity with low dislocation count is extremely important from a research standpoint. The researchist can then discern through experiment the intrinsic characteristics of the crystal. The purification of silicon and germanium is an excellent example of this. Many meaningful experiments have been accomplished since the advent of these pure elemental semiconductors that would have been worthless otherwise. For this reason, it seems valuable to make some comment regarding endotaxy (endo-within and taxios-arrangement). The discussion will include the implications of crystal growth theories, means of purification, and means of removing line and surface defects.

The methods presently employed in growing single crystals can be classified into three groups as follows:

1. Growth from the vapor phase

    a. Sublimation

    b. Reaction in the vapor phase

    c. Thermal decomposition

    d. Disproportionation

2. Growth from the liquid phase

    a. Growth from the melt

        1. Directional freezing

        2. Crystal pulling

        3. Zone melting

        4. Pedestal pulling

        5. Tip fusion

    b. Growth from an alloy

     c.   Growth from solvents (molten salts)

     d.   Growth from liquid solutions (water, alcohol,

3.   Growth from the solid phase

     a.   Recrystallization

     b.   Solid state reaction

     c.   Growth by tarnishing reaction

The nearest method to endotaxial crystal growth is item 3c. This has
an advantage of initially forming a single crystal (usually a thin mem-
brane) if a metal single crystal is used. However, this has severe
limitations. The transition from a defect experiment to crystal grow-
ing is relatively simple. The temperature is raised, the crystal
membrane is oriented, and the partial pressures using $(P^1_M)_2$
are adjusted to give the highest rate of growth consistent with
quality.

       The method of arrival at the endotaxially growing surface
of the atomic species involved is drastically different than the present
crystal growth techniques. One of the two atomic species is already
chemically combined with crystal. In the case of metal atom inter-
stitials they will be ionized to some extent, and as they arrive on the
surface will chemically react with the stoichiometric number of
metalloid atoms. Thus, the type and number of ionic and covalent
bonds to be formed are different.

       In the ideal membrane, the diffusion of (e. g.) the inter-
stitial species would be uniform over all areas. Thus, the entire
growing surface will have a uniform distribution of new atoms arriving
by interstitial or interstialcy diffusion of the metal species. A funda-
mental question now emerges. Is it necessary to have screw dislo-
cations for crystal growth by this method? The answer to this ques-
tion may have fundamental significance. The number of chemisorbed
or adsorbed metalloid atoms on the growing surface versus the num-
ber of arriving interstituals is another parameter. The surface mobil-
ity of the arrived metal atom is still another parameter. Unlike
growth from the vapor phase, the chemical formation of a unit cell has
to occur on the surface (the metal vapor pressure is necessarily small
because of the high metalloid vapor pressure). Crystallographic

c ientation can be controlled by the seed crystal for the optimum growing surface. When the stoichiometric partial pressure can be spanned, the crystal can be grown on either surface as in Case 12. If $(P_{X_2})_1 > (P_{Y_2})_2 > (P_{X_2})_S$ or if $(P_{X_2})_S > (P_{X_2})_1 > (P_{X_2})_2$ then Case 1, 2, 3 or 4 may be used for growth. The difference in the growth by having metalloid atoms arriving on surface 2, versus, the growth by having metal atoms arriving on surface 1, will be most interesting and enlightening. The variation of the partial pressures and temperatures leads to great versatility. In fact, electric fields may be used to enhance the diffusion of ionized interstitials.

The rate of growth will, in general, be slower than most other crystal growing techniques. However, in almost all crystal growing techniques the perfection of the crystal is inversely propoi - tional to the rate of growth. From a research standpoint the rate of growth if not important, but the mere ability to grow and acquire a high perfection crystal is important. If application of a crystal device requires high perfection, then the rate of growth is important as re- flected by the cost. Each crystal growing technique has its own type of crystals which can be grown. The introduction of a new technique such as endotaxy and the investigation of this technique will likely yield certain crystals which can be grown larger and of higher purity and perfection than can be grown by any other technique.

As yet, there is no general consolidated theory for the growth of crystals. Thus, the investigation of a new technique will yield experimental data necessary for correlation with theory.

If surface reaction rates and electron transports are not con- trolling, the diffusion of the imperfections through the crystal will determine the rate of growth. The rate of growth can be determined by the following equations

$$\frac{dx}{dt} = \frac{\Omega}{a} j_M \quad \text{for surface 1 growth} \tag{83}$$

$$\text{or} \quad \frac{dx}{dt} = \frac{\Omega}{b} j_X \quad \text{for surface 2 growth.} \tag{84}$$

where dx is the increase in crystal thickness, Ω is the unit cell volume, and $j = $ No. of atoms/cm^2 sec arriving at the growing surface by diffusion.

The rate of growth for constant environmental conditions is dependent upon the thickness of the crystal because of the decrease in concentration gradient with an increase in crystal thickness. A moving boundary condition differential equation has to be solved to determine the rate growth versus time. A reasonable approximation, however, and general discussion of technique is of importance here.

First, however, it is necessary to derive the meaning of the terms in Fick's Law and to show a clear picture of steady-state mass diffusion. Diffusion is an activated process. For example, if we consider the energy of an interstitial atom as it moves from one interstitial position to another in a diffusion jump, there is an intermediate position of high energy. This intermediate position of high energy is the activated complex. The activated complex in reaction rate theory can be treated as any other atomic species, and an equilibrium constant K_{act} can be employed for the formation of this complex. The free energy of formation of the activated complex is related to the equilibrium constant by:

$$- \Delta F = RT \ln K_{act} \qquad (85)$$

According to the second fundamental assumption of reaction rate theory the rate of transition of the activated complex into a product is a universal constant equal to $\frac{kT}{h}$ where k is Boltzmann's constant, T is the absolute temperature and h is Planck's constants ($\frac{kT}{h} = 2.1 T \times 10^{10}$/sec.) The specific rate constant is

$$r = \frac{kT}{h} K_{act} \qquad (86)$$

and the specific rate constant times the concentration gives the number of transitions/cm^3 sec.

Thus, at a plane where the concentration of interstitials is denoted by C, where the average pump distance is denoted by $\lambda*$, and the fraction of sites in the forward direction is denoted by $1/m$, the flux of atoms in the forward direction

$$j_f = \frac{kT}{h} K_{act} C \frac{\lambda*}{m} \qquad (87)$$

where $\qquad \lambda* = \frac{\Sigma \lambda}{2} \left(\cos \alpha \right) \quad$ (for a centrosymmetric crystal system) $\qquad (88)$

39

The flux in the reverse direction at the plane $x + \lambda *$, if the concentration changes with distance, is

$$j_r = \frac{kT}{h} K_{act} \frac{\lambda *}{h} \left(C + \lambda * \frac{dc}{dx} \right) \qquad (89)$$

The difference between these two equations is the net flux in the forward direction, or

$$J = -\frac{kT}{h} \frac{\lambda^2}{m} K_{act} \frac{dc}{dx} \qquad (90)$$

Now

$$K_{act} = e^{\frac{-\Delta H_{act}}{kT}} e^{\frac{\Delta S_{act}}{k}} \qquad (91)$$

where ΔH_{act} and ΔS_{act} are the enthalpies and entropies associated with the activated complex. Thus,

$$j = \frac{-kT}{h} \frac{(\lambda *)^2}{m} e^{\frac{\Delta S_{act}}{k}} e^{-\frac{\Delta H_{act}}{kT}} \frac{dc}{dx} \qquad (92)$$

Since Fick's law is usually written

$$j = -D \frac{dc}{dx} \qquad (93)$$

or

$$j = -D_o e^{-\frac{\Delta H}{kt}} \frac{dc}{dx} \qquad (94)$$

it is clear that

$$D_o = \frac{kT}{h} \frac{\lambda^2}{m} e^{\frac{\Delta S_{act}}{k}} \qquad (95)$$

then

$$\Delta H = \Delta H_{act} \qquad (96)$$

The prime purpose of this derivation is to point out that if the concentration gradients of diffusing species is already present in the

crystal, the entropies and enthalpies involved in D are only those associated with the activated complex for motion. This is in marked contrast to the value for D in a tracer isotope experiment where vacancy diffusion is involved. In tracer isotope diffusion by vacancies the fraction site has to be changed from $\frac{1}{m}$ to $\frac{V_{S.F}}{m}$, where, $V_{S.F}$ is the vacancy site fraction or the probability that the $\frac{1}{m}$ site is vacant. $V_{S.F} = \frac{[V_m]}{n}$, where, $[V_m]$ is the concentration/cm^3 of vacant sites, and n is the concentration/cm^3 of M sites. For example, a Frenkel type defect

$$V_{S.F} = \frac{A}{n} e^{-\frac{Q_F}{2kT}} \qquad (97)$$

Since, in a tracer diffusion experiment one looks at the tracer atoms, the $\frac{dc}{dx}$ term is the concentration gradient of tracer atoms. However, in a steady-state mass diffusion experiment one looks at the diffusion of the vacancies or interstitials themselves, the site fraction factor remains essentially $\frac{1}{m}$ (actually it is $\frac{[M_m] - [V_m]}{m[M_m]} \approx \frac{1}{m}$ for mass diffusion of vacancies) and

$$j = \frac{kT}{h} \frac{\lambda^2}{m} e^{\frac{\Delta S_{act}}{k}} e^{-\frac{\Delta H_{act}}{kT}} \frac{dc}{dx} = D_o e^{-\frac{\Delta H_{act}}{kT}} \frac{dc}{dx} \qquad (98)$$

where C is the concentration gradient of imperfections.

It is now interesting to look at some numbers to see if endotaxial growth is practical. By substituting 98 in 93 one gets ($a = 1$)

$$\frac{dx}{dt} = \Omega D_o e^{-\frac{\Delta H_{act}}{kT}} \frac{\Delta c}{\Delta x} \qquad (99)$$

41

Some reasonable numbers are

$$\Omega = 40 \times 10^{-24} \text{ cm}^3$$

$$D_o = 5 \times 10^{-2}$$

$$\Delta H_{act} = .5 \text{ ev} \quad \text{for motion}$$

$$\Delta c = 5 \times 10^{19}/\text{cm}^3$$

$$\Delta X = .5 \text{ cm}$$

which are probable at high temperatures. This yields

$$\frac{dx}{dt} \approx 400 \overset{o}{A}/\text{sec} \quad \text{at } 1200C \tag{100}$$

This means that in one day $400 \times 10^{-8} \times 8.6^{4} = 0.344$ cm/day, or in ~ 3 days a 1 cm thick crystal can be grown. This is, in fact, probably too fast if high quality is desired.

A crystal of high quality would have a low foreign impurity concentration, and a small number of dislocations per cm^2.

1. Purification and Growth of High Purity Crystals.

Let us first consider the problem of impurities in the seed crystal. Impurities are either substitutional or interstitial. Consider only metallic impurities and growth by an interstitial mechanism.

A concentration gradient of the host crystal cation interstitials will be driving the diffusion. It is easily seen that the foreign ion interstitials also will be driven out of the crystal. This is true because the interstitial site fraction in the rearward direction will be reduced when the host cation interstitial arrives at jump site immediately behind foreign ion interstitial. Thus, the probability for a rearward direction diffusion jump is decreased with the result that the impurities are driven out of the crystal. If the foreign ion is a substitutional ion and the interstitialcy mechanisms predominates, the substitutional sites will be emptied (if the binding energy is lower than the host atom). If the cation vacancy is the imperfection causing the

crystal growth, then purification will occur. If $D_F < D_H$, where D_F is the diffusivity of the foreign species, and D_H is the diffusivity of the host specie, the crystal will have a higher concentration of foreign ion near the growing surface. If $D_F \gtrsim D_H$, then the crystal will be purer near the growing surface. By the use of zone-refined metals for the metal vapor pressure the addition of foreign impurities can be kept to a low value. By using a thin membrane the concentration of foreign impurities is reduced by an order of magnitude if the thickness is increased by a factor of 10, even if the initial impurities act as a completely soluble species. The production of five to six nines purity crystals appears easily available. The next problem concerns the dislocation concentration.

2. Dislocation Climb

The ability to grow crystals and the purification techniques leads one to the question as to whether or not the line imperfections can be removed from a crystal. The two types of line imperfections, i. e., edge dislocations and screw dislocations, have different properties and must be considered separately.

An edge dislocation has a region of compression in the extra half plane and a region of tension on the other side of the dislocation line. Interstitial ions can reduce the energy associated with the dislocation by diffusing into the region of tension. Substitutional ions of larger size than the substituted ion also tend to move towards the region under tension to relieve the strain energy. Similarly, vacancies and smaller substitutional ions move toward the region of compression. Thus, dislocations tend to cluster foreign impurities. However, the motion of native imperfections to the dislocation will cause the dislocation to climb. The extra half plane is usually considered to be stoichiometric in a polyatomic crystal. Therefore, for climb to occur, all atomic species must diffuse to or from the dislocation for negative or positive climb. (Negative climb occurs when the extra half plane increases in area.)

Now, consider Case 10 and Case 11 of Table 2. As described in the discussion of Case 10, there is a stoichiometry plane in the interior of the crystal where the concentration of metal and metalloid vacancies has the stoichiometric ratio. As pointed out, these vacancies will tend to associate, but they also will be driven either singly, or, as an associated defect towards the region of compression associated with the dislocation. Thus, dislocation climb will occur, but since the climb can only continue to occur as long as all vacancy species move

towards the dislocation, the rate of dislocation climb will decrease the further the dislocation climbs away from the stoichiometric plane. Thus, the proper thing to do is to move the stoichiometric plane through the crystal at the rate the dislocation climb. The position of the stoichiometric plane can be controlled by the relative partial pressures in association with the diffusion constants. Consider Figure 6.
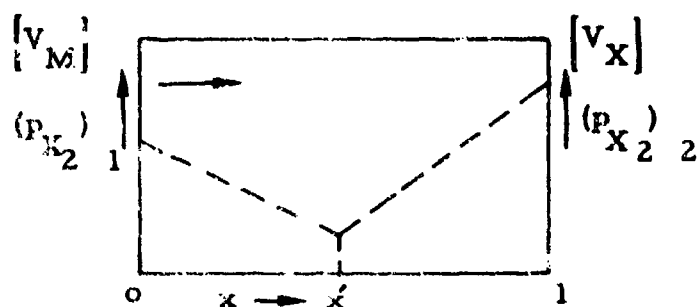

Figure 6. Stoichiometric Plane at $x = x'$

Both vacancies will diffuse toward x' according to their respective equations.

$$j_{V_M} = -D_{V_M} \frac{d\left[V_M\right]}{dx} \tag{101}$$

$$j_{V_X} = -D_{V_X} \frac{d\left[V_X\right]}{dx} \tag{102}$$

A good approximation for $d\left[V_M\right]$ if $\left[V_M\right]_{x=0} \gg \left[V_M\right]_{x=x'}$ is $d\left[V_M\right]_x = \left[V_M\right]_{x=x'} - V_{M\ x=0} \approx -\left[V_M\right]$. Similarly a good approximation for $dV_X \approx +\left[V_X\right]_{x=\ell}$

Therefore, the two equations become

$$j_{V_M} = -D_{V_M} \frac{-\left[V_M\right]_{x=0}}{x'} = D_{V_M} \frac{\left[V_M\right]_{x=0}}{x'} \tag{103}$$

44

$$j_{V_X} = -D_{V_X} \frac{|V_X|_{x=\ell}}{\ell - x'} \tag{104}$$

The condition for stoichiometry at plane x' is that the number of vacancies arriving is in the stoichiometric ratio or that,

$$\left| \frac{j_{V_M}}{j_{V_X}} \right| = \frac{a}{b} \tag{105}$$

Now, combining Equations 103, 104, and 105 and solving for x', one obtains,

$$x' = \frac{\ell}{1 + \frac{a}{b} \frac{D_{V_X}}{D_{V_M}} \left[\frac{|V_X| \ell}{|V_M|} \right]_0} \tag{106}$$

Now x' can be made small by $\dfrac{|V_X|_2}{|V_M|_1}$ being large. This can be accomplished by having $(p_{X_2})_1 = (p_{X_2})_s$ and $(p_{X_2})_2 < (p_{X_2})_s$; therefore, $|V_M| \to 0$. x' also can be made large by having $(p_{X_2})_2 = (p_{X_2})_s$ and $(p_{X_2})_1 > (p_{X_2})_s$; therefore, the denominator approaches 1.

In other words, one could start with $(p_{X_2})_1 = (p_{X_2})_s$ and increase in pressure while $(p_{X_2})_2$ (which was initially much less than $(p_{X_2})_s$) approaches $(p_{X_2})_s$. Now, to sweep out both positive and negative edge dislocations (with respect to $\cdot$) would require a reverse

sweep of the stoichiometric plane. By geometrical arguments one can see that any edge dislocation having any orientation would be swept out of the crystal by thi method.

Case 11 is the condition where metal and metalloid inter-stitials move from the surfaces towards the internal stoichiometric plane. In this case, the dislocations would undergo negative climb, i. e., the half plane would grow. Similar equations can be derived for the position of the stoichiometric plane and its position controlled by the relative pressures on either side of the boundary.

The motion of a screw dislocation is always glide. A force causing it to glide is not immediately apparent. However, an immediate effect one can visualize by the following arguments. The elastic energy of a screw dislocation is associated with the shear stress and varies as b/r times a periodic function of θ where b is the Burgers vector and r, θ are cylinder coordinates. The elastic energy could be reduced by the stoichiometric association of vacancies of both kinds in the region of small r. This would amount to the formation of a hollow cylindrical tube the center of which would be the position of the original screw. The size of this hole would be determined by the inc :ase in the surface free ener y in relation to the reduction in the elastic energy.

Grain boundaries on surface defects could climb out of the crystal in either Case 10 or Case 11 in the same manner as edge dis-locations.

III. EXPERIMENTAL PROCEDURE

A. EXPERIMENTAL APPARATUS

The diffusion experimental apparatus was designed to hold
a thin ~1mm crystal disk sample between two different atmospheres
at elevated temperatures. Thermocouples were placed on either side
of the sample and the oxygen atmosphere was monitored by a precision
volume measuring U tube. Provision was made to hold the oxygen
volume reservoir at controlled temperatures (by a liquid bath). The
furnace was controlled by a centrally located Pt - Pt-13 percent Rh thermo-
couple placed in close proximity to the furnace winding. A Leeds and
Northrup precision set point control unit controlled a 3 kw saturable
reactor.

The gases used were Matheson's High Purity grade O_2,
CO, H_2, Argon and Linde's CO_2. The gas-flow rates were controlled
by calibrated Matheson flow meters. The specimens were oriented by
X-ray back reflection techniques and sliced with a diamond saw pre-
cision wafering machine. The specimens were then ground and polished
by conventional optical lapping techniques to size (flat and parallel to
less than four fringes) and then ground to a circular shape in a special
lathe chuck.

Platinum washers were prepared from 9.9 mil sheet stock
with a 0.750 in. OD and a 0.400 ID. The ceramic rings were cut and
ground from high purity high density alumina plates to a thickness of
0.0 to 0.2 mil thinner than the specimens with a 0.750 OD and a 0.625 ID.
The specimens were then placed inside the ceramic ring and two plati-
num washers were then placed on either side. This arrangement was
then loaded between the two alumina atmosphere containing tubes and
then the furnace was lowered into place.

The polycrystalline samples were prepared from Research
Organic 99.99 percent pure TiO_2 powder. Polyvinyl alcohol was used
as a binder. The mixture was then dried and formed into a boule and
hydrostatically compressed inside a balloon with 20,000 lb/sq in., in
a pressure vessel. The formed boule was then heated at 300C for 48
hours and then slowly brought up to 1250C in a helium atmosphere and
allowed to sinter to 94.5 percent theoretical density for 72 hours. The
sample disks were then prepared in the usual manner.

47

Weight loss measurements were performed by reducing the sample in a controlled atmosphere and quenching in an inert atmosphere as shown in Figures 7 and 8. The samples were then weighed on a Mettler precision microgram balance, reoxidized in a 1 atm O_2 atmosphere, and reweighed.

The outer tube served to contain the controlled atmosphere and was surrounded by the furnace winding. The inner pedestal tube held a polished sapphire disk which served as the sample dish. An approximately 1 gram cubically cut TiO_2 single crystal was then placed on the dish and allowed to achieve equilibrium with the atmosphere. The tube was then lowered rapidly into the lower chamber which contained the inert atmosphere for quenching.
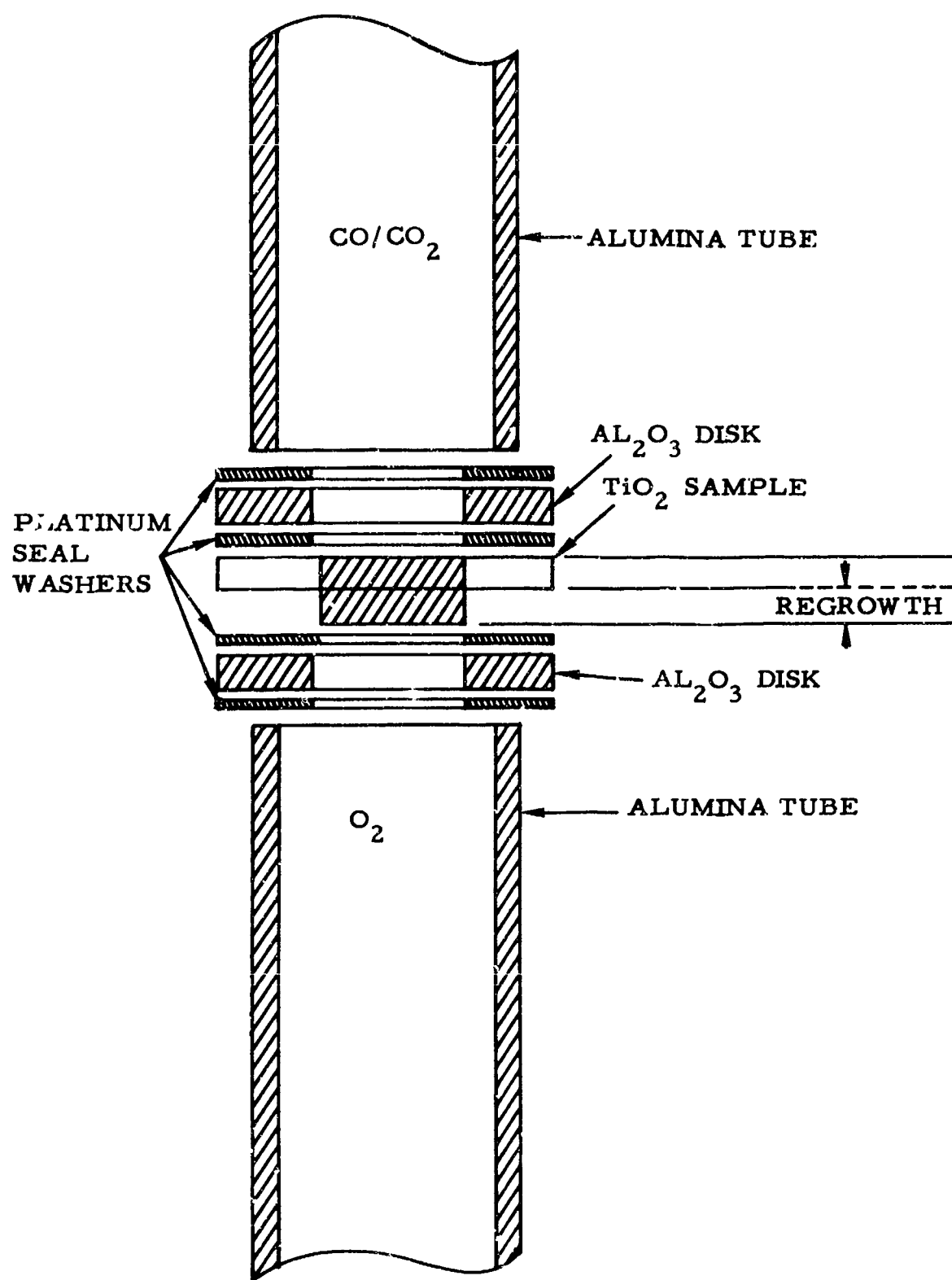
Figure 7. Details of Sample Holder Showing
Growth of the TiO$_2$ Disk
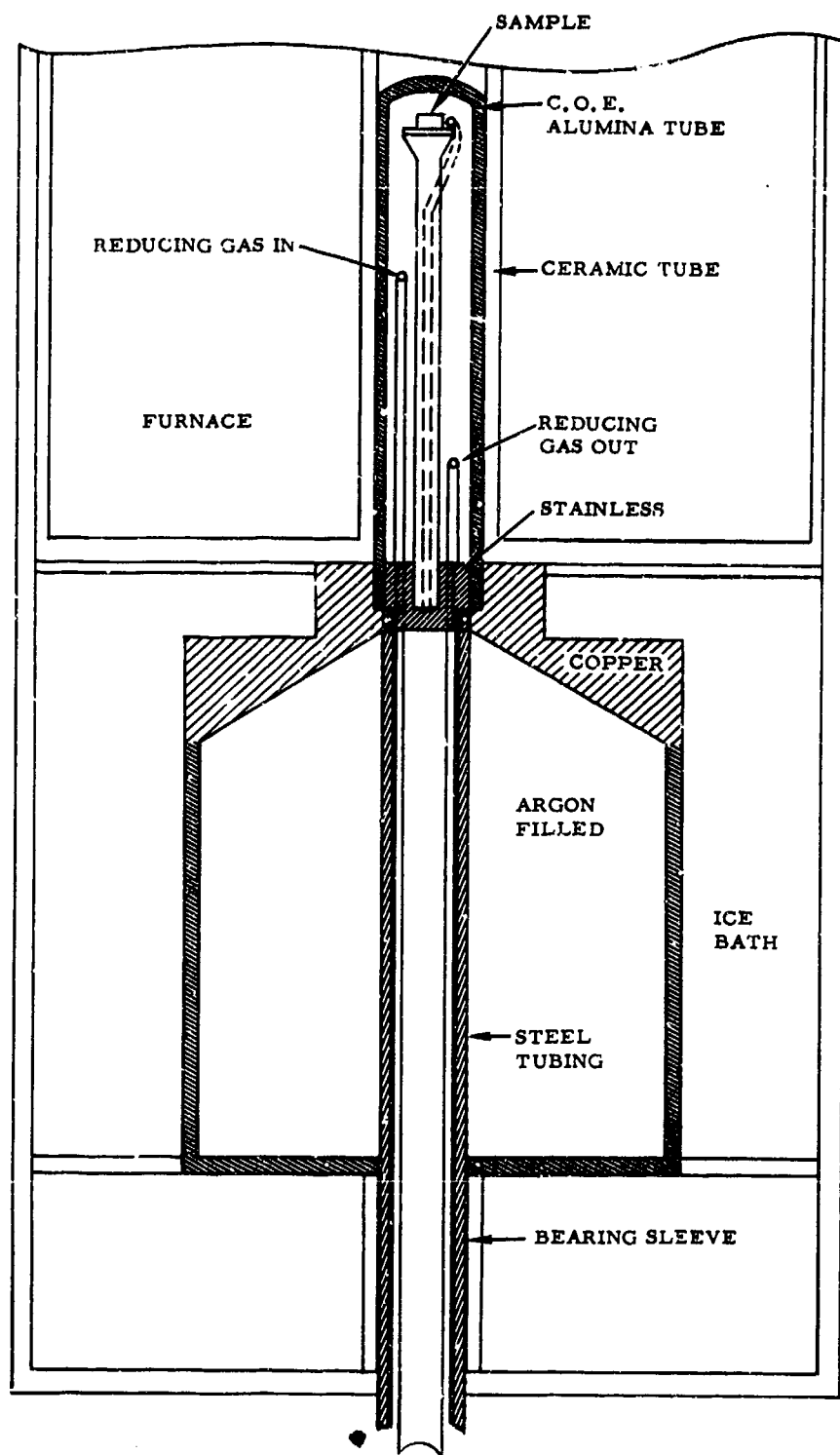
Figure 8. Furnace Modification for Nonstoichiometry
Determination

IV. EXPERIMENTAL PROGRAM

The experimental program was divided into two parts.

(1) To determine either the oxygen diffusion
due to oxygen vacancies or to determine
the titanium interstitial diffusion effects.

(2) To determine if consistent weight loss
measurements could be made by reduction,
quenching and then weighing procedures.

The initial diffusion experiment resulted in crystal regrowth
on the high pressure surface. The work then proceeded to determine
the following:

(1) What experimental results would be obtained
by using a polycrystalline disk?

(2) What experimental results would be obtained
by using single crystal disks having (100)
faces and (001) faces?

(3) What experimental results would be obtained
by using H_2/H_2O, CO/CO_2 atmospheres,
and a 10^{-2} TORR partial pressure of O_2 on
surface 2?

(4) What experimental results would be obtained
by varying the surface preparation?

(5) What experimental results would be obtained
by using Fe as a diffusing species?

A. POLYCRYSTALLINE MEMBRANE

Polycrystalline samples of 94.2 percent theoretical density
were prepared and polished flat to within 2 to 4 fringes. The sample
thickness was 0.76mm. The alumina ceramic ring was prepared to
a thickness 0.000 to 0.005 mm thinner than the sample. The platinum
seals were then placed on both sides and the arrangement placed

51

between the ceramic tubes inside the furnace. A $CO/_{CO_2}$ gas ratio equal to one and pure O_2 were used on either side. Both gases were at one atmosphere pressure.

An initial run at 1000C for four hours led to nonstoichiometric diffusion etching on the $CO/_{CO_2}$ surface. No growth was visible on the O_2 surface. However, a cross-section revealed that densification was occurring in the center of the membrane. A second sample was then run for 32 hours at 1100C. Densification and growth to and beyond the original O_2 surface occurred.

Figures 9 and 10 are photographs of the unpolished sample cross-section. Figures 11 and 12 are photographs of the polished cross-sections of the sample. Figure 13 reveals the densification occurring in the sample. Figures 14 and 15 are photographs of the O_2 surface. Figure 16 is a photograph of the $CO/_{CO_2}$ surface.

Figure 9 is particularly interesting. The platinum seal serves as a marker. The regrowth is beyond the original surface which would be a line drawn between the inner edges of the platinum seal through the regrowth region. Upon cooling from 1100C, the platinum contracts more than the oxides because of the differences in the coefficients of expansion. For this reason, polishing has to be performed with great care due to the residual compressional stresses. The platinum seal is slightly distorted near the regrowth region for this reason. The platinum seal is always bonded to the TiO_2 on the oxygen side. The platinum seals are never bonded to the TiO_2 on the $CO/_{CO_2}$ surface.

Five distinct regions exist in the membrane as a result of the nonstoichiometric diffusion gradients. These are depicted in the sketch of Figure 17.

Region one is an area of regrowth beyond the original surface. Region two is an area of densification of the polycrystalline material. The difference in thickness of this region probably reflects local variations in original density. Region three is an area of densification under the platinum seal extending up the inside surface of the ceramic seal. Region four is an area essentially unscathed. Region five is a "scale" area that separated from Region two due to the dynamics of the diffusion.

52

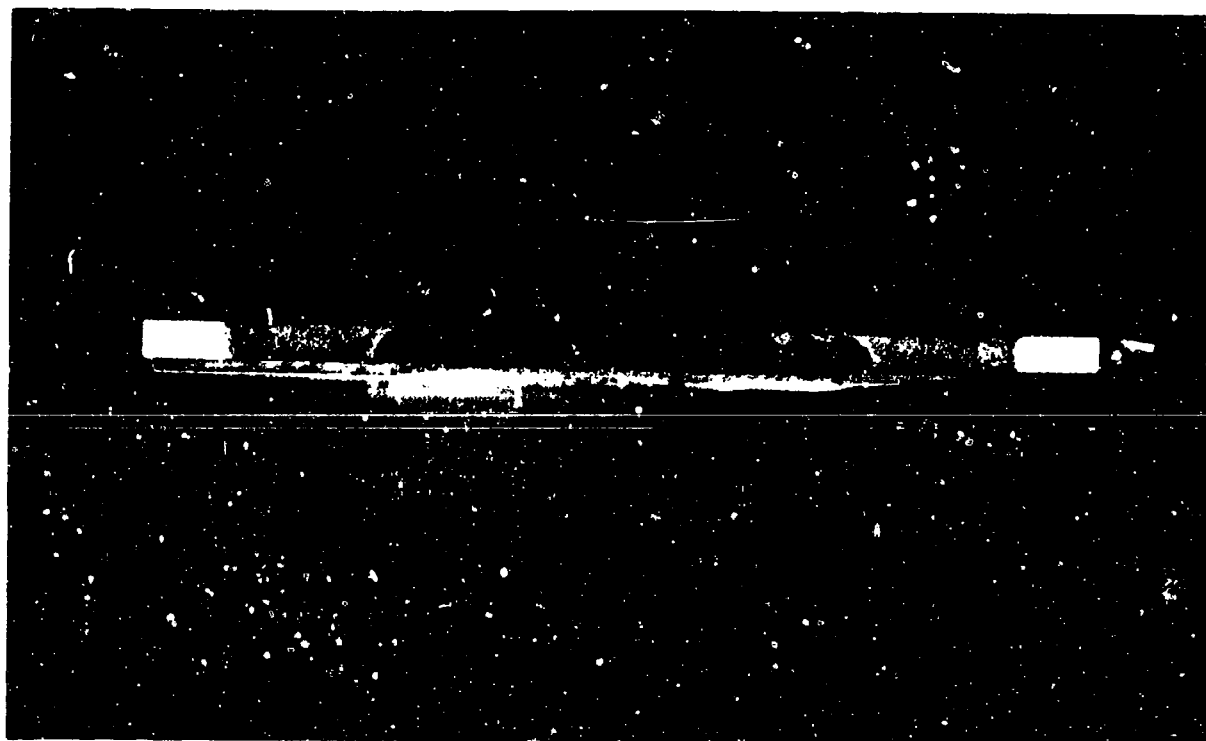Figure 9.   Polycrystalline Unpolished Cross Section

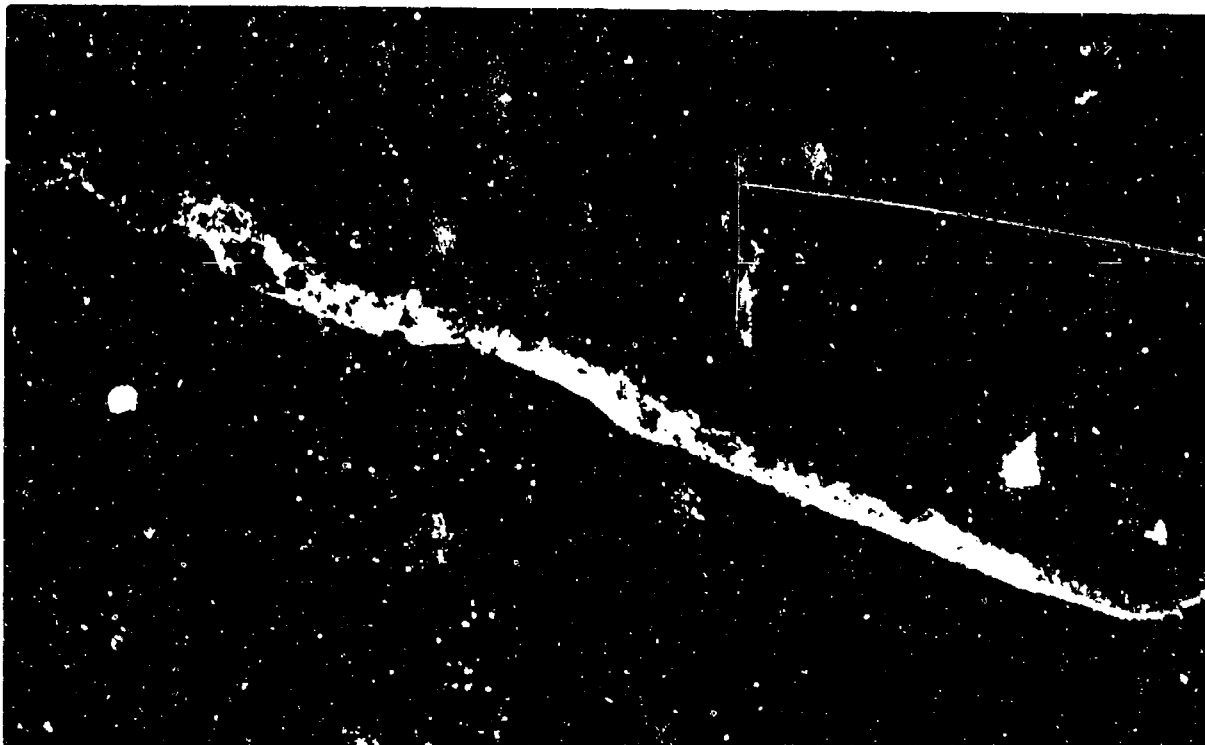Figure 10.   Polycrystalline Unpolished Cross Section

Figure 11. Polycrystalline Polished Cross Section. Center
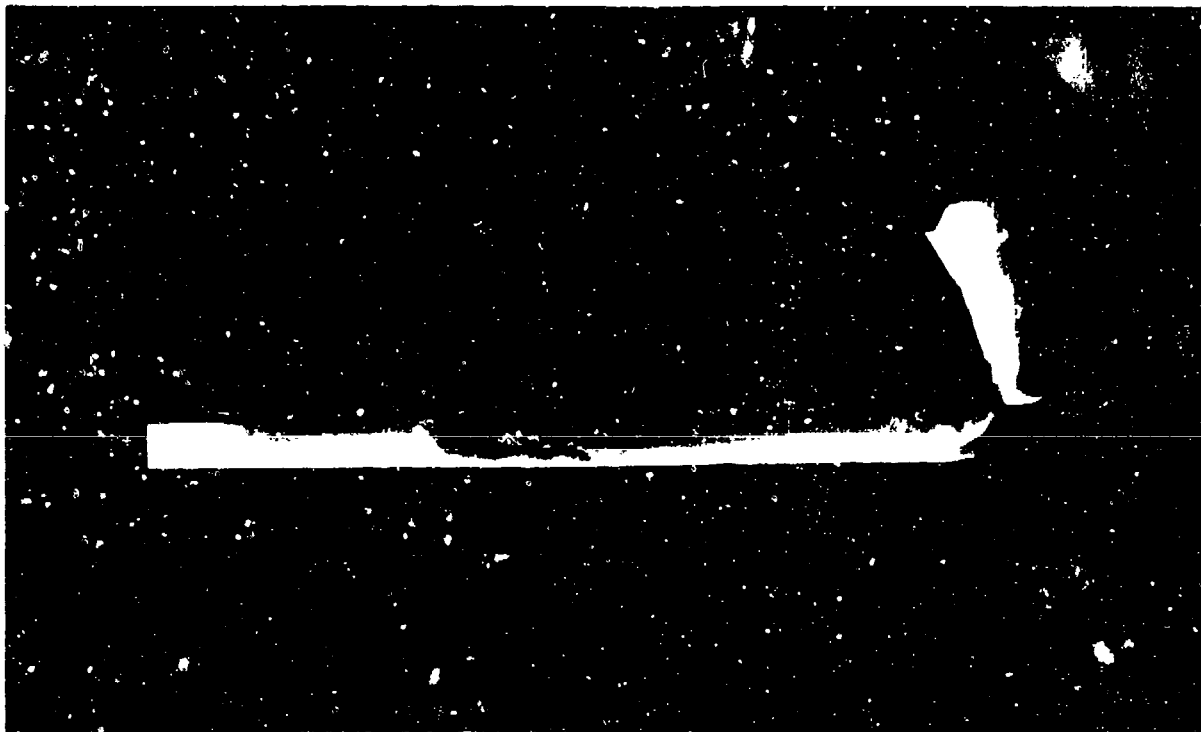Portion of Sample Shown in Figure 10 (X 14.5)

Figure 12. Polycrystalline Polished Cross Section of Sample
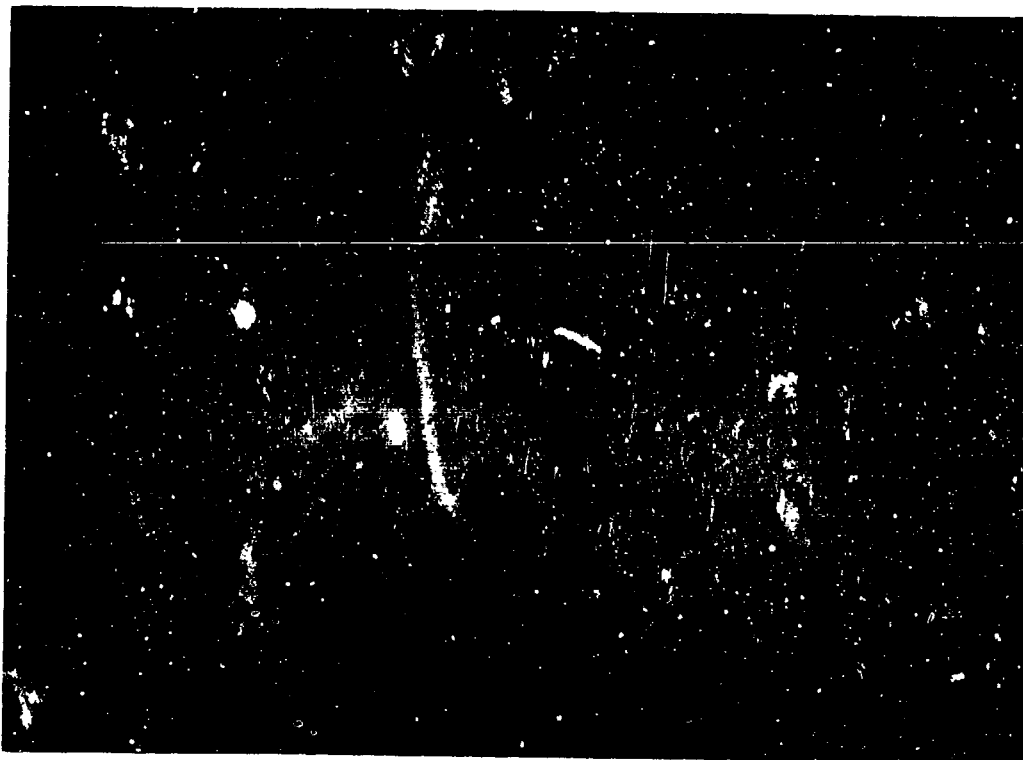Section Shown in Figure 9 (X 7.25)

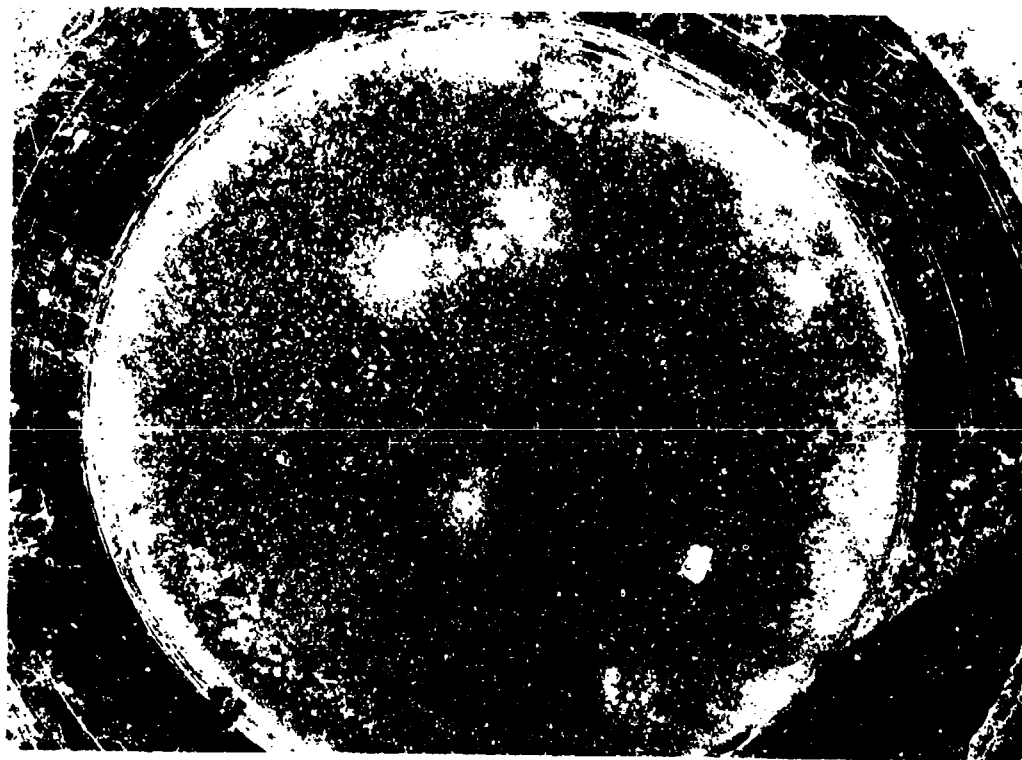Figure 13.   Enlargement of Figure 12 Cross Section (X 94. 3)

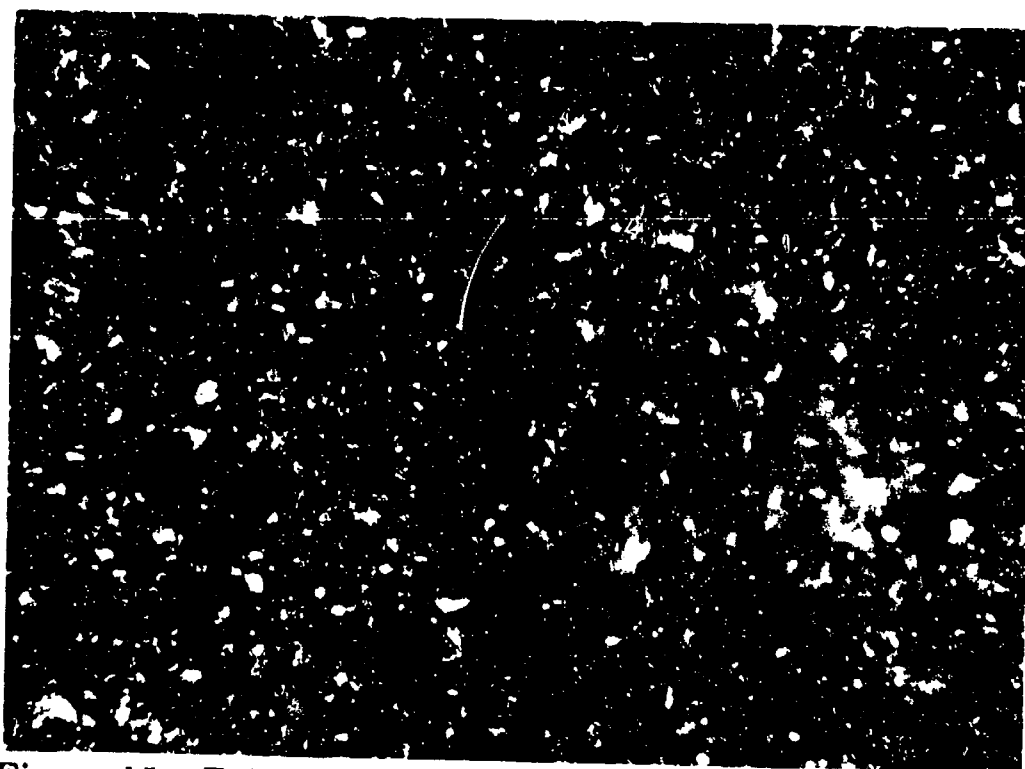Figure 14.   Polycrystalline High Partial Pressure
             O_2 Surface (X 10)

Figure 15.   Enlargement of Figure 14—O_2 Surface (X 67.5)
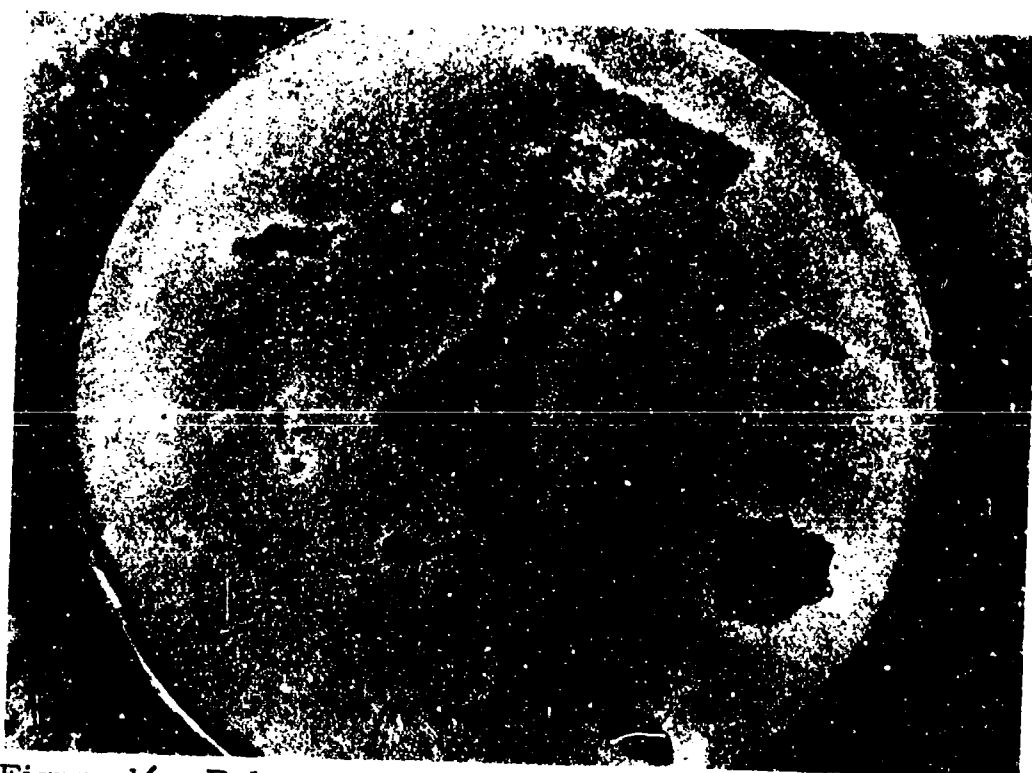
Figure 16.   Polycrystalline Sample—CO/CO_2 Surface (X 70)
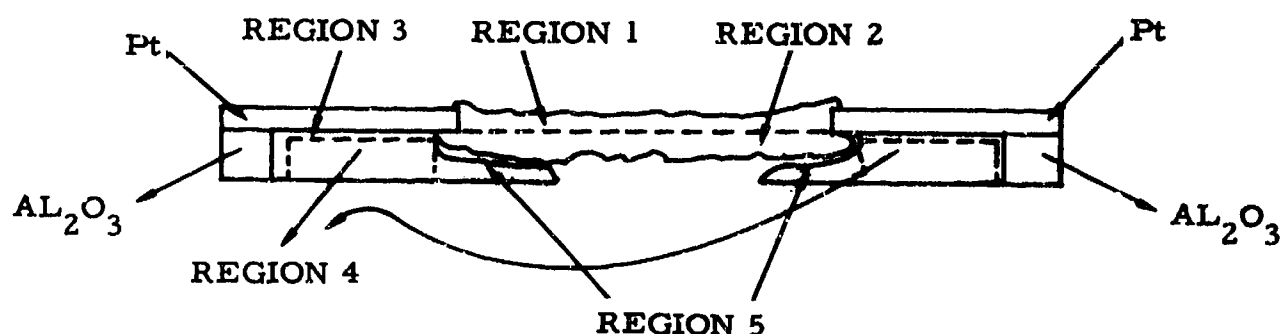
Figure 17. Sketch Depicting Various Regions
of Diffusion Results

The dynamics of the diffusion and regrowth is considered to
take place as follows. The polycrystalline sample is impervious to
gaseous flow. However, a 5.8 percent void volume is present. The
CO/CO_2 surface is not microscopically flat due to the intersection of
voids. This microscopically uneven surface approaches non-stoichio-
metric equilibrium with the CO/CO_2 atmosphere. Consider Figure 18
depicting the upper surface with intersecting voids.

Iso-nonstoichiometric concentration lines (INCL) are
depicted by the dashed lines in Figure 18. A microcrystal such as A
in Figure 18 will tend towards a uniform nonstoichiometric concentra-
tion because of the solid gas reaction on all of its surfaces. However,
the nonstoichiometric gradients are causing diffusion of the imperfection
specie. Therefore, the iso-nonstoichiometric concentration lines would
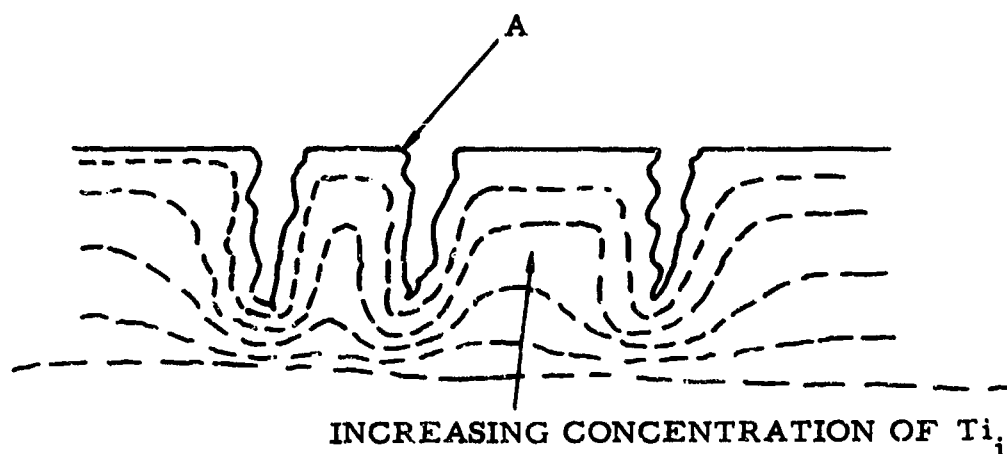
Figure 18. Iso-Nonstoichiometric Concentration
Lines

be separated by greater distances near the actual macroscopic surface.
The INCL's would tend toward a straight line in the interior of the
sample. The INCL's would be closer together in the region just below
the lowest point of the surface void. The diffusion of the nonstoichio-
metric species would therefore be greatest in this region. This would
tend to lower and widen the lowest point of the surface void even
further because of removal of unit cells by titanium interstitial
diffusion and evolution of O_2. This process continues reaching new
voids. The widening continues until the Region 5 is separated from
the membrane. At this time, Region 5 is at a uniform nonstoichio-
metric composition and no diffusion occurs. Titanium interstitial con-
centration gradients now exist in Region 2. Consider Figure 19 depicting
the INCL's in a Region 2 with a void.

The INCL's closer to the CO/CO_2 Region 2 surface represent
a higher concentration of titanium interstitials intersecting the void
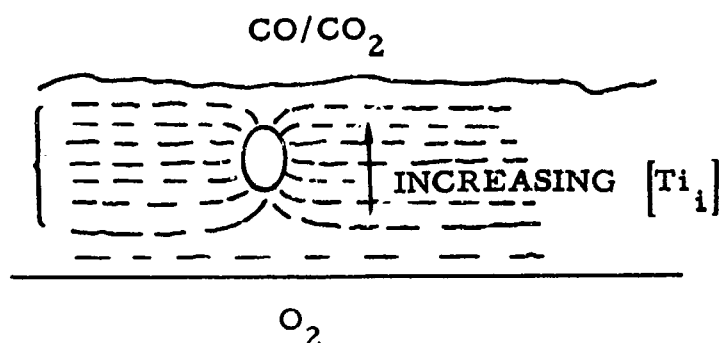
CO/CO$_2$

INCREASING [Ti$_i$]

O$_2$

Figure 19. INCL's in Region 2 With a Void

surface. Equilibrium tends to exist within the void, that is, every portion of the interior void surface, if no concentration gradients exist, would be in equilibrium with the void gas according to the following reaction.

$$TiO_2 \rightleftharpoons Ti_i^{+4} + O_2(g) \tag{107}$$

However, a concentration gradient of Ti$_i$ exists. The upper void surfa e has a higher concentration of Ti$_i$ than the lower void surface. The upper portion of the void surface therefore reacts with the O$_2$(g) within the void driving the reaction from right to left. Therefore, the interior upper surface moves toward the outer O$_2$ gas reservoir. However, since the PO$_2$ within the void is now lowered by this reaction, the lower portion of the void is now supplying the O$_2$ from unit cells on its surface. The entire void therefore moves toward the O$_2$ gas reservoir.

This effect is clearly seen in Figure 13. There are fewer voids near the CO/CO$_2$ reservoir than near the O$_2$ reservoir. Figure 20 is a photograph of Region 1, and the interface with Region 2 under
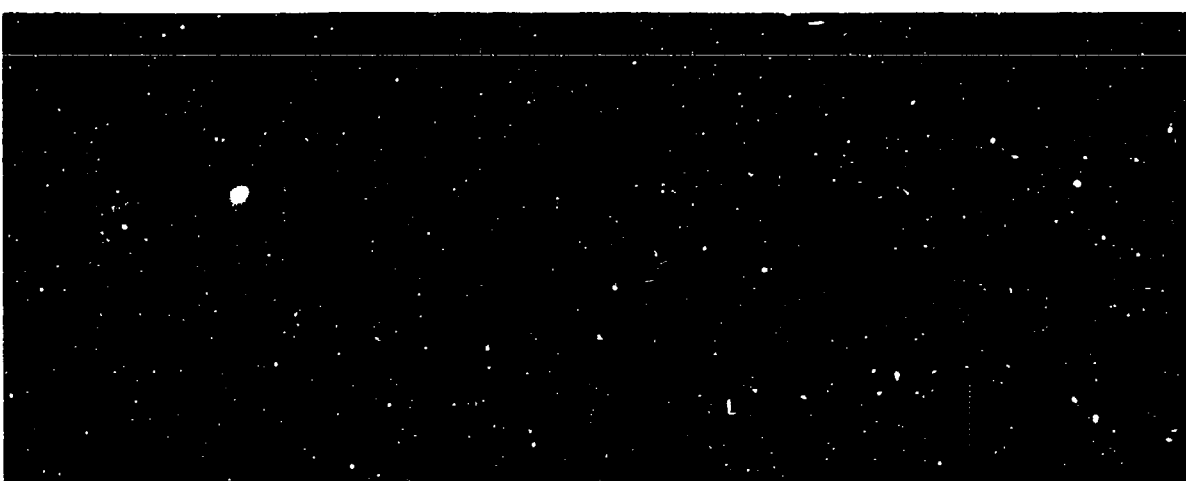
59

Figure 20. Enlarged Cross Section of Figure 12 Under
Varying Illumination Conditions (X 91)

varying illumination. The dynamics at the O_2 surface with the arriving of titanium interstitials is the inverse of what happens on the CO/CO_2 surface. That is, the surface voids fill up first and then crystalline growth continues in Region 1. This line of demarcation between Region 1 and Region 2 is clearly seen in Figures 10, 11, 12 and 20. The interface between Region 1 and Region 2 has microcrystals up to 200 microns across versus an initial 5 to 10 micron particle size.

Region 3 is an area of densification due to titanium interstitials forming unit cells by combining with oxygen available due to leaking seals.

Region 4 has no large defect concentration gradients and this region remains essentially intact.

B. a-Cut Crystals

Single crystal TiO_2 was machined and optically polished (to within 2-4 fringes) to a thickness of 0.61 mm. Ceramic rings were prepared with a thickness 0.000 to 0.005 mm thinner than the TiO_2 disks. The orientation is depicted in Figure 21.

The samples were chemically polished in fuming H_2SO_4 for a minimum of three hours to remove the work hardened surface. CO/CO_2 and O_2 gases were used.
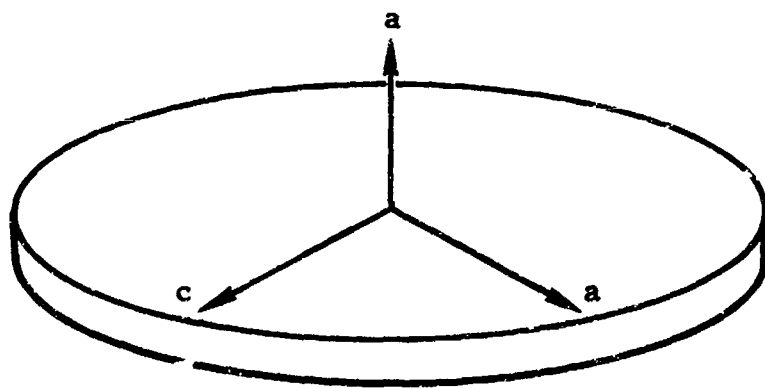

Figure 21. a-Cut Crystal Orientation

61

The results of four samples are shown in Figures 22a, 23a, 24a, and 25a. Figures 22b, 23b, 24b, and 25b are photographs of $O_2(g)$. surface. The samples were run at temperatures of 900 C, 1000 C, 1000 C, and 1100 C for 8, 6, 8 and 6 hours, respectively.

All samples show single crystal regrowth on the O_2 surface. All samples show nonstoichiometric diffusion etching in channels along the c-axis direction on the CO/CO_2 side. The regrowth of Figure 22a was determined by Laue X-ray techniques to be single crystal. Growth layers on this surface are nucleated in many positions and extend in the c-axis direction. The 1000 C samples show a slightly changed surface growth condition resulting in fewer nucleation steps and a smoother surface. This could be due to higher surface mobility and/or more uniform diffusion of titanium interstitials to the surface.

The photograph of the surface in Figure 25b shows lighter regions which proved to be voids between the original O_2 surface and the outer crystal growth. These voids were connected by nonstoichiometric diffusion etch tunnels to the CO/CO_2 surface.

Crystal growth occurred between the Al_2O_3 ceramic ring and the TiO_2 membrane disk as indicated in Figures 22b, 23b, 24b, and 25b. In general, this growth was more predominant along arcs of the outer perimeter that could be connected to the center exposed portion of the crystal by lines parallel to the c-axis. The interface at the Al_2O_3 ceramic ring was reddish in color indicating iron impurities. More will be said about this later. The original CO/CO_2 exposed surface showed more nonstoichiometric diffusion etching than those areas originally covered by the platinum seal.

Figure 25 shows very straight nonstoichiometric diffusion etched tunnels (under the partially covered CO/CO_2 surface) in the c-direction that are connected to the lowered center region, and therefore, exposed to the CO/CO_2 gas. Enlarged photographs of this tunneling in this sample are shown in Figures 26, 27 and 28. The tunnels in general have flat interior surfaces (the curvature of the tunnels is caused by a pin cushion effect in the optics). The surfaces are (110) as indicated in Figure 29.
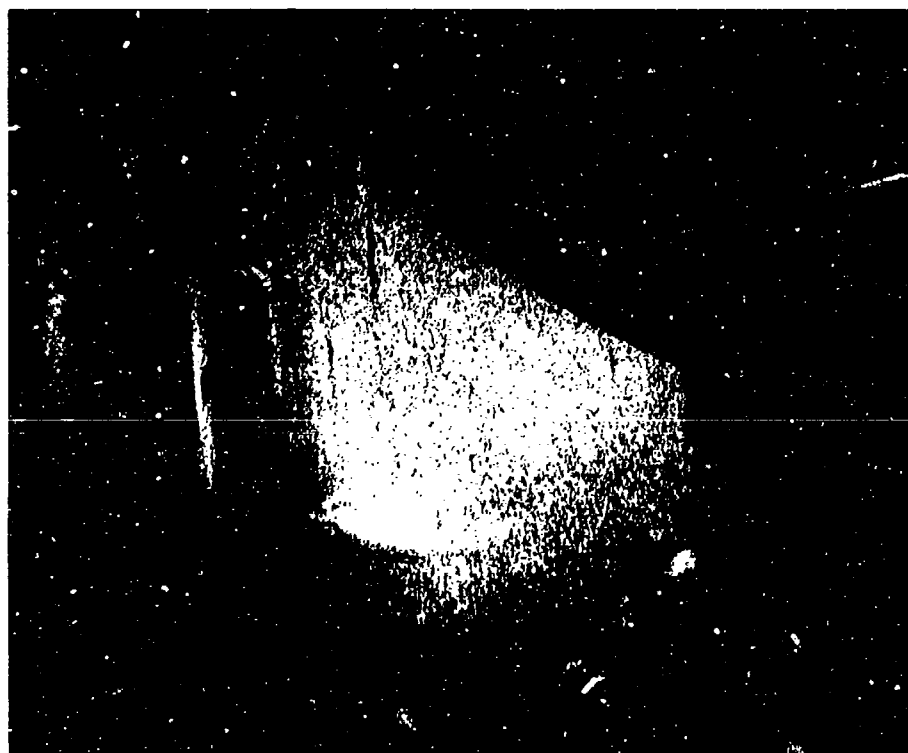
62

Figure 22a. a-Cut Sample O_2 Surface (X 6.0)

Figure 22b. a-Cut Sample CO/CO_2 Surface (X 6.0)

Figure 23a.   a-Cut Sample O_2 Surface (X 7.6)

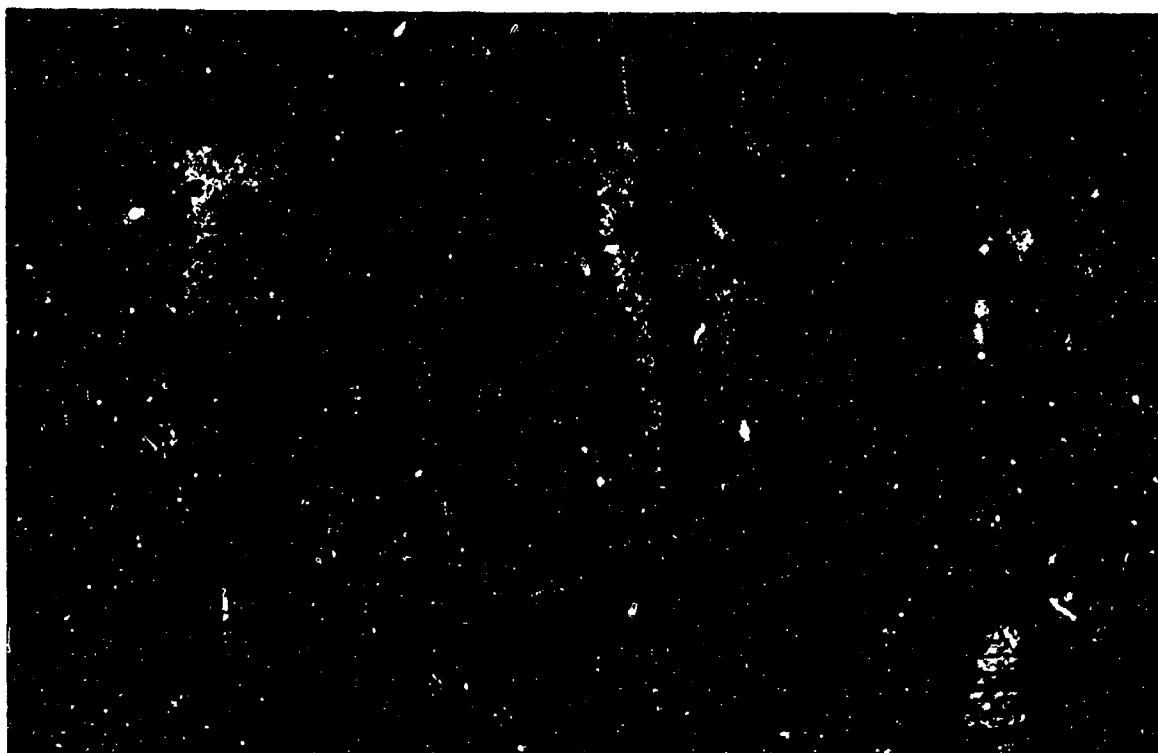Figure 23b.   a-Cut Sample CO/CO_2 Surface (X 5.1)

Figure 24a.   a-Cut Sample O_2 Surface (X 7.1)

Figure 24b.   a-Cut Sample—CO/CO_2 Surface (X 5.1)

65
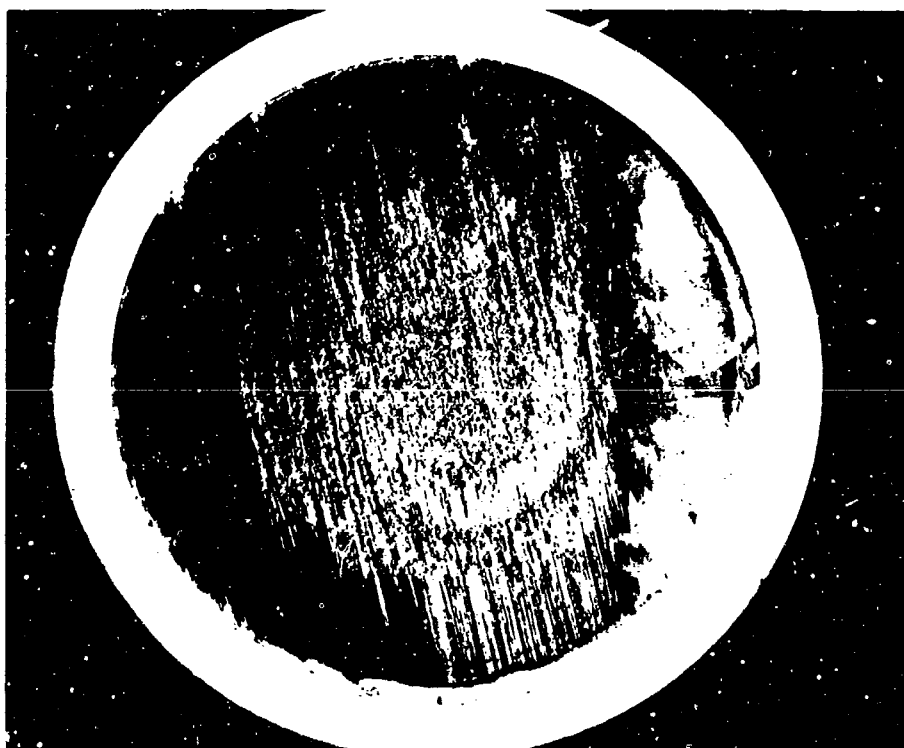
Figure 25a. a-Cut Sample O_2 Surface (X 7.6)

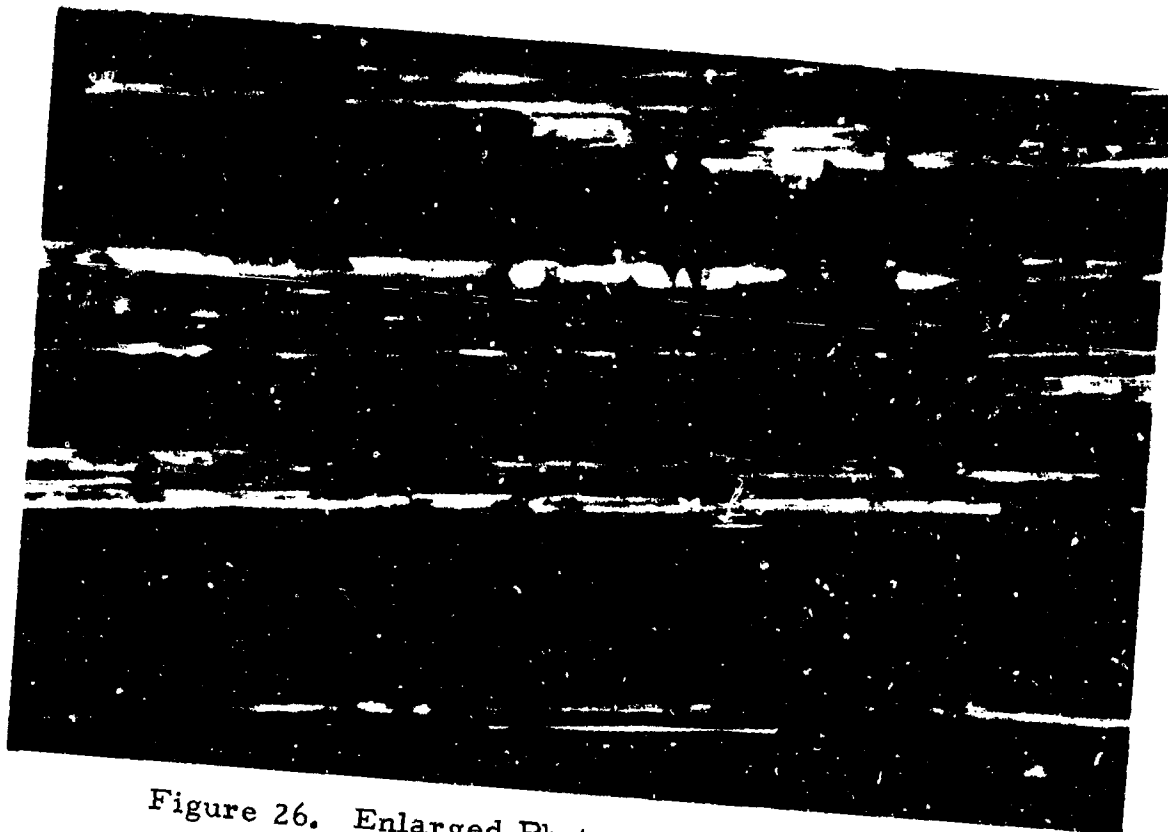Figure 25b. a-Cut Sample CO/CO_2 Surface (X 5.6)

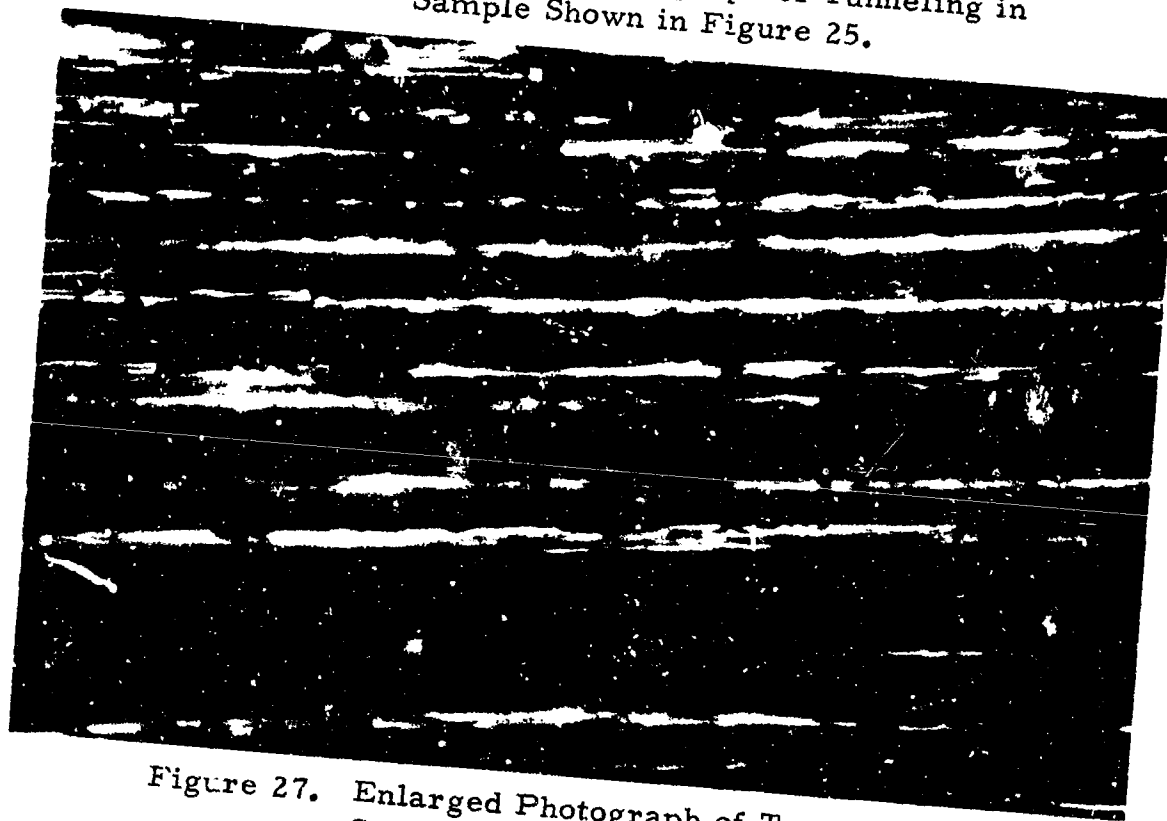Figure 26. Enlarged Photograph of Tunneling in Sample Shown in Figure 25.

Figure 27. Enlarged Photograph of Tunneling in Sample Shown in Figure 25.

67

Figure 28.   Enlarged Photograph of Tunneling
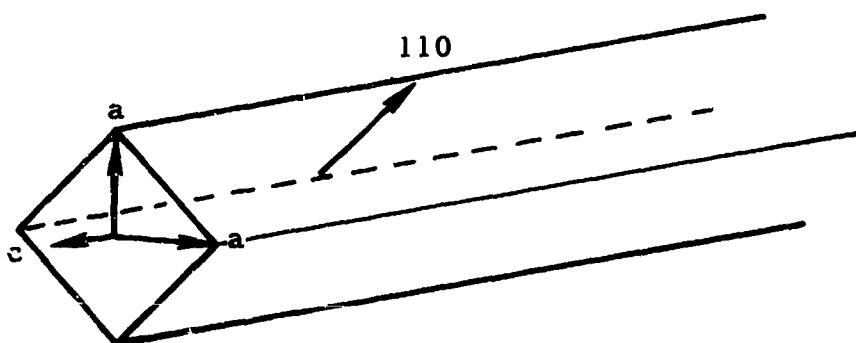of Sample Shown in Figure 25.

Figure 29.   Geometry of Tunnels

The very end of the tunnel seems to be quite flat, having a (001) face and of somewhat smaller area than the tunnel cross-section area. Unusual tunneling was observed as shown in Figure 28 along changing axial directions.

Unusual tunneling sometimes occurred as shown by a very randomly oriented tunnel as shown in Figure 30. From the size and circular cross shape of this tunnel, it is apparently a nonstoichiometric diffusion etching of a screw dislocation. Tunnels similar to this have been observed to change their cross-sectional shape from circular to straight rectangular tunnels and then back to ever changing circular tunnels again. This is probably due to the dislocation changing from screw to edge to screw.

Great care had to be exercised during cross-sectioning and polishing to prevent further fracture of the samples. Typical cross cross-sectioning is shown in Figures 31 and 32 of the sample shown in Figure 24a and 24b. The regrowth region has grown above the 0.248 mm thick platinum marker. This sample was diffused at 1000 C for eight hours.

The sample shown in Figure 23a and 23b fractured in the process of sectioning but the fracture surface revealed a very interesting marker of the regrowth region. The fracture shows an interface line between the original surface and the regrowth region. This is indicated by arrows in Figure 33. This line does not continue across the entire fracture surface, indicating that regrowth is in regions of an integral extension of the crystal. This edge was tipped slightly and the optics focused deeper so that the nonstoichiometric diffusion etching is revealed. This is shown in Figure 34.

This etching is in the a-axis direction so that temperature differences produce different etching tunnels. The surface etching is along grooves in the c-axis direction to some interior layer and then become a-axis tunnels. The a-axis tunnels are not as straight and uniform in direction as the c-axis tunnels.

The cross-section of the 1100 C sample of Figure 25a and Figure 25b is shown in Figures 35 and 36. The original interface is indicated by the arrows. Heavy nonstoichiometric diffusion etching as expected by the higher temperature is apparent.

69
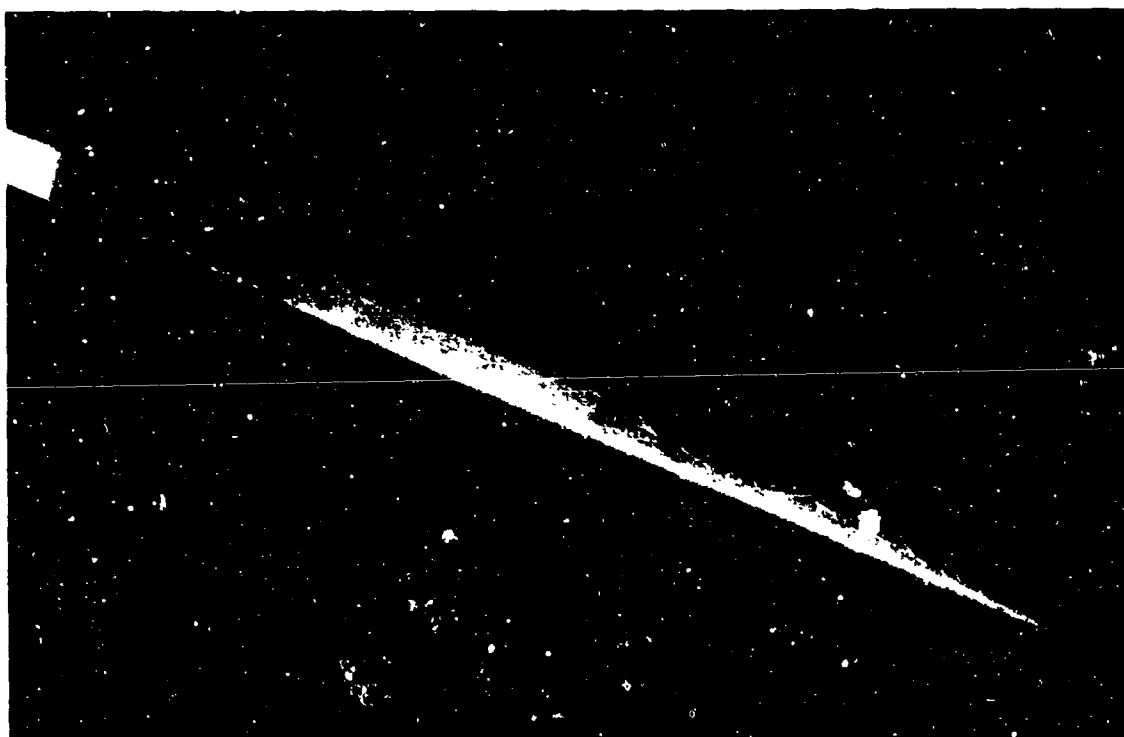
Figure 30. Randomly Oriented Tunnel.

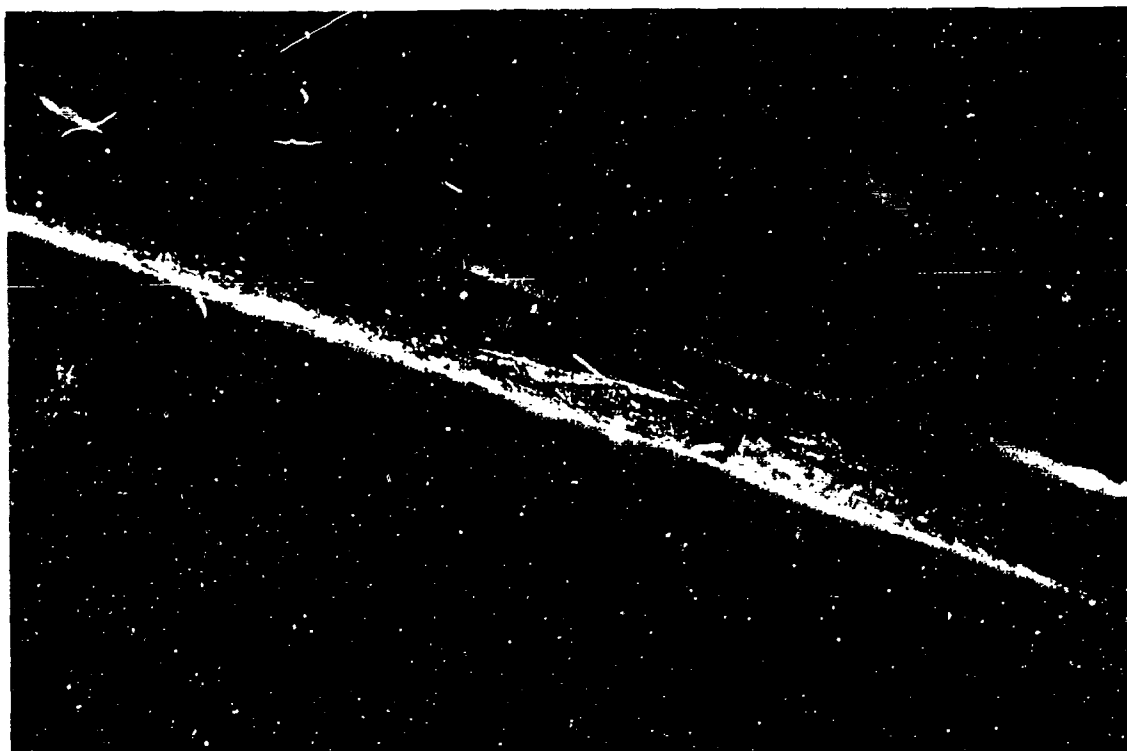Figure 31. Cross Section of Sample Shown in Figure 24.

70

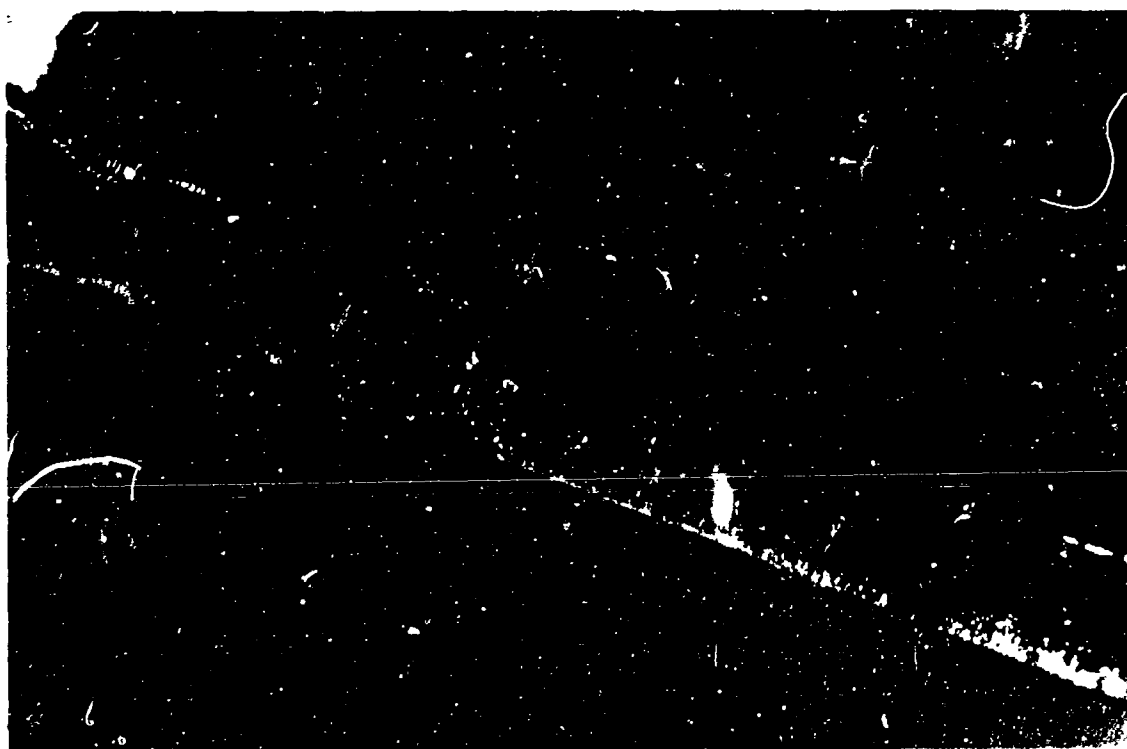Figure 32. Cross Section of Sample Shown in Figure 24 (X 15.2).

Figure 33. Cross Section of Sample Shown in Figure 23 (X 23).
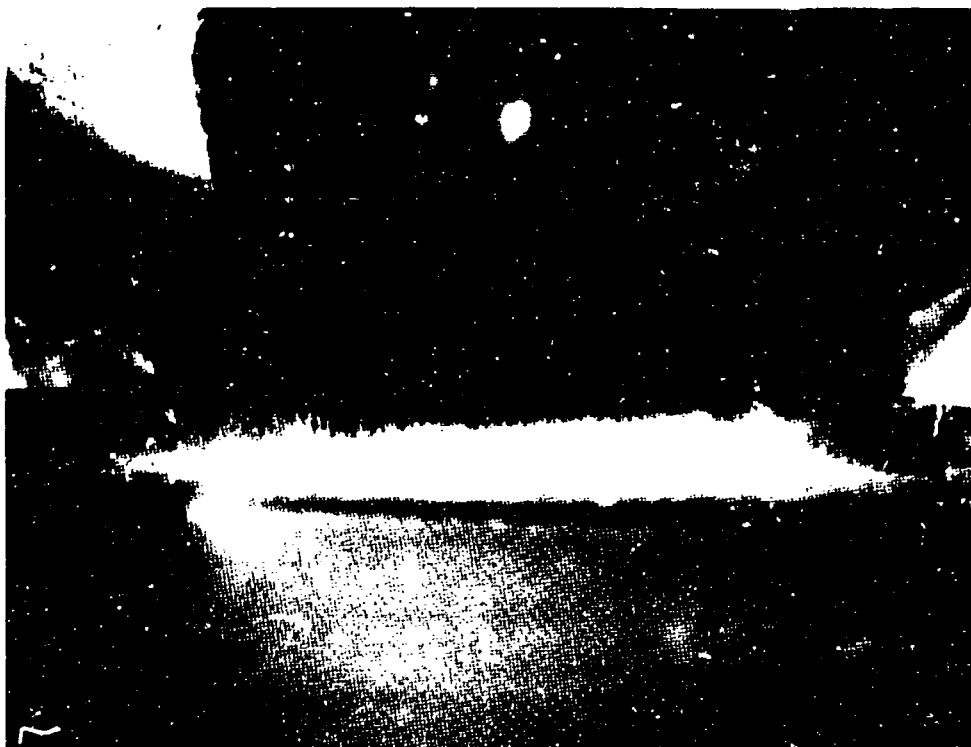
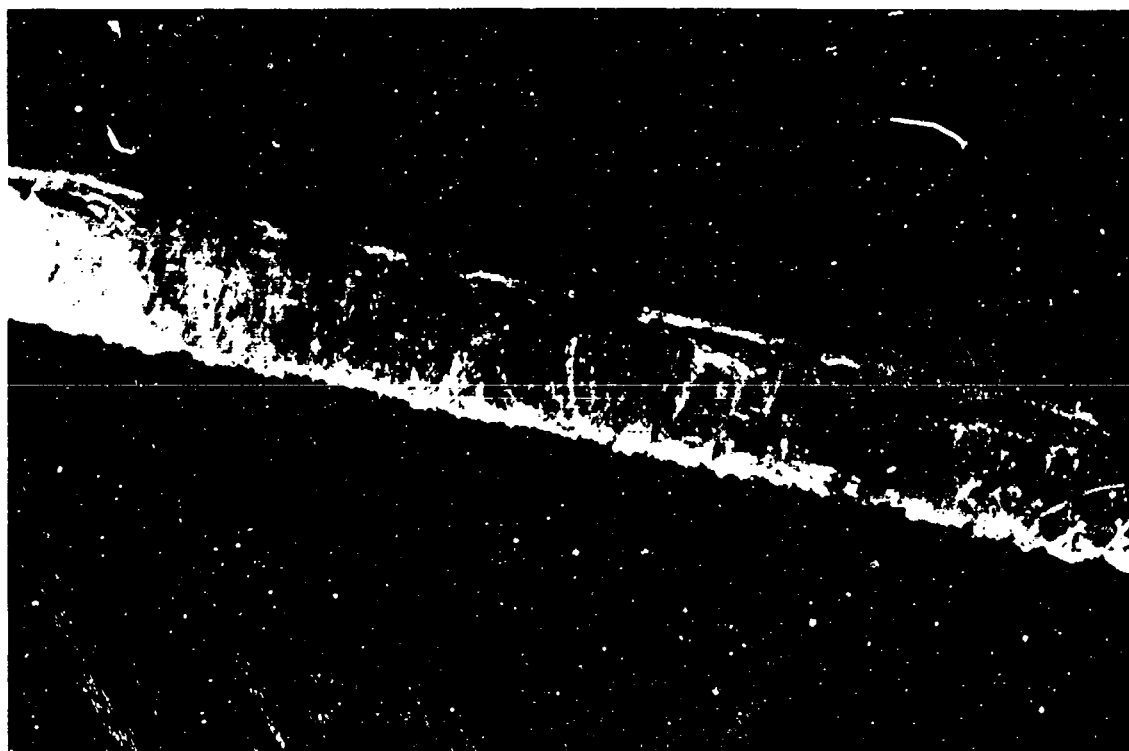Figure 34. Cross Section of Sample Shown in Figure 23 (X 12.3).

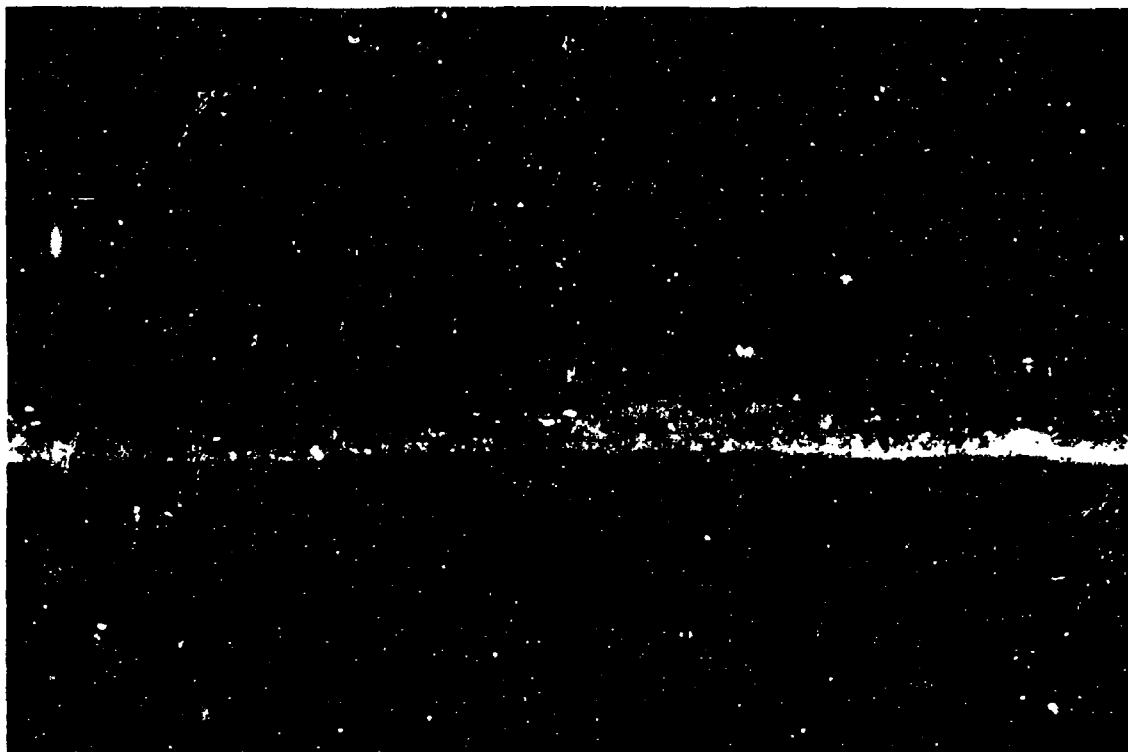Figure 35. Cross Section of Sample Shown in Figure 25 (X 20.1).

Figure 36. Cross Section of Sample Shown in Figure 25 (X 20.1).

C. c-AXIS CRYSTALS

The crystals were oriented by X-ray techniques, machined and polished flat to within 2 to 4 fringes. The crystal membranes were oriented as shown in Figure 37.

The (001) crystal disk experiments were performed early in the program. The initial run was performed in one atmosphere of CO and one atmosphere of O_2 at 1150C for 96 hours on a 1-mm thick sample. The exposed region of the crystal showed regrowth to a distance 1.5mm below the original O_2 surface. Portions of the original CO exposed surface remained at the original level. Non-stoichiometric diffusion etching permeated the entire exposed region so that the sample was pervious to gas flow. X-ray analysis showed the crystallographic orientation to be predominantly c-axis. The sample showed a profusion of flat ribbon whiskers and circular whiskers.

The time and temperature was then reduced and Figures 38 and 39 are the result of a 1-mm sample exposed to CO and O_2 atmospheres for 23.5 hours at 962C. As in all cases, the O_2 platinum seal is "bonded" to the sample and fracture of the original surface occurs when removal is attempted. Figure 40 shows a polished cross-section of this sample. This sample was not chemically etched in fuming H_2SO_4 and large areas of the exposed surface remain intact as indicated in Figure 39. The area under the platinum seal is attacked, however, and the greater portion of the titanium interstitial diffused from this region. Figure 40 shows a polished cross section of this sample showing variations in the nonstoichiometric diffusion etching.
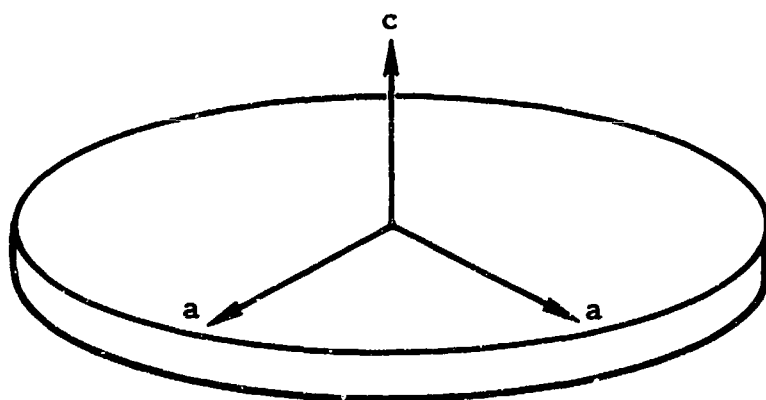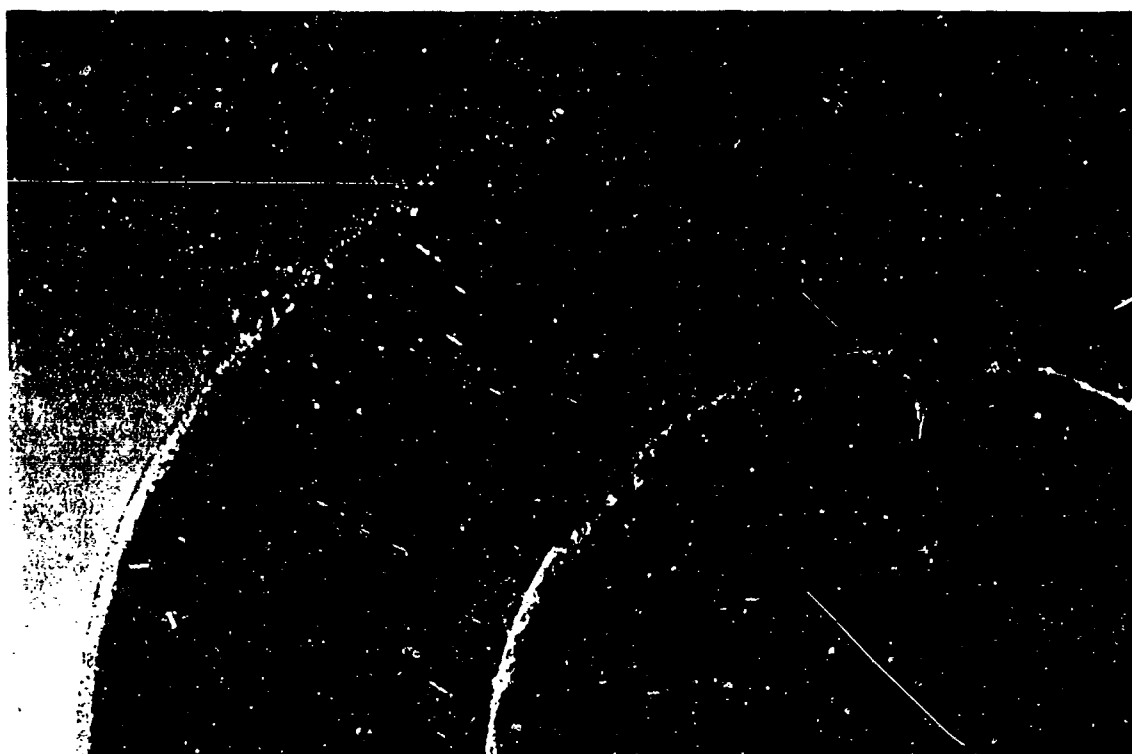

Figure 37. c-Axis Orientation

Figure 38. c-Axis Sample — No Chemical
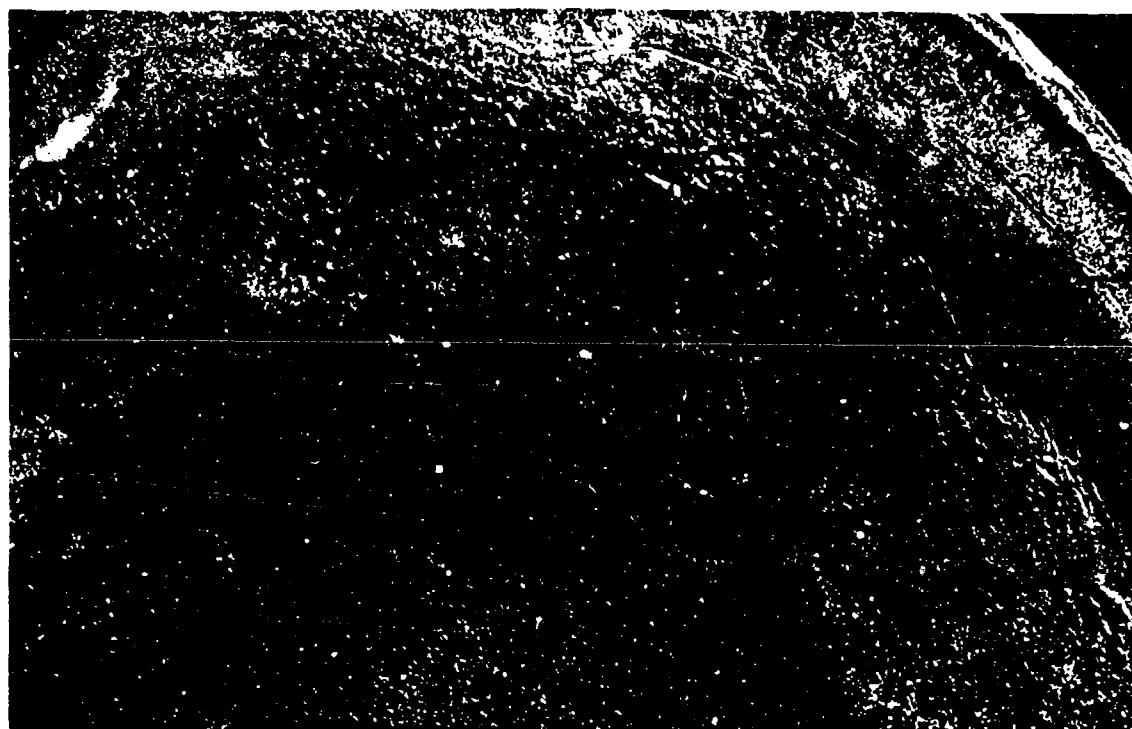Pre-etching O_2 Surface (X 7. 75)

Figure 39. c-Axis Sample — No Chemical
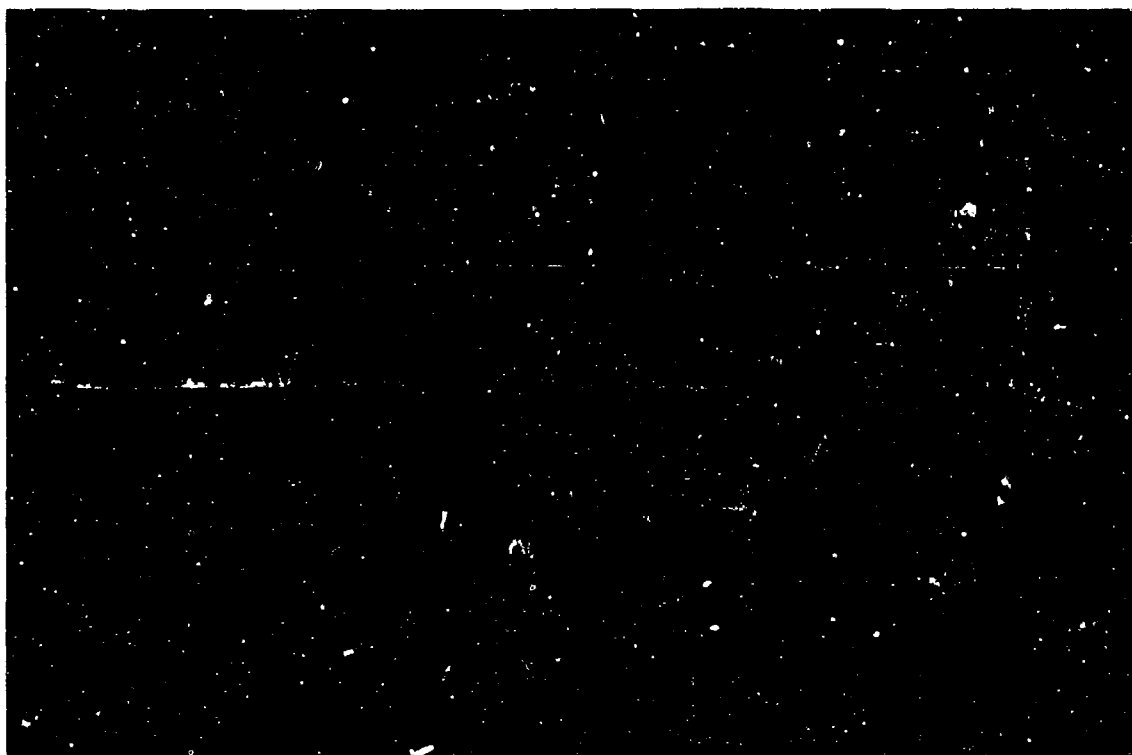Pre-etching CO Surface (X 7. 75)

Figure 40. Nonstoichiometric Diffusion Etching
and Regrowth (X 6.7).

An outer ceramic ring was not used in this experiment so
that the crystal grew beyond the original diameter of the circular
membrane. Thus, there was no chance that the crystalline regrowth
occurred by surface diffusion from one surface to the other. The
initial diffusion to the O_2 platinum seal results in some diffusion to
the unexposed O_2 surface. Thus, the region around the inner edge of
the platinum seal on the O_2 side has always shown greater regrowth.
However, as soon as the platinum seals to the TiO_2 disk, the majority
of the diffusion would be volume diffusion. The crescent or circular
shape of the cross-sectional regrowth region is to be expected. The
INCL would be in the form as shown in Figure 41.

Since the INCL's are closer together at Region 1 and
Region 2, the crystal would grow faster due to an increased diffusion
in this region. Thus, the center portion of the crystal more closely
represents the true diffusivity across the sample. However, due to
the nonstoichiometric diffusion etching, the distance across the
sample becomes an unknown. As pointed out in the theoretical section,
a real partial pressure of metal would eliminate this problem and
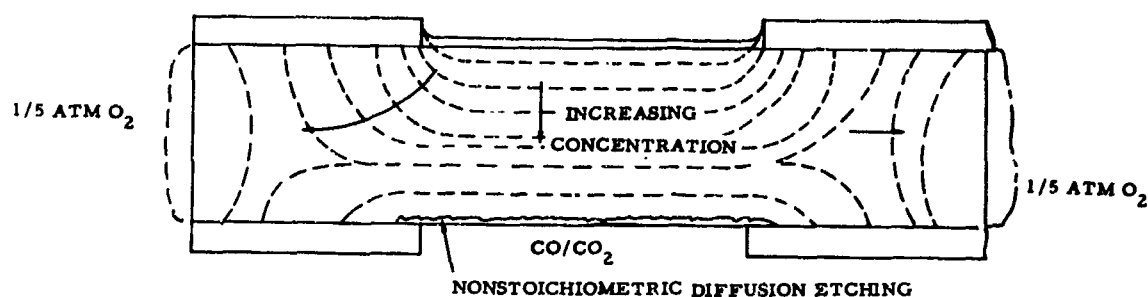nonstoichiometric diffusion parameters could be measured.

1/5 ATM O₂ ... INCREASING CONCENTRATION ... 1/5 ATM O₂

CO/CO₂

NONSTOICHIOMETRIC DIFFUSION ETCHING

Figure 41. INCL's in Membrane Cross Section

One c-cut sample was diffused by using a CO atmosphere on one side and a partial pressure of 20 microns O_2 produced by floor pump for 24 hours at 965C. A cross-section of this sample is shown in Figure 42. The growth on the O_2 surface was predominantly single crystal with some polycrystalline formation on the outer layer of the regrowth surface which extended 0.11 mm below the original O_2 surface. The nonstoichiometric diffusion etching was quite uniform to a depth of 0.4 mm to 0.5 mm.

Figures 43 and 44 are cross-sections of a c-cut sample that contained either an aggregate of impurities near the CO surface or the surface had some foreign object which enhanced the surface reaction rate. The result was a nonstoichiometric diffused tunnel through the membrane which destroys the concentration gradients.

The appearance of a red coloration on all c-axis sample membranes on the outer O_2 surface of the regrowth region suggested iron impurity diffusion. A comparison emission spectographic analysis of material removed from the two surfaces by a diamond tipped tool was performed. The results are shown in Table 5.

77
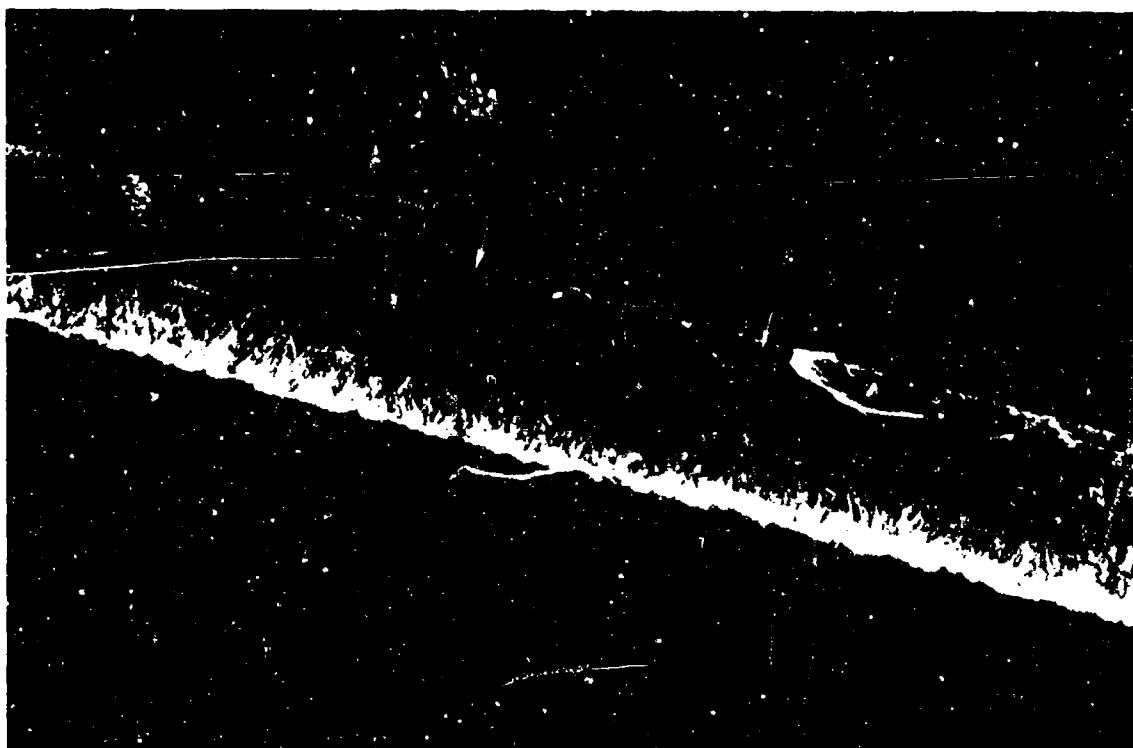
Figure 42. Growth by Using CO and 20 TORR O_2 (X 16.5).
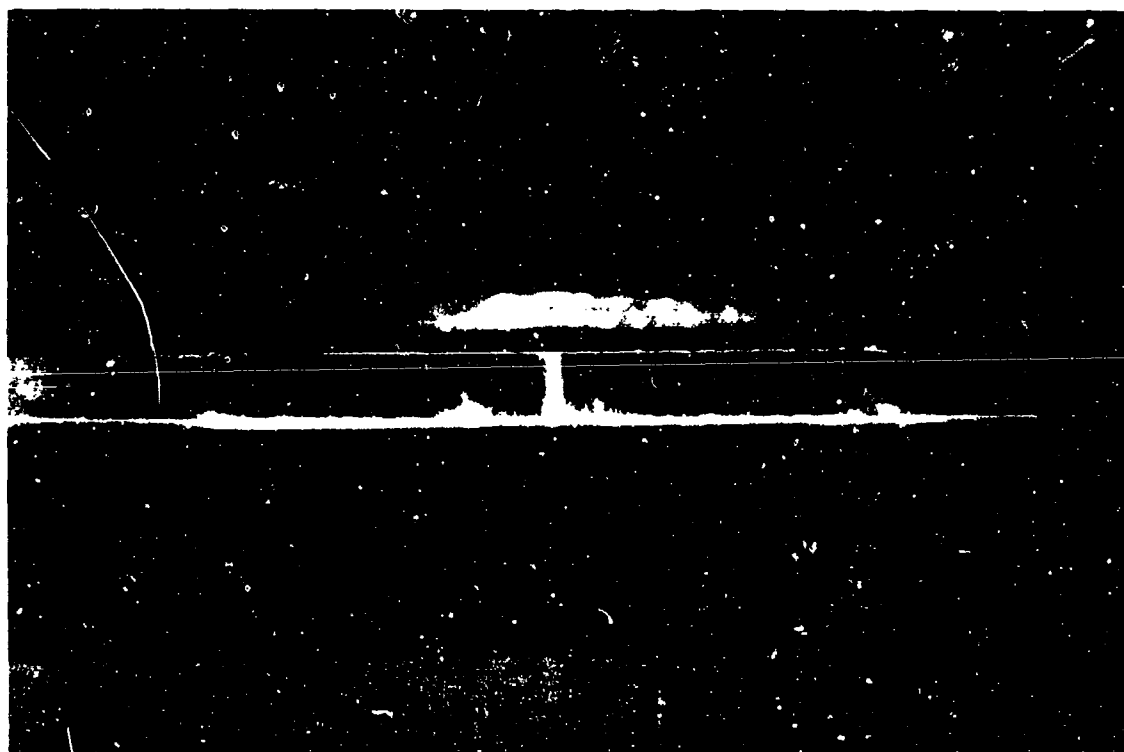
Figure 43. Cross Section of c-Cut Sample Showing
Nonuniform Diffusion Tunnels (X 6.8).
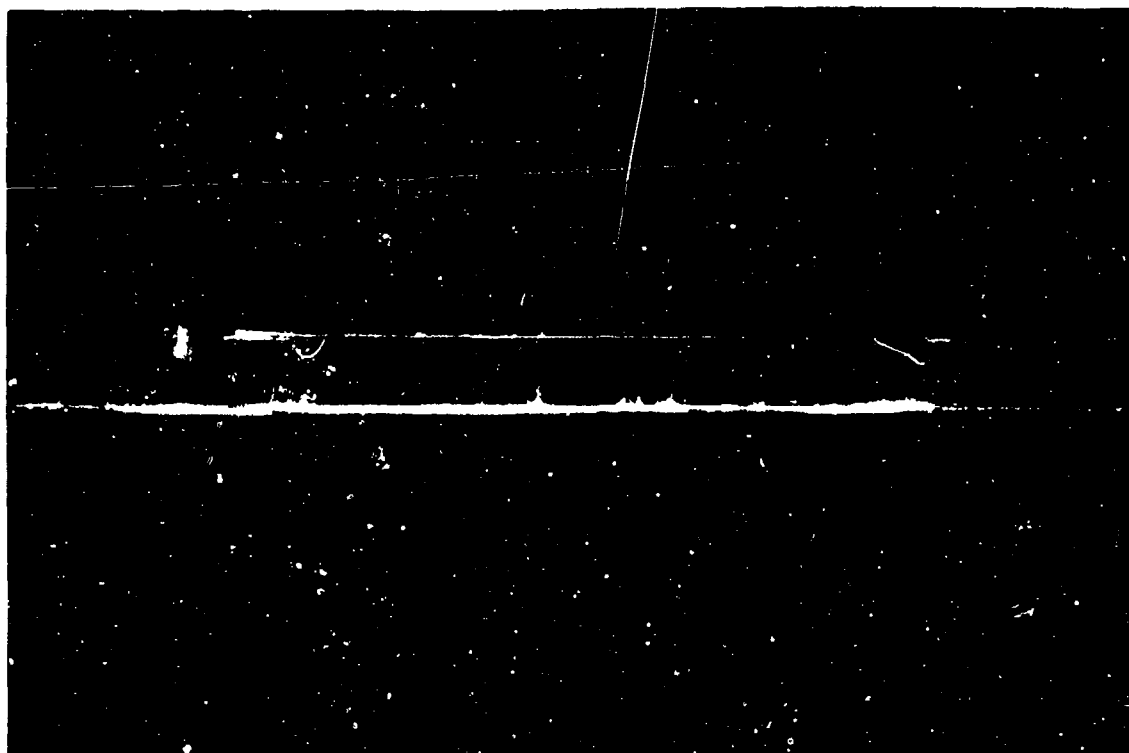
Figure 44. Other Half of Sample Shown in Figure 43 (X 7.1).

Table 5. Emission Spectographic Analysis of Material
Removed From the Two Surfaces

O_2 Surface		CO/CO_2 Surface	
Titanium - Major		Titanium - Major	
	%		%
Aluminum	>0.001 - <0.01	Aluminum	>0.001 - <0.01
Copper	>0.0001 - <0.001	Copper	>0.0001 - <0.001
Calcium	>0.0001 - <0.001	Calcium	>0.0001 - <0.001
Iron	>0.0005 - <0.005	Not detected	
Silver	>0.0001 - <0.001	Not detected	
Magnesium	>0.0002 - <0.002	Not detected	

No other metals detected.

79

Iron, silver and magnesium are thus removed from the crystal due to the titanium interstitial gradients. Cu, Ca and Al however, did not diffuse to the O_2 surface. By the argument presented in the theoretical section this strongly suggests that Fe, Ag and Mg are interstitial foreign impurities, whereas, Cu, Ca, and Al reside in substitutional positions.

The previous spectrographic analysis led to the conclusion that Fe, Ag, and Mg were interstitial. As an additional check to see if this diffusion was indeed occurring, a small amount of iron oxide was placed on the low partial pressure oxygen surface.
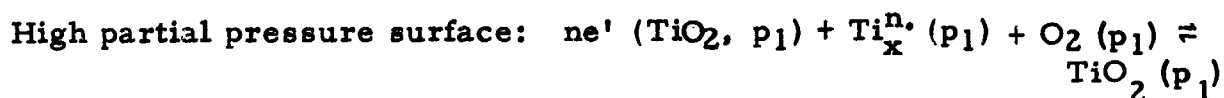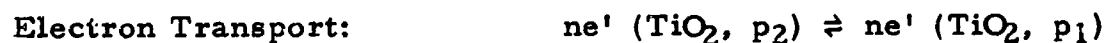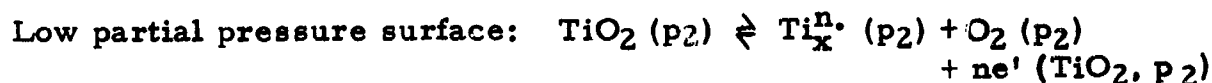
The entire process of nonstoichiometric diffusion is equivalent to the transport of oxygen across the membrane regardless of the nature of the defect. The steps are as follows:

Low partial pressure surface: $\quad TiO_2 (p_2) \rightleftharpoons Ti_x^{n\cdot} (p_2) + O_2 (p_2)$
$$+ ne' (TiO_2, p_2)$$

Volume Diffusion: $\quad Ti_x^{n\cdot} (p_2) \rightleftharpoons Ti_x^{n\cdot} (p_1)$

Electron Transport: $\quad ne' (TiO_2, p_2) \rightleftharpoons ne' (TiO_2, p_1)$

High partial pressure surface: $\quad ne' (TiO_2, p_1) + Ti_x^{n\cdot} (p_1) + O_2 (p_1) \rightleftharpoons$
$$TiO_2 (p_1)$$

Net Process: $\quad TiO_2 (p_2) + O_2 (p_1) \rightleftharpoons TiO_2 (p_1) + O_2 (p_1)$

where Ti_x^n can represent either $Ti_{Ti}^{n\cdot}$ or $Ti_i^{n\cdot}$. In the first case diffusion would occur by vacancies in the titanium sublattice and in the second case by titanium interstitials. For the net process, the free energy change is

$$\Delta F = RT \ln \frac{p_2}{p_1} + RT \ln \frac{a\{TiO_2 (p_1)\}}{a\{TiO_2 (p_2)\}} \qquad (108)$$

where a represents the activity. Unless defect-defect interactions lead to a large change in the activities, the first term in the above equation is much greater than the second. (Note: Therefore, galvanic cell measurements would not separate these parts of ΔF; and therefore,

no information can be gleaned from classical thermodynamics about the defect structure. Thus, atomic details have to be assumed to determine the nature of the defect as was done in the theoretical section.)

If foreign metallic oxides were present on the low pressure surface, an identical set of transport equations could be written with Fe_3O_4 in place of the TiO_2, if the same iron oxide was formed on the high partial pressure oxygen surface.

However, as always, atomic details are outside the realm of classical thermodynamics. If the iron atoms become interstitial impurities the diffusion should be rapid (assuming Fe_i^{3+} -free energy of motion low), the iron should become interstitial first and then the titanium ions next $(\Delta F_{Fe_3O_4} > \Delta F_{TiO_2})$; thus the iron should be transported to the high partial pressure first. This would be determined by a short diffusion experiment. Also, since iron oxide produces a red color on the surface, it should serve as an indirect check for volume diffusion and surface mobility.

The results of this diffusion are shown in Figures 45 and 46 which are photographs of the high partial pressure O_2 surface and the low partial pressure O_2 surface after diffusion.

The diffusion took place at 1050C for one-half hour under a CO/CO_2 ratio of one and one atm of O_2. The corresponding areas on the two surfaces are circled. A pit is produced on the low partial pressure surface opposite the deposition of iron oxide and some growth of TiO_2 on the high partial pressure surface. The smaller of the two circled areas indicates that even at low concentration of foreign impurities bulk diffusion of both Ti and Fe took place. In the larger of the two areas, iron titanate may have been formed because of the large iron concentration which could lead to other possibilities. Thus it is evident that volume diffusion of both the Fe and Ti did occur. Notice that the remainder of the surface did not show appreciable growth in this short diffusion time experiment .

1. Nonstoichiometric Diffusion Using H_2/H_2O Gas

The nonstoichiometry produced by hydrogen reducing gases occurs at lower temperatures and is believed to form an O-H bond with an O_o. This could have an effect upon the diffusion of Ti_i by lowering the concentration gradient because of a large number of H_i.
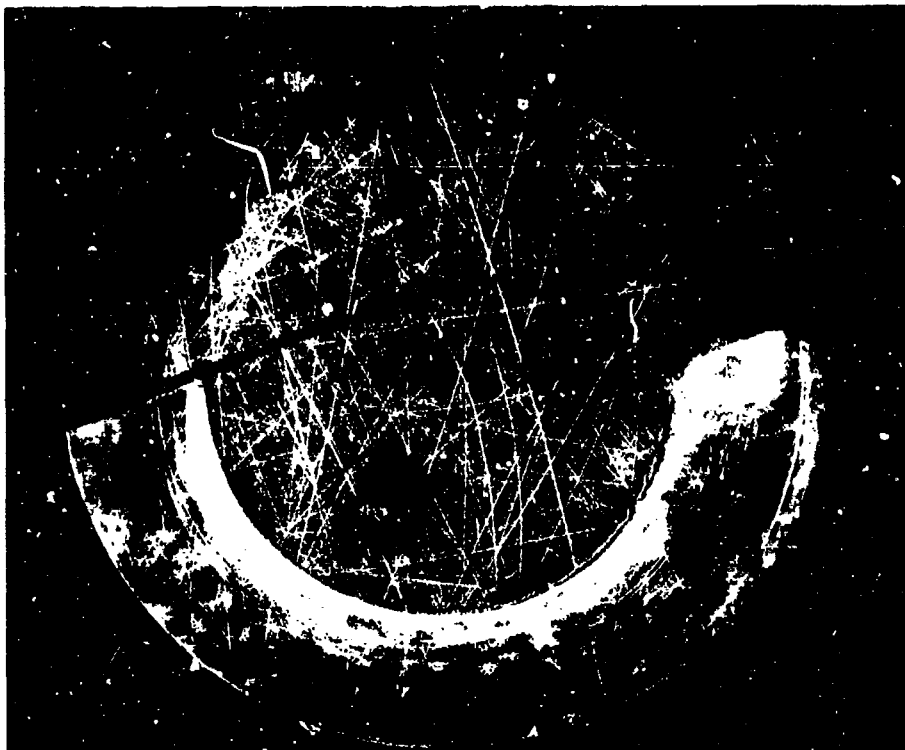
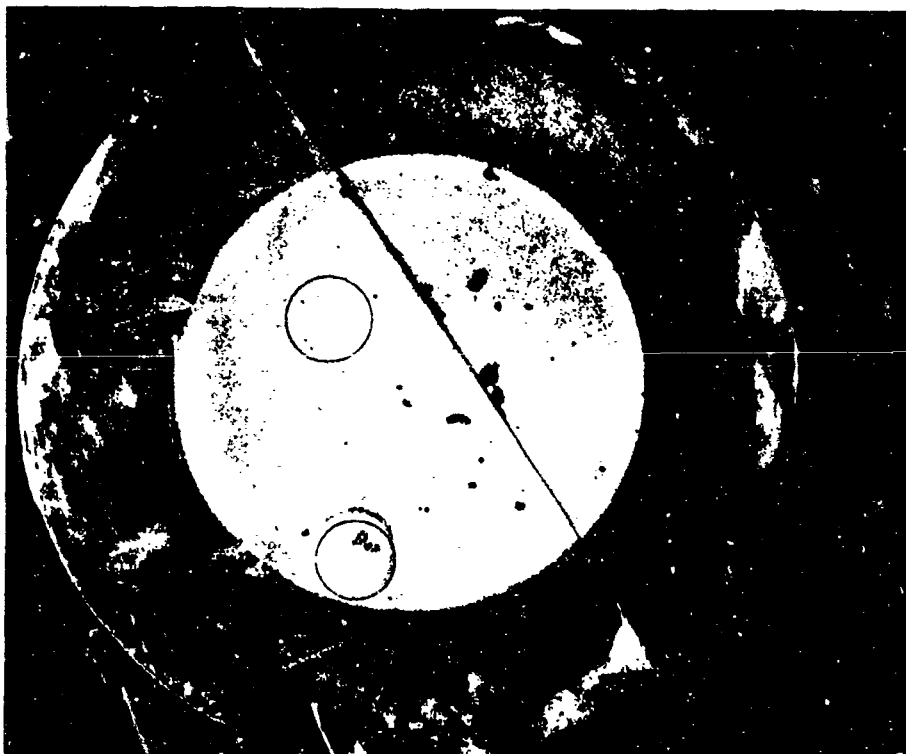Figure 45. O_2 Surface of Fe Diffusion Sample (X 5. 65)

Figure 46.   CO Surface of Fe Diffusion Sample (X 5. 65).

Two experiments were performed using $H_2/H_2O = 10^6$ and O_2 on either side of the c-cut membrane. Figure 47a and 47b show the O_2 and the H_2/H_2O surfaces, respectively. A polished cross-section is shown in Figure 48.

This diffusion was performed at 885C for 4-1/6 hours. The entire character of the diffusion has changed. The production of nonstoichiometric diffusion tunnels did not occur. The surface attack was quite uniform and some crystal growth did occur. However, the amount of "reduction" by $H_2/H_2O = 10^6$ at these temperatures results in a much larger weight loss. This would indicate that the concentration of Ti_i would be even larger. The activation energy for motion of Ti_i is apparently between 0.5 ev and C.75 ev from the CO/CO_2 results. Thus, one would expect a rapid regrowth on the O_2 surface. This author considers that the H_2 reduction leads to H_i and to a reduced concentration of Ti_i with the weight losses only apparent due to loss of T_i from the solid as a result of a gaseous species. Also, the O-H bond would increase the activation energy for diffusion.
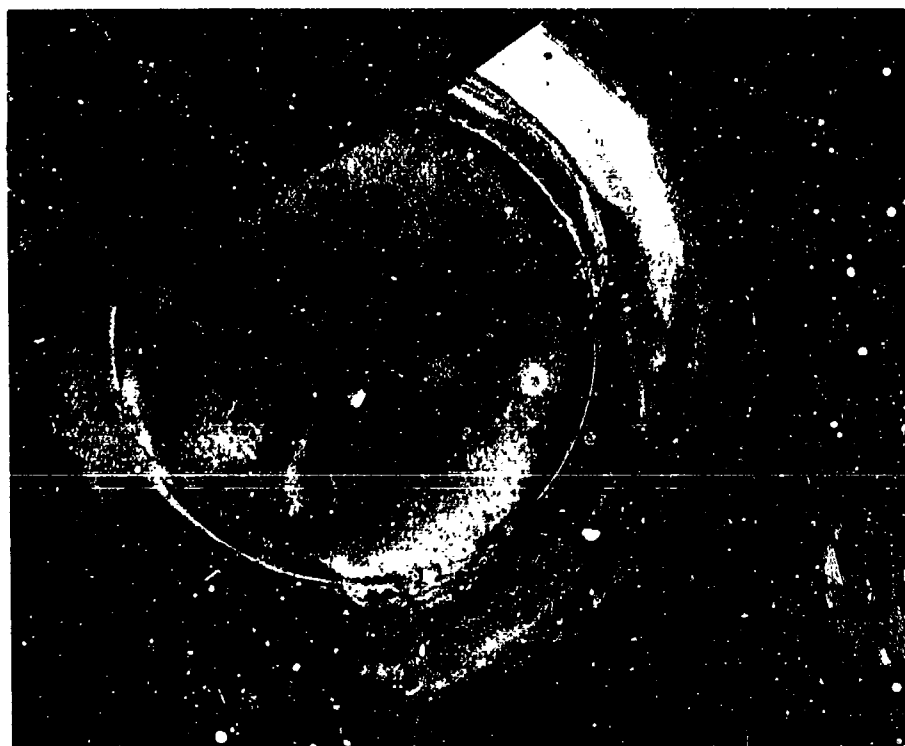

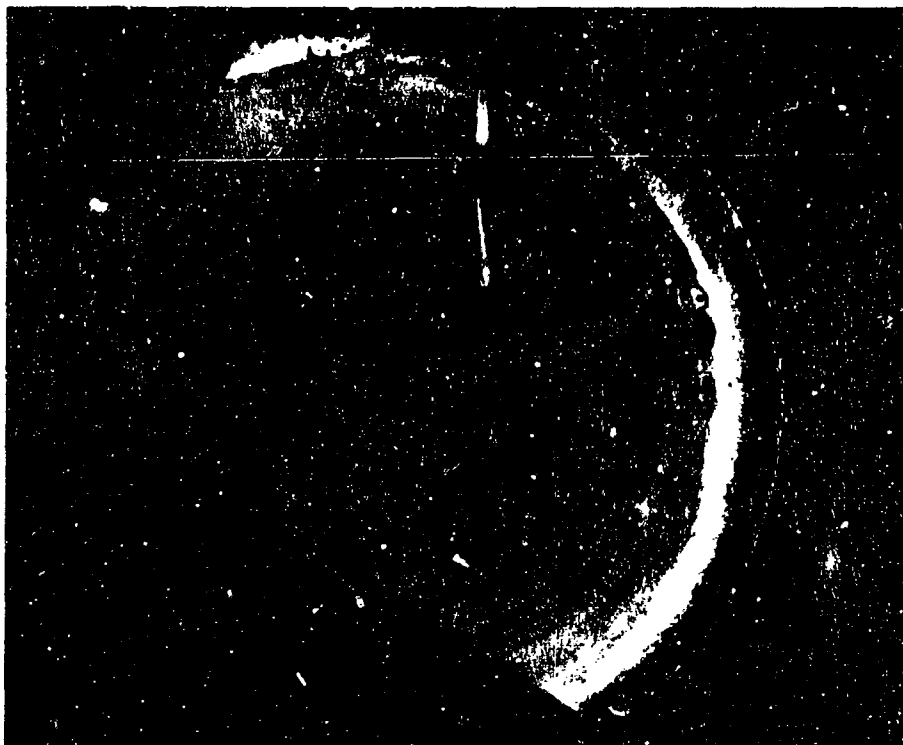Figure 47a. O_2 Surface Using H_2/H_2O and O_2 Gases (X 5.7)

Figure 47b. H_2/H_2O Surface Using H_2/H_2O and O_2 Gases (X 5.7)
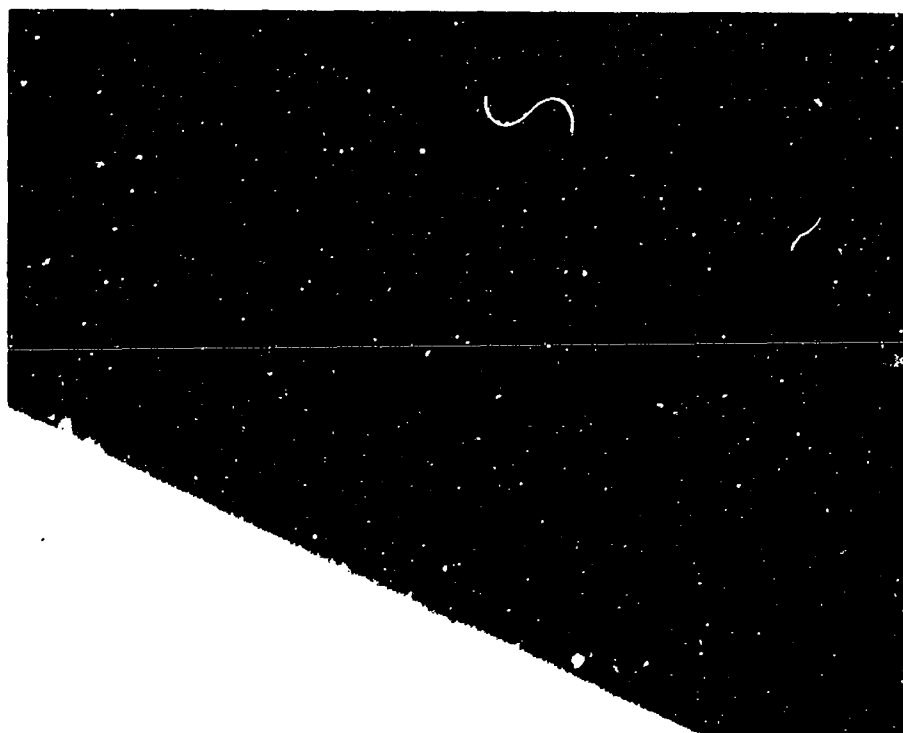

Figure 48. Cross Section of Sample Shown in Figure 47 (X 72)

The hydrogen atom would be in a void position that would reduce the fraction of interstitials sites available for forward diffusion jumps.

2. Loss of Weight Data

There have been two previous thermogravimetric studies performed on TiO_2 and published. (Reference 10 and 11.) This portion of the experimental work was performed to see if similar results could be obtained and to determine which gases could be considered interacting and noninteracting, and to see if consistent results could be obtained with different samples cut from a vernuel flame fusion grown TiO_2 boule. The TiO_2 boules are known to have considerable impurities and a variation in impurities with position in the boule.

The initial experiments were performed with argon gas having the following impurities

$$N_2 \longrightarrow 5 \text{ ppm.}$$
$$O_2 \longrightarrow 5 \text{ ppm.}$$
$$H_2 \longrightarrow 5 \text{ ppm.}$$
$$CO_2 \longrightarrow 1 \text{ ppm.}$$
$$\text{Hydrocarbons} \longrightarrow <1 \text{ ppm.}$$

If one excludes the hydrocarbons the partial pressure of oxygen is approximately 2.5×10^{-6} mm. Hg. the equivalent percent loss of oxygen which would result in either oxygen vacancies or titanium interstitials. The data was quite scattered as indicated in Table 6 .

Table 6. Reduction Data

Temp	Equivalent percent loss of oxygen.
872	0.00025
1084	0.00799
1086	0.00175
1179	0.00234
1249	0.0140
1258	0.0132
1275	0.0262

The two samples at 1084C and 1086C gave very widely scattered results indicating that the number of samples necessary to yield a 95 percent confidence limit would be considerable. The results at 1249C and 1258C were more consistent than the 1085C samples. An increase in temperature did show an increase in reduction in spite of the wide scatter.

Two samples were reduced in a vacuum of 10^{-6} mm Hg. at 1179C and 1275C. The results are shown in Table 7.

Table 7. Vacuum Reduction

Temp	Equivalent percent loss of oxygen.
1179C	0.0325%
1275C	0.0357%

One sample was reduced in H_2 at 745C resulting in 2.12 percent loss of oxygen.

Three samples were reduced in CO and are shown in Table 8.

Table 8. CO Reduction

Temp	Equivalent percent loss of oxygen.
786C	0.0357 % loss of oxygen.
1002C	0.307
1002C	0.251

At 1002C the scatter appears quite large showing that many samples would be needed for a 95 percent confidence limit.

3. Calculation of the Diffusivity

The rate of growth can be approximated by the following equation:

$$\frac{dx}{dt} = \Omega D \frac{\Delta c}{\Delta x}$$

where

dx = increases in Δx with time

Ω = unit cell volume of TiO_2

86

$$D = D_o \exp(-\Delta H_m / KT)$$

Δc = concentration on reducing surface

Δx = original thickness of crystal.

This is only a rough calculation for the following reasons:

1. Nonstoichiometric diffusion etching causes an indeterminal variation in Δx and Δc. The variation with time is also unknown.

2. Growth on the O_2 surface is greater at the edges of the platinum seals with local variations in thickness across the O_2 surface.

3. Surface impurities and preparation may impede surface reaction rates so that concentration gradients are less than that expected from equilibrium conditions.

However, an order of magnitude calculation can be made that fits most of the experimental by assuming the following:

1. $\Delta x \approx 0.75$ the original thickness

2. Δc equal to the equilibrium concentration using Kofstead's data on the reduction surface and assuming Ti_i rather than V_o.

3. dx equal to the growth thickness in the center of the O_2 surface.

Using these approximations, the value of D that fits within an order of magnitude is $D = 10^{-5}$ cm^2/sec.

The quenching of the concentration gradient was attempted several times but the nature of the apparatus would not allow quenching from diffusion temperatures to room temperature in less than 20 minutes. The blue color, significant of reduced TiO_2, was never apparent in the CO/CO_2 reduced samples. However, this is not surprising for the activation energy of formation is significantly greater than the activation energy for motion. The production of Ti_i would be reduced greatly with a reduction in temperature but, the diffusion and oxidation of Ti_i on the O_2 surface could still occur. The H_2/H_2O samples, however, had

87

the nonstoichiometric color which would indicate that the activation energy of motion is higher or that the nonstoichiometry is due to O-H bonds.

D. EXPERIMENTAL CONCLUSIONS

This experiment proves the existence of titanium interstitials as a nonstoichiometric species in TiO_2. The concentration of defects varies inversely with oxygen pressure. N-type conductivity exist in nonstoichiometric TiO_2. Therefore, two possibilities exist for the nonstoichiometric specie, i.e., Ti_i or V_o; Ti_i is the only defect of the two that could produce regrowth on the O_2 surface. Any existence of V_o could be determined by the use of a real partial pressure of Ti "gas" on one surface as explained in the theoretical section.

The experimental results show that this experiment can be used as a general tool for the determination of defects using either polycrystalline or single crystal material. The impurity diffusion resulting from a concentration gradient of Ti_i shows that Fe, Ag, and Magnesium are interstitial impurities and that Cu, Ca and AL are substitutional impurities. This correlates with previous results concerning iron impurities (Reference 16) and aluminum impurities (Reference 17).

This experiment results in a new method of revealing dislocations by nonstoichiometric diffusion etching producing tunnels at dislocations.

This experiment results in a new method of producing ~ 100 percent theoretically dense polycrystalline TiO_2.

This experiment reveals the difference between interacting (H_2/H_2O) and noninteracting (CO/CO_2) reduction gases.

This experiment shows the influence of surface preparation on the nonstoichiometric diffusion.

E. GENERAL CONCLUSIONS

A new experimental tool, which relies only on unquestionable fundamental assumptions, has been derived theoretically that will determine the nature of the nonstoichiometric defect in a single experiment.

A new method of crystal growth termed endotaxy has been described which could produce single crystals of high purity.

A new method of reducing the number of edge dislocations has been explained in metal-metalloid systems.

A new method of increasing the density of polycrystalline material has been explained and demonstrated.

If interstitialcy diffusion does not occur this experiment amounts to a new experimenta tool to prove that foreign atoms are either in substitutional positions or interstitial positions if the native imperfection is a metal interstitial.

New purification techniques by a membrane experiment h. been explained.

V RECOMMENDATIONS

This experimental and theoretical study has a wide range of applications as indicated in the following table.

Field	Reason
Solid State Physics	Determination of the types of native defect in metal-metalloid systems. Determination of the nature and type of foreign atom impurities. Production of high purity low-dislocation density crystals for the intrinsic study of metal-metalloid systems. Insight into the cohesive properties of crystals. New diffusion studies possible.
Chemistry	Theoretical implications for crystal growth. Surface properties of crystals. Gas-solid reactions and equilibrium constants.
Metallurgy	Oxidation and tarnishing reactions on metals. Defect studies in order alloys.
Ceramics	Production of high density polycrystalline ceramics. Defect studies in oxides.
Electrical Engineering	New p-n, p-i-n, and perhaps tunnel diodes. High quality sensors. Relation between nature of defect and electrical properties.

The USAF, the DOD, and the scientific community in general have many interests and needs which this theoretical and experimental work may fulfill. For example, the cost in time and money of determining the nature of defects can now be decreased. Nevertheless, the quality of the defect information has increased with additional knowledge gained for each crystal system.

The next program is strongly recommended to be a program to classify the native imperfections in metal-metalloid crystals according to their atomic species and crystalline structure. Either polycrystalline or single crystal samples can be used. The more important oxides and sulfides should be determined first.

From this study important facts can be determined for use in the fields of chemistry, metallurgy, ceramics, electrical engineering and other aspects of solid state physics. The second program is strongly recommended to be a study of endotaxial growth using metal partial pressures. This study would determine the quality and extent of endotaxy.

The third program should be a determination of the equilibrium constants which will yield an accurate description of the native imperfection concentrations. The method of separation of D and C by Rosenburg's techniques are recommended. (Reference 17.)

The applications in the fields of electrical engineering, metallurgy, and ceramics will unfold as the above programs are in progress. A theoretical investigation should be instigated to study the applicability of these experimental techniques to all ordered systems, e.g., the metal-metal ordered alloys.

REFERENCES

1. Grant, F. A.,"Properties of Rutile," Rev. of Mod. Phys. 31, 646, 1959

2. Grant, F. A., "Properties of Rutile," National Bureau of Standards Report Project No. 0900-11-4475, 1959

3. Hannay, N. B. "Semiconductors" Rheinhold Publishing Co., Chapter 14, New York, 1959

4. Kroger, F. A., "Chemistry of Imperfect Crystals," John Wiley and Sons, New York, 1962

5. Swalm, R. A., "Thermodynamics of Solids,"John Wiley and Sons, New York, 1962

6. Read, W. T., Jr., "Dislocations on Crystals," McGraw Hill, Inc., New York, 1953

7. Shewmon, P., "Diffusion in Solids," McGraw Hill, Inc., New York, 1963

8. Bardeen, J., Herring, C., "Diffusion in Alloys and the Kirkendall Effect, Atom Movements," American Society Metals, Cleveland, Ohio, p. 87, 1951

9. Amelinckx, S., "The Direct Observation of Dislocations," Supplement 6, Solid State Physics, Academic Press, New York, 1964

10. Buessem, W. R., Butler, S. R.,"Defects in TiO_2, Kinetics of High Temperature Processes," Kingery, W. D., Editor, p. 13, John Wiley and Sons, Inc., New York, 1959

11. Kofstad, P., "Thermogravimetric Studies of the Defect Structure of Rutile (TiO_2)," J. Phys. Chem. Solids 23, p1579 (1962)

12. Yahia, J., "Dependence of the Electrical Conductivity and Thermoelectric Power of Pure and Aluminum-Doped Rutile on Equilibrium Oxygen Pressure and Temperature," Physical Review, 130, p1711, 1963

13. Haul, R., Just, D. "Sauerstoffdiffusion in Oxyden, Reactivity in Solids, " Elsevier, 1961

REFERENCES (CONT'D)

14. Johnson, O. W., "One-Dimensional Diffusion of Id in Rutile," Phys Rev 136, pA284 1964

15. Von Hippell, H., et al, "Protons, Dipoles and Charge Carriers in Rutile," J. Phys Chem Solids 23, p779, 1962

16. Cronemeyer, D. C., "Infrared Absorption of Reduced Rutile TiO_2 Single Crystals," Phys. Rev. 113, p1222, 1959

17. Rosenberg, A. J., "Separation of Defect Concentration and Diffusion Coefficient in Diffusion Limited Scaling Reactions," J. Elec. Chem. Soc. 107, p795, 1960

94

1. ORIGINATING ACTIVITY (Corporate author)	2a. REPORT SECURITY CLASSIFICATION
Autonetics Navigation Systems Division Anaheim, Calif.	Unclassified
	2b. GROUP N/A

3. REPORT TITLE

Determination of Native Defects and Endotaxial Growth of Metal-Metalloid Crystal Systems. Experimental Results in TiO_2 (Rutile)

4. DESCRIPTIVE NOTES (Type of report and inclusive dates)

Technical Documentary Report, April 28, 1964 to April 28, 1965

5. AUTHOR(S) (Last name, first name, initial)

Farb, Norman E.

6. REPORT DATE	7a. TOTAL NO. OF PAGES	7b. NO. OF REFS
September 1965	94	17

8a. CONTRACT OR GRANT NO. AF 33(615)1552 b. PROJECT NO. 7350 735001 c. d.	9a. ORIGINATOR'S REPORT NUMBER(S)
	9b. OTHER REPORT NO(S) (Any other numbers that may be assigned this report) N/A

10. AVAILABILITY/LIMITATION NOTICES

Qualified requestors may obtain copies from DDC. DDC release of report to CFSTI is prohibited.

11. SUPPLEMENTARY NOTES	12. SPONSORING MILITARY ACTIVITY
	RTD AFML (MAMC) W-P AFB, Ohio

13. ABSTRACT

Single and polycrystalline TiO_2 (Rutile) membrane experiments were performed using two different partial pressures of O_2 at temperatures from $900^{\circ}C$ to $1200^{\circ}C$. Crystalline regrowth on the high partial pressure O_2 surface under a variety of conditions is convincing proof of the existence of the titanium interstitials. Diffusion tunneling of dislocations occurred in the single crystal experiments. Purification of the single crystals of foreign impurities (Fe, Ag, and Mg) occurred. The regrowth of the polycrystalline sample approached 100 percent theoretical density. The general determination of nonstoichiometric defects and endotaxial crystal growth is considered theoretically.

DD FORM JAN 64 **1473**

14. KEY WORDS	LINK A		LINK B		LINK C	
	ROLE	WT	ROLE	WT	ROLE	WT
Nonstoichiometry						
Oxides						
Defects						
Crystal Growth						
Dislocations						
Titanium Dioxide						
Purification						

INSTRUCTIONS

1. ORIGINATING ACTIVITY: Enter the name and address of the contractor, subcontractor, grantee, Department of Defense activity or other organization (corporate author) issuing the report.

2a. REPORT SECURITY CLASSIFICATION: Enter the overall security classification of the report. Indicate whether "Restricted Data" is included. Marking is to be in accordance with appropriate security regulations.

2b. GROUP: Automatic downgrading is specified in DoD Directive 5200.10 and Armed Forces Industrial Manual. Enter the group number. Also, when applicable, show that optional markings have been used for Group 3 and Group 4 as authorized.

3. REPORT TITLE: Enter the complete report title in all capital letters. Titles in all cases should be unclassified. If a meaningful title cannot be selected without classification, show title classification in all capitals in parenthesis immediately following the title.

4. DESCRIPTIVE NOTES: If appropriate, enter the type of report, e.g., interim, progress, summary, annual, or final. Give the inclusive dates when a specific reporting period is covered.

5. AUTHOR(S): Enter the name(s) of author(s) as shown on or in the report. Enter last name, first name, middle initial. If military, show rank and branch of service. The name of the principal author is an absolute minimum requirement.

6. REPORT DATE: Enter the date of the report as day, month, year; or month, year. If more than one date appears on the report, use date of publication.

7a. TOTAL NUMBER OF PAGES: The total page count should follow normal pagination procedures, i.e., enter the number of pages containing information.

7b. NUMBER OF REFERENCES: Enter the total number of references cited in the report.

8a. CONTRACT OR GRANT NUMBER: If appropriate, enter the applicable number of the contract or grant under which the report was written.

8b, 8c, & 8d. PROJECT NUMBER: Enter the appropriate military department identification, such as project number, subproject number, system numbers, task number, etc.

9a. ORIGINATOR'S REPORT NUMBER(S): Enter the official report number by which the document will be identified and controlled by the originating activity. This number must be unique to this report.

9b. OTHER REPORT NUMBER(S): If the report has been assigned any other report numbers (either by the originator or by the sponsor), also enter this number(s).

10. AVAILABILITY/LIMITATION NOTICES: Enter any limitations on further dissemination of the report, other than those

imposed by security classification, using standard statements such as:

(1) "Qualified requesters may obtain copies of this report from DDC."

(2) "Foreign announcement and dissemination of this report by DDC is not authorized."

(3) "U. S. Government agencies may obtain copies of this report directly from DDC. Other qualified DDC users shall request through

_____."

(4) "U. S. military agencies may obtain copies of this report directly from DDC. Other qualified users shall request through

_____."

(5) "All distribution of this report is controlled. Qualified DDC users shall request through

_____."

If the report has been furnished to the Office of Technical Services, Department of Commerce, for sale to the public, indicate this fact and enter the price, if known.

11. SUPPLEMENTARY NOTES: Use for additional explanatory notes.

12. SPONSORING MILITARY ACTIVITY: Enter the name of the departmental project office or laboratory sponsoring (paying for) the research and development. Include address.

13. ABSTRACT: Enter an abstract giving a brief and factual summary of the document indicative of the report, even though it may also appear elsewhere in the body of the technical report. If additional space is required, a continuation sheet shall be attached.

It is highly desirable that the abstract of classified reports be unclassified. Each paragraph of the abstract shall end with an indication of the military security classification of the information in the paragraph, represented as (TS), (S), (C), or (U).

There is no limitation on the length of the abstract. However, the suggested length is from 150 to 225 words.

14. KEY WORDS: Key words are technically meaningful terms or short phrases that characterize a report and may be used as index entries for cataloging the report. Key words must be selected so that no security classification is required. Identifiers, such as equipment model designation, trade name, military project code name, geographic location, may be used as key words but will be followed by an indication of technical context. The assignment of links, rules, and weights is optional.